Heterogeneity of human bone marrow plasma cells: transcriptional and *in situ* studies

vorgelegt von
M.Sc.
Antonia Niedobitek

an der Fakultät III – Prozesswissenschaften
der Technischen Universität Berlin
zur Erlangung des akademischen Grades

doctor rerum naturalium
Dr. rer. nat.

genehmigte Dissertation

Promotionsausschuss:

Vorsitzender:	Prof. Dr. Jens Kurreck
Gutachter:	Prof. Dr. Hyun-Dong Chang
Gutachter:	Dr. Henrik Mei

Tag der wissenschaftlichen Aussprache: 5. Oktober 2022

Berlin 2022

ABSTRACT

Plasma cells are highly adapted to the demanding task of antibody production against an encountered antigen, thereby providing humoral immune memory. They are the only antibody secreting cells of the immune system, apart from their short-lived precursors, the plasmablasts, and are capable of persisting for long time periods. As major components of humoral immune memory, many of them are stored in the bone marrow where they are supported in microenvironments consisting of niche cells and accessory cells that supply important survival factors. While it is known that the durability of the antibody titers differs greatly depending on the antigen, it is not yet understood by which mechanism humoral immune memory is regulated at the level of plasma cells. According to current knowledge, an array of intrinsic and extrinsic factors can influence the survival of plasma cells.

It is becoming increasingly acknowledged that plasma cells are not uniform regarding their phenotype and biology. Current evidence indicates that plasma cells lacking the expression of the B cell surface antigen CD19 are enriched in the bone marrow and provide humoral immune memory by producing antibodies specific for childhood antigen. Therefore, it is speculated that $CD19^-$ plasma cells contain long-lived plasma cells. In addition, plasma cells lacking CD19 and CD45 expression in the small intestine were found to be of increased age compared to their CD19- and CD45-expressing counterparts. The phenotypic heterogeneity of plasma cells is therefore likely relevant for the variable durabilities of immune memory. The presence of plasma cells expressing the adhesion molecule CD56 in diseases such as some multiple myeloma lead to our interest in assessing whether this plasma cell phenotype is indeed restricted to malignant plasma cells or whether they may be found in healthy humans.

The aim of this study was to delineate the phenotypic heterogeneity of plasma cells of the human bone marrow regarding CD19, CD45 and CD56 expression. We also aimed to assess whether these surface antigens distinguish transcriptionally diverse human bone marrow plasma cell populations with potentially different capacities of long-term survival based on intrinsic survival factors. In addition, we studied the spatial distribution of plasma cells in the human bone marrow in relation with the differential expression of CD19 and CD45.

We have identified novel subpopulations of plasma cells with differential expression of CD19, CD45 and CD56 that are a part of the normal human bone marrow. Specifically, substantial proportions of human bone marrow plasma cells lacked the expression of CD45 or expressed CD56, and these phenotypes were enriched among $CD19^-$ bone marrow plasma cells. These subpopulations were transcriptionally diverse regarding adhesion properties, metabolism and intrinsic resilience. Importantly, $CD19^-$ bone marrow plasma cells were characterized by transcriptional features indicative of improved retention and intrinsic resilience, and within this group, the loss of CD45 expression and gain of CD56 expression identified plasma cells with features of increased maturity. In particular, CD56 expression appeared to mark a subpopulation

that contains bone marrow plasma cells which may potentially derive from primary immune responses, possibly a long time ago, due to lower rates of mutation of their immunoglobulin genes. Our immunohistochemical study of plasma cells in the human bone marrow reveals a division of plasma cells according to their distribution *in situ*, in that a large fraction of plasma cells localized to perivascular sites in clusters. This perivascular localization of plasma cells appears to be restricted to non-sinusoidal blood vessels, therefore indicating that this is not a result of accumulation at the entry site for newly generated plasma cells into the bone marrow. Importantly, perivascular bone marrow plasma cells were enriched for $CD45^-$ cells, which, together with our transcriptional data, suggests that more mature, resilient BMPC may find a supportive environment in this specific site.

In conclusion, this work suggests a hierarchy of maturation progressing from $CD19^+$ $CD45^+$ $CD56^-$ to $CD19^-$ $CD45^-$ $CD56^+$ bone marrow plasma cells. Our data suggest that the loss of CD45 and gain of CD56 in bone marrow plasma cells is connected with the habitation of different, potentially more supportive bone marrow niches as well as advanced maturity. Future efforts to elucidate the contribution of these phenotypes to humoral immune memory will be required. This will contribute to a better understanding of the regulation of humoral immune memory, and, in practical terms, be of use for the development of highly efficient vaccination strategies as well as the targeted therapy of plasma cell disorders.

ZUSAMMENFASSUNG

Plasmazellen sind auf die Produktion großer Mengen von Antikörpern spezialisiert, durch die das humorale Immungedächtnis gegen vergangene Antigene gewährleistet wird. Abgesehen von ihren kurzlebigen Vorläufern, den Plasmablasten, sind sie die einzigen Antikörper-sezernierende Zellen des Immunsystems, und können vermutlich über sehr lange Zeiträume überleben. Langlebige Plasmazellen werden großenteils im Knochenmark gespeichert, wo ihr Überleben in einem Mikromilieu bestehend aus sogenannten Nischenzellen und akzessorischen Zellen, die wichtige Überlebensfaktoren liefern, unterstützt wird. Außerdem sind einige intrinsische, für das Plasmazellüberleben wichtige Faktoren bekannt. Obwohl man bereits weiß, dass die Halbwertszeit von Antikörpertitern nach Infektion oder Impfung sehr unterschiedlich sein kann, ist noch unklar, durch welche regulatorischen Mechanismen die großen Unterschiede zustande kommen.

Es wird zunehmend deutlich, dass Plasmazellen hinsichtlich ihres Phänotyps und ihrer Biologie nicht einheitlich sind. Gegenwärtig wird angenommen, dass Plasmazellen, die das B-Zell-Oberflächenantigen CD19 herunterreguliert haben, im Knochenmark angereichert sind, und dort durch die Produktion von Antikörpern, die zum Beispiel gegen eine Impfung während der Kindheit gerichtet sind, zum humoralen Immungedächtnis beitragen. Daher werden langlebige Plasmazellen innerhalb der Gruppe der $CD19^-$ Plasmazellen vermutet. Zudem hat man festgestellt, dass $CD19^-$ und $CD45^-$ Plasmazellen im Dünndarm langlebiger sind als $CD19^+$ und $CD45^+$ Plasmazellen. Daher ist die phänotypische Heterogenität von Plasmazellen relevant, um die Variabilität der Lebensdauer des Immungedächtnisses zu erklären. In diesem Zusammenhang wirft die Expression des Adhäsionsmoleküls CD56 auf malignen Plasmazellen, wie zum Beispiel den Zellen des Multiplen Myeloms, die Frage auf, ob CD56 auch in normalen, nicht-malignen Plasmazellen exprimiert wird.

Zielsetzung dieser Arbeit ist die Beschreibung der phänotypischen Heterogenität von Plasmazellen des menschlichen Knochenmarks hinsichtlich der Expression von CD19, CD45 und CD56. Des Weiteren beabsichtigten wir die transkriptionelle Charakterisierung von Knochenmarksplasmazellen mit differentieller Expression dieser Moleküle in Hinblick auf möglicherweise unterschiedliche Überlebenskapazitäten. Außerdem analysieren wir die räumliche Verteilung von Plasmazellen im menschlichen Knochenmark in Verbindung mit der differentiellen Expression von CD19 und CD45.

Wir beschreiben in dieser Arbeit bislang unbekannte Subpopulationen normaler Knochenmarksplasmazellen mit differenzieller Expression von CD19, CD45 und CD56. Merkmale dieser neuen Subpopulationen sind das Fehlen von CD45 und eine hinzukommende Expression von CD56, wobei diese Phänotypen interessanterweise innerhalb der $CD19^-$ Knochenmarksplasmazellen angereichert sind. Diese Subpopulationen unterscheiden sich auf transkriptioneller Ebene voneinander bezüglich der Expression von Adhäsionsmolekülen, sowie

metabolischer Eigenschaften und intrinsischer Widerstandsfähigkeit. Insbesondere haben $CD19^-$ Knochenmarksplasmazellen mit differentieller Expression von CD45 und CD56 transkriptionelle Eigenschaften, die auf eine verstärkte Verankerung im Knochenmark und eine erhöhte intrinsische Beständigkeit hindeuten, wobei zusätzlich innerhalb dieser Population eine fehlende Expression von CD45 und eine hochregulierte Expression von CD56 mit transkriptionellen Merkmalen von zunehmender Reifung assoziiert sind. Interessanterweise deutet der Zusammenhang zwischen CD56-Positivität und niedrigen Mutationsraten in den Immunglobulingenen darauf hin, dass $CD56^+$ Knochenmarksplasmazellen möglicherweise aus primären Immunreaktionen entstanden sind, die auf das Kindheitsalter zurück zuführen sein könnten. Aus immunhistochemischen Analysen ergibt sich, dass sich Knochenmarksplasmazellen nicht nur transkriptionell sondern auch hinsichtlich ihrer Verteilung im Knochenmark unterscheiden. Ein großer Anteil an Knochenmarksplasmazellen ist in perivaskulären Arealen angehäuft angesiedelt, während die übrigen vereinzelt im Knochenmark verteilt sind. Da es sich bei den Blutgefäßen, um die sich perivaskuläre Plasmazellen ansiedeln, um nicht-sinusoidale Gefäße handelt, ist davon auszugehen, dass diese Lokalisierung nicht auf kürzliche Immigration neu gebildeter Plasmazellen ins Knochenmark zurückzuführen ist. Zudem waren perivaskuläre Knochenmarksplasmazellen signifikant für $CD45^-$ Zellen angereichert, was zusätzlich zu den transkriptionellen Merkmalen darauf hindeutet, dass die perivaskuläre Lokalisierung insbesondere für besonders reife, widerstandsfähige Plasmazellen eine geeignete Umgebung bietet.

Diese Ergebnisse legen nahe, dass die identifizierten Phänotypen normaler Knochenmarksplasmazellen eine Hierarchie zunehmender Reife von $CD19^+$ $CD45^+$ $CD56^-$ zu $CD19^-$ $CD45^-$ $CD56^+$ Knochenmarksplasmazellen beschreiben. Der Verlust von CD45 und die Hochregulierung von CD56 in Knochenmarksplasmazellen sind assoziiert mit der Bewohnung von Nischen mit unterschiedlichen Eigenschaften sowie zunehmender intrinsischer Überlebenskapazität. Um aufzuklären, in welchem Maße diese Phänotypen zum protektiven humoralen Immungedächtnis beitragen, werden weitere Untersuchungen erforderlich sein. Insgesamt liefern die Ergebnisse dieser Arbeit die Grundlage für ein besseres Verständnis der Regulierung des humoralen Immungedächtnisses, und können zukünftig zur Entwicklung hocheffizienter Impfstrategien sowie die gezielte Therapie von Plasmazellkrankheiten beitragen.

Contents

1. Introduction

An organism is constantly exposed to a plethora of pathogens, such as viruses, bacteria or parasites, which may potentially cause disease. The defense against pathogen invasion through an immune system that detects and disarms extraneous microbes is conserved throughout many species. A highly complex network of effector functions and cells ensures that hosts rarely become ill despite constant confrontation with often harmful microorganisms.

1.1. The innate immune system

The innate branch of the immune system comprises a range of first-line functions deployed against infection. These are physical and chemical barriers, e.g., the skin or antimicrobial proteins on mucosal surfaces, inflammatory response, the complement cascade, together with the functions of innate leukocytes such as mast cells, macrophages and dendritic cells (DC). These cells express so-called pattern recognition receptors that recognize conserved microorganism-derived molecules, termed pathogen-associated molecular patterns, e.g., bacterial lipopolysaccharides or peptidoglycans. Upon their activation by recognition of pathogen-associated molecular patterns, cells of the innate immune system exert specific functions with the purpose of elimination of the intruder through phagocytosis by e.g., macrophages and DC, or the recruitment of other immune cells. DC can take up antigens and then migrate to the secondary lymphoid organs where they present this antigen, thereby activating cells of the adaptive immune system [1].

1.2. The adaptive immune system

Unlike innate immunity with its conserved response to broad categories of pathogens, the cells of adaptive immunity can adapt their functions to encountered antigens and store acquired specificity to past antigens as so-called immunological memory. This information is stored in highly specific receptors on B and T lymphocytes, as well as in the form of highly diverse antibody repertoires released into circulation by plasma cells (PC), the terminal effector B cells (BC). B and T cells are the cellular components of the adaptive immune system and they primarily develop in the bone marrow and thymus, respectively [1].

Naive T cells (TC) circulate through blood and peripheral organs until they encounter antigen and differentiate into different types of effector TC. There are two main effector T cell types, namely $CD4^+$ or $CD8^+$ TC. While $CD8^+$ TC, also called cytotoxic TC, directly recognize and eliminate infected cells, $CD4^+$ TC subdivide into T helper cell or regulatory T cell subpopulations that exert functions through direct cell-contact or the secretion of cytokines. Importantly, T follicular helper cells localized in BC follicles are specialized to interact with BC thereby activating them and promoting the production of antigen-specific antibody [1].

After primary BC development in the bone marrow (BM), they leave the BM as immature BC, and their further maturation takes place in the periphery. Some of them populate the marginal zone in the spleen where they respond to antigen with and without T cell help in extrafollicular foci, rapidly yielding short-lived plasmablasts producing low-affinity antibodies in the early phase of an immune response. The

majority of BC circulate through spleen and lymph nodes as follicular BC and can follow two paths in an immune response. They can either establish an extrafollicular plasmablast reaction, similar to marginal zone BC, generating short-lived plasmablasts, or they can seed germinal centers (GC) by embedding in follicular DC stroma. In the GC, BC undergo iterative rounds of proliferation, somatic hypermutation (SHM) of B cell receptor (BCR) genes and selection based on the affinity of their BCR to the antigen, with highest-affinity cells being favored in obtaining T cell help for successful differentiation into PC with the potential to become long-lived PC (LLPC). GC BC with low-affinity BCRs egress as memory BC while GC BC expressing non-functional BCRs die via apoptosis [1,2].

1.3. The B cell receptor and the antibody repertoire

The BCR is a transmembrane protein composed of a membrane-bound immunoglobulin (Ig) and a signal-transducing component. It serves as a receptor for the recognition of antigen and, upon antigen binding, is internalized and processed into peptides that are presented on the cell surface via major histocompatibility complex class II (MHC II) molecules. The displayed peptide:MHC II complex, in turn, is recognized by cognate T helper cells which then, through the secretion of cytokines, support the proliferation and differentiation of BC into antibody-secreting cells (ASC) or memory BC. Antibodies are encoded for by the same genes that also encode for the BCR, which is why the BCR is also termed membrane immunoglobulin. Upon antigen binding and differentiation into PC, they produce monoclonal antibodies with the identical antigen specificity as the BCR. Antibodies are present in extracellular fluids of the body and act to retain and eliminate pathogen through neutralization, opsonization and complement activation [1].

The theoretical size of the human antibody repertoire is presumed to be in the range of 10^{13} different specificities [3]. This enormous diversity of antibodies is established through a number of processes prior to or during response to antigen. Immunoglobulins consist of two kappa or lambda light chains, and two heavy chains which are encoded in clusters of gene segments. The gene clusters for both chains are subdivided into so-called “variable” (V), “diversity” (D), “joining” (J) and “constant” (C) segments, each containing individual sets of genes. In the process of somatic DNA recombination, or V(D)J rearrangement, during BC development, these gene segments are rearranged and assembled to form a complete antigen receptor gene that is one of many possible combinations. Upon BC activation, SHM in GC further diversifies Ig genes through the introduction of various types of mutations, and BC with high affinity for the antigen are selected for survival, a process termed affinity maturation [1].

Each antibody is composed of a crystallizable fragment (Fc) and an antigen-binding fragment (Fab) of which the latter further consists of a constant and a variable region (Fv) which in turn each have a heavy (V_H) and a light (V_L) chain. The Fv is diversified through V(D)J rearrangement before antigen recognition. Upon antigen encounter, SHM further diversifies the Fv region. In doing so, the complementarity determining regions (CDR) of the Fv are modified by the introduction of mutations in order to enhance antibody specificity. Of the three CDR of each V_H or V_L chain, CDR-H3 is the most diverse carrying the highest hypermutation loads. The so-called framework acts as a scaffold for the CDR and plays a role in the structural shape of the Fv [3,4].

In humans, there are five classes, or isotypes, of immunoglobulins (Ig) some of which are further subdivided into subclasses (IgM, IgD, IgG1, IgG2, IgG3, IgG4, IgA1, IgA2, IgE). The Ig isotypes determine

effector functions of immunoglobulins such as allergic responses and mucosal immunity. Naïve BC express IgM and IgD. During GC reactions, in addition to SHM, BC are induced to switch to different Ig heavy chains (IgA, IgD, or IgG) through changes to their heavy chain constant region, in a process termed class switch recombination (CSR). In mature, antigen experienced BC, the predominant isotype classes are IgG and IgA. Some BC retain IgM expression, and IgM comprises under 10% of immunoglobulin in plasma. The fraction of IgD and IgE antibodies is usually the smallest [1].

IgM antibodies are usually low affinity as they are produced early during an immune response when SHM has not yet occurred. They form large pentamers found mainly in blood and are effective activators of the complement system, e.g., in controlling infections in the bloodstream. In contrast to IgM pentamers, IgG, IgA and IgE are smaller and can exit the bloodstream into the tissues. IgA can dimerize but IgG and IgE are monomeric [1].

IgE is found at minor levels in blood or extracellular fluids and can bind to receptors on mast cells in skin, mucosa and near blood vessels in connective tissue. Upon antigen-recognition by cell-associated IgE, allergic reactions such as coughing and sneezing are effected with the aim of expelling the antigen. IgE is also involved in immune defense against parasites [1].

IgA is predominant in secretions from epithelial tissue lining the intestines and respiratory tracts. Most IgA in circulation is of the subclass IgA1, while IgA2 predominates in the gut. Generally, IgA is a weak opsonin and activator of complement, and mainly acts through neutralization [1].

IgG is the most prominent protein in human serum, accounting for up to 20% of serum protein. In blood and extracellular fluids, it activates complement and opsonizes antigens for them to be engulfed by phagocytes. Class switching into one of the four IgG subclasses is influenced by the type of antigen. Protein antigens cause class switch skewing towards IgG1 or IgG3, although switching toward IgG4 or IgE is also possible. IgG1 is generally the most frequent IgG subclass, followed by IgG2, while IgG3 and IgG4 normally represent the minor fractions of all IgG. Polysaccharide antigens almost exclusively induce production of IgG2. IgG4 is the least abundant of IgG subclasses, and it is the only class able to form hybrid antibodies by reassembly of two different heavy- and light chain pairs to form an IgG4 antibody with two different specificities [1,5].

Thus, class switching ultimately defines the effector functions of antibodies, and it was found to depend on the CD40-CD40-ligand interaction with T helper cells. Hyper IgM syndrome occurs in individuals with CD40-ligand deficiency, and causes them to accumulate exceptionally high levels of IgM in serum while lacking other Ig isotypes, ultimately causing severe immunodeficiency [1]. The decision for switching to a particular Ig isotype is also regulated by cytokines produced by T follicular helper cells or other cells during an immune response. In humans, interleukin 21 (IL-21) drives class switching towards IgG1 [6], interferon γ (IFN-γ) directs it towards IgG2 [7] and in the presence of transforming growth factor β (TGF-β), IgA1 or IgA2 antibody production is induced [8].

1.4. Immune memory

The recognition that undergoing a disease can protect an individual against contracting the disease another time goes back to reports on the plague in Athens by the Greek historian Thucydides in 430 B.C. [9]. Although so-called variolation, i.e., the inoculation with infected material from smallpox victims, was practiced across Asia, Africa and Western Europe for centuries before, it was only in 1796 when Edward Jenner provided scientific proof of this by demonstrating that inoculation of individuals with cowpox provided them protection against infection with smallpox two months after inoculation. A century later, Emil von Behring and Shibasaburo Kitasato discovered that antibodies in the serum of an organism immune to diphtheria or tetanus have a protective activity against the effects of these pathogens. This work marks the basis of the principle of vaccination which, nowadays, is performed using deactivated strains of pathogens or nonhazardous components thereof [1]. Vaccination has become a medical tool that has disarmed various serious, infectious diseases. National organizations such as the Standing Committee on Vaccination (STIKO) for Germany, Switzerland and Austria or the European Centre for Disease Prevention and Control (ECDC) are committed to developing recommendations for vaccinations, thus constantly setting standards in order to keep preventable infections in check through immunization of the broad population.

The principle of vaccination relies on the formation of immunological memory following an immune response to an antigen. Immunological memory manifests in form of memory cells which enable a faster and more efficient response upon a second encounter of the antigen. Within the group of BC, memory BC and PC comprise important components of immune memory. While memory BC do not secrete antibody and maintain an antigen-specific BCR on their surface, PC are terminally differentiated BC that have switched their expressed immunoglobulin from membrane-bound to the secreted form and are classically presumed to have lost responsiveness to antigen, although this dogma has recently been challenged [10,11]. Pre-existing antibody in serum acts as an immediate defense against infection.

1.5. Plasma cells

PC are the only ASC apart from their precursors, the plasmablasts. They are commonly defined as terminally differentiated BC which have stopped proliferating and provide humoral immune memory by secreting high-affinity antibodies after an antigenic challenge [12–14]. It is assumed that once they arrive in the BM, PC become sessile and are supported by a survival niche [15–17]. Although it is becoming increasingly acknowledged that PC are more than mere antibody producers that can modulate their environment by producing cytokines [18,19], they are most famous as the central mediators of humoral immunity.

The persistence of PC as components of immune memory not only promotes health but can also be disadvantageous in autoimmune diseases or PC malignancies. PC neoplasms, for example plasmacytoma and multiple myeloma (MM), are PC disorders in which monoclonal PC expand mainly in the BM in other tissues and can cause clinical symptoms such as anemia, bone lesions or renal dysfunctions [20]. In antibody-mediated diseases such as multiple sclerosis or systemic lupus erythematosus, malignant PC produce autoantibodies which target host proteins, ultimately leading to a wide range of symptoms affecting various organs. For example, in multiple sclerosis, autoantibodies are produced that target myelin proteins in the central nervous system [21].

It has been established that LLPC can contribute to autoimmune disease [22,23]. Furthermore, treatment with rituximab, which targets CD20-expressing cells, is not effective in reducing autoantibody titers because CD20 is not expressed on already existing PC [24]. Therefore, pathogenic LLPC are major contributors of autoimmune disease, and a way of targeting them specifically while sparing protective plasma cells remains an objective of ongoing research [25].

1.6. The generation of plasma cells

PC originate from immune responses to antigen in either TC-independent or TC-dependent manner. TC-independent immune responses take place outside of BC follicles and can be mounted by marginal zone BC in a network of DC. TC-dependent responses can occur either in GC upon embedding of follicular BC in the follicular DC stroma, or from follicular BC that leave the follicles and differentiate into extrafollicular plasmablasts, but in both cases involving TC help. Although it cannot be excluded that TC-independent responses may also yield PC that are potentially long-lived, it is assumed that the majority of LLPC emerge from GC [26,27]. It was believed for a long time that LLPC emerged exclusively from GC, and that SHM took place only in GC but it is becoming apparent that it also takes place in extrafollicular responses, and recent evidence suggests that long-lived antibody responses can result from extrafollicular reactions [28,29].

The differentiation of BC into PC occurs by a switch of transcriptional programs from the BC program, determined by e.g., Paired Box 5 (Pax5) and B cell lymphoma 6 (Bcl6), to the PC program, orchestrated by three transcription factors, i.e., interferon regulatory factor 4 (IRF-4), B lymphocyte-induced maturation protein 1 (Blimp-1) and X-box binding protein 1 (Xbp-1). IRF-4 not only plays a role in PC generation by regulating genes important for GC reactions, e.g., activation-induced cytidine deaminase (*AICDA*) and *BCL6*, and upregulating Blimp-1 expression [18]. It has also been implicated in PC maintenance as induced ablation of *IRF4* gene expression in existing PC led to their significant reduction [30]. A major event in the switch from BC to PC is the induction of the transcriptional repressor Blimp-1 that shuts down proliferation and BC activation genes, such as BTB Domain And CNC Homolog 2 (*BACH2*), *PAX5*, *BCL6* and *AICDA* [18]. Blimp-1 also supports Ig production and secretion, e.g., by enhancing expression of Xbp-1. There is conflicting scientific evidence regarding the question whether Blimp-1 is needed for maintenance of PC or not [30,31]. As a result of Pax5 repression by Blimp-1, Xbp-1 is upregulated through induction of activating Transcription Factor 6 (ATF6) and activated by splicing of Xbp-1 mRNA by Inositol-requiring enzyme 1 (IRE1). Once this occurs, Xbp-1 promotes unfolded protein response (UPR) genes, thereby preparing PC for the demanding task of high throughput antibody production. PC produce antibody molecules in the range of 10^5 per cell per second [32], underlining the importance of cellular adaptation ensuring the expansion of the endoplasmic reticulum (ER), quality control through the UPR machinery, meeting metabolic and amino acid demands, as well as efficient recycling of faulty proteins by autophagy [33,34].

1.7. Migration of plasma cells to the bone marrow

In the first day or two of an immune response, PC generated in extrafollicular foci can migrate towards C-X-C motif chemokine 12 (CXCL12) in the red pulp of the spleen via expression of C-X-C chemokine receptor type 4 (CXCR4) [35]. While most of these PC die rapidly, the class-switched, highly affine PC generated in GC later during the immune response migrate to the BM via the CXCL12-CXCR4 axis where

they potentially persist for a long time. Chemotactic responsiveness is lost upon arrival in the BM, and PC are thought to be sessile with hardly any movement in the BM [16,36]. PC dock onto BM stromal cells (SC) and are thought to stay in constant contact with these cells through integrin-ligand-interactions such as that of the PC integrin α4β1, also called very late antigen-4 (VLA-4), with vascular cell adhesion molecule 1 (VCAM-1) or fibronectin. Interactions between SC and PC through the PC integrin αLβ2, also called lymphocyte function-associated antigen 1 (LFA-1), with intercellular adhesion molecule (ICAM) are also crucial for PC retention [37]. LFA-1 has several other potential binding partners but their relevance in PC niches is not clear. Furthermore, the cell adhesion molecule CD44 expressed by PC was implicated in PC survival and can bind to fibronectin [37,38].

CXCR4-deficient mice show an impaired accumulation of plasma cells in the first 9 after immunization, this negative effect appears to be compensated through other mechanisms later on, suggesting that other unidentified factors also play a role in PC homing to the BM [39].

1.8. The bone marrow as a residence for plasma cells

Once PC have migrated to the BM, they populate survival niches consisting of supportive cells that provide factors favoring the maintenance of PC. The fact that PC die quickly when extracted from the body supports the notion of a niche providing exogenous survival factors. The niche concept is based primarily on the association of PC with SC and other accessory cells, for example DC, macrophages or megakaryocytes, that serve as sources of soluble survival factors such as a proliferation-inducing ligand (APRIL) and interleukin 6 (IL-6) [2,40]. The main, most stable component of the BMPC niche appear to be non-proliferative, VCAM-1$^+$ CXCL12$^+$ reticular stromal cells [17]. Because the frequency of PC among BM cells was found to be constantly around 0.1 to 1 % in healthy subjects [41], it has been deducted that the number of survival niches for PC in the BM must be limited.

SC comprise a poorly defined, heterogeneous cell category that includes cells such as neurons, endothelial cells and mesenchymal stromal cells (MSC). MSC can differentiate into osteoblasts, chondrocytes or adipocytes. Some MSC are CXCL12-producing, i.e. CXCL12-abundant reticular (CAR) cells, nestin$^+$ MSC and osteoblasts [2]. Apart from its role in chemotactic attraction, CXCL12 can have a positive effect on PC survival [42]. Although CXCL12-secreting cells are distributed all over the BM [43], their positioning may be important for the PC or accessory cells that access them. However, since SC comprise a poorly defined heterogeneous class of cells, it is not known whether SC that constitute the PC niche comprise a specialized subset of SC [44].

Accessory cells provide PC with soluble factors that were found to be mostly redundant for PC survival. Although the importance of IL-6 for PC survival is debatable because PC can survive in the absence of IL-6, it does have a positive effect on maintenance and antibody production *in vitro* [45]. Moreover, in IL-6 deficient mice, BMPC numbers were significantly reduced, even though only a fraction of PC seemed affected and this effect was not seen in splenic PC [46]. APRIL is secreted by eosinophils, megakaryocytes, monocytes, macrophages and DC [18]. APRIL is bound by the receptors transmembrane activator and CAML interactor (TACI) and B cell maturation antigen (BCMA) on PC, an interaction which leads to upregulation of the anti-apoptotic factor Mcl-1 and downregulation of the pro-apoptotic factor Bim [46]. Interestingly, CD138 expression was found to increase APRIL- and IL-6- signaling [47]. BCMA deficiency ablated most

BMPC [48], indicating that APRIL provides important survival signals. In an APRIL-deficient patient, immunoglobulin production was impaired, suggesting an impact of the deficiency on PC survival [49].

The BM can be separated into two anatomical regions, i.e., the endosteum and the central, perivascular area. The endosteum, comprised of osteoprogenitors, osteoblasts, osteocytes and vascularized by small arterioles and capillaries, lines the inner surface of bony tissue and makes up about 10% of the BM. This area is also characterized by relatively higher local oxygen tension than the sinusoidal area [50]. The central, perivascular BM region accounts for the remaining 90% of the BM and includes vasculature surrounded by cells like MSC, pericytes, neurons and adipocytes. The BM is vascularized by small arterioles which branch into a network of thin-walled sinusoids with large lumina surrounded by CXCL12-secreting MSC. It is unknown whether PC localization to any of these BM areas has any particular effect on their maintenance. From research on hematopoietic stem cells (HSC), there are indications that these anatomical areas differ in their qualities to support resting or active HSC lifestyles [51]. The endosteum was found to harbor the more primal HSC and the cellular environment here promotes HSC quiescence, while more active HSC were located towards the sinusoids [2,51,52]. Sinusoids have fenestrated endothelia and discontinuous basal membranes, and were found to be a preferred entry site for hematopoietic cells owing to low blood flow velocities in this vascular segment [53].

Aging may also have effects on the nature of the BM niches. It has been shown that in very young mice, APRIL concentrations in BM are very low and, therefore, PC persistence is compromised at this early stage in life and, only at a certain age, APRIL-levels sufficient for PC survival are established [54]. Another age-related factor in the composition of the BM is the accumulation of adipocytes which contain large fat vacuoles. Although there are no indications of a role for fatty tissue in the maintenance of PC, it is likely that these cells indirectly shape the BM cellular composition, at least by influencing the available space for PC and other cells in the BM. Additionally, obesity may negatively affect immune responses, as found during the influenza pandemic in 2009 [55]. Moreover, due to aging, inflammatory signals through elevated levels of, e.g., IL-6 or TGF-ß can occur [51].

1.9. Intrinsic cellular adaptations to plasma cell biology

1.9.1. Transcription factors of the plasma cell lineage

The expression of the PC transcription factors has profound effects on the function and survival of these cells. The expression of Blimp-1 not only inhibits BC activation genes and proliferation, but in also enhances immunoglobulin gene expression as well as expression of genes that support Ig secretion [56]. Xbp-1 is an important mediator of UPR which PC are crucially dependent on due to their high rates of protein production. Xbp-1 is regulated by Blimp-1. While Blimp-1 was found to be non-essential for PC survival, the PC lineage transcription factor IRF-4 was shown to be indispensable for PC survival [30,57]. IRF-4 is upregulated during PC differentiation and leads to enhanced expression of *PRDM1*, encoding for Blimp-1, while repressing several genes of unknown functions [58]. More recently, IRF-4 was implicated in the regulation of PC identity genes such as BCMA, as well as glycolytic and mitochondrial metabolism [57].

1.9.2. Unfolded protein response and autophagy

The UPR functions as a quality control mechanism for newly synthesized antibody molecules. It allows the cell to sense the accumulation of misfolded proteins through stress sensors at the ER, and to respond accordingly by either promoting cell survival or death. This mechanism is a vital adaptation for PC to cope with the stress of large-scale protein synthesis [59]. PC also depend on the capability to degrade misfolded proteins for the recycling of building blocks for new protein synthesis [60].

An important adaptation of PC in response to the stress of producing large amounts of antibody is the recycling of intracellular components and organelles, termed autophagy. The autophagy related gene 5 (ATG5) was found to be essential for PC maintenance. Work with ATG5-deficient mice revealed that autophagy mediated by ATG5 acted as a negative regulator of ER capacity and Ig production and secretion with the object of saving energy and keeping ER stress levels low [34,61].

1.9.3. Metabolism

Due to their colossal rates of antibody production, PC have high demands of energy and amino acids. In mice, LLPC were distinguished from short-lived PC (SLPC) by higher glucose uptake which is utilized primarily for antibody glycosylation. Moreover, LLPC showed a greater pyruvate-dependent respiratory capacity than LLPC. They appeared to depend on the mitochondrial pyruvate carrier 2 (Mpc2) as its genetic deletion led to loss of LLPC. LLPC also expressed higher levels of CD98, an amino acid transporter, and LLPC were able to utilize glutamine not only as a source of amino acid building blocks but also in mitochondrial respiration. Strikingly, these fundamental differences in metabolism were not reflected on transcriptional levels either by bulk RNA sequencing or single cell RNA sequencing [33,62]. Interestingly, Blimp-1 enhances expression of CD98 [63].

1.9.4. Regulation of apoptosis

A further intrinsic process that determines PC survival is the molecular circuitry regulating programmed cell death, also called apoptosis. Apoptosis can be induced by either extrinsic triggers such as stimulation of the death receptor, Fas, or by intrinsic pathways in response to stress signals, e.g., ER stress, while the latter was found to be the main pathway of cell death in PC [64]. Cell death is executed by the formation of the mitochondrial outer membrane pore (MOMP) which releases cytochrome c into the cytoplasm and leads to activation of caspases such as caspase 3, ultimately killing the cell and recruiting macrophages to get rid of the cell remnants. The initiation of apoptosis is regulated through a complex balance of anti-apoptotic factors such as Bcl-2 or Mcl-1 and pro-apoptotic factors, e.g., Bax, Bak, Bim and Noxa. Anti-apoptotic proteins bind pro-apoptotic proteins that can initiate MOMP formation, thus preventing the onset of apoptosis. In turn, other pro-apoptotic proteins can act as competitors to the anti-apoptotic factors [65]. Mcl-1 appears to be a key factor for PC survival as its genetic deletion resulted in rapid and almost complete loss of PC [46]. Moreover, IRF-4 was also implicated as a mediator of PC survival although the authors of this study found that it appeared to do this only in part through the prevention of apoptosis and caspase activation, and it did not regulate the expression of Mcl-1 [57].

1.9.5. Other factors involved in plasma cell maintenance

Some surface proteins expressed by PC have also been implicated in their maintenance. CD93 is expressed in a subset of PC and was found to be important for the survival of LLPC in mice [66]. $CD93^+$ PC were also associated with higher glucose uptake [33]. The precise function of CD93 in PC is not known but this molecule has been associated with angiogenesis and support of integrin function [67,68]. CD138 is widely used as a PC marker, and its deletion had a large impact on BMPC survival. It appeared that the heparan sulfate proteoglycan improved the capture of APRIL and IL-6, thereby enhancing pro-survival signaling through Mcl-1 and Bcl-2 [47]. Furthermore, CD28 which is expressed upon downregulation of PAX5 [69] is expressed on PC. Rozanski et al. found it to be essential only in LLPC survival [70], while work by Njau et al. provides evidence that it regulates Ab production and survival in both short- and long-lived PC [71]. Interestingly, signaling through CD28 stimulated glucose uptake, mitochondrial respiratory capacity and IRF-4 expression [72]. Moreover, CD28 is discussed as a factor by which PC niches may be restricted. CD28 may interact with CD80/86 on the surface of DC, an interaction which was suggested to be disturbed by regulatory TC that express CTLA, an alternative binding partner of CD80/86 [73]. This may represent a way of limiting PC niches involving DC. Zbtb20, a transcription factor and direct target of IRF4, was not only found to be important for expression of Mcl-1 but also supported PC survival depending on the adjuvant used in the immunization model. Wang et al. showed that Zbtb20-deficiency affected PC survival in alum-adjuvanted immunization but not when immunization involved toll like receptor (TLR) stimulation [74,75]. The CD44 isoforms CD44v6 and CD44v9 were found to mediate the adhesion of PC cell lines to BM stromal cells and, moreover, CD44v9 induced IL-6 secretion by stromal cells [76]. In addition, PC survival was supported synergistically by CD44 and IL-6 [45].

1.10. Maintenance and adaptation of humoral immune memory

The duration of humoral immunity has been shown to vary greatly depending on the pathogen. By longitudinal monitoring of serum antibody titers in a cohort of 45 individuals for up to 26 years, Amanna and colleagues (2007) extrapolated serum antibody titer half-lives against vaccinia, measles, mumps, rubella, Epstein-Barr (EBV) and varicella-zoster virus (VZV), as well as against the non-replicating protein antigens tetanus and diphtheria [77]. They found that viral antibody levels had overall highly durable half-lives, as these ranged from 50 years, as found for VZV, up to 114 years for rubella, 542 years for mumps, and even 3014 for measles. In contrast, the half-lives for tetanus and diphtheria were shorter, with 11 years and 19 years, respectively. From these results, they concluded that the duration of humoral immunity was generally very stable over many years and was likely to depend to some extent on the type of antigen.

Since antibodies produced by PC have a limited serum half-life ranging from hours to days [78], it is evident that the stability of antibody titers over many years depends on continuous antibody production. In the attempt to explain how this is conferred, one model suggests that memory BC can continuously become activated and differentiate into PC, thereby replenishing the PC pool and increasing antigen-specific antibody levels. In this case, either antigen-specific stimulation by repeated infection or persisting antigen in immune complexes [79], or antigen-independent stimulation, e.g., via bystander T-cell activation or TLR engagement, leads to the activation of memory BC and their differentiation into PC [80]. Ever since this idea emerged, several studies involving BC depletion have provided indications that humoral memory may be maintained to a great extent independently of memory BC. In rhesus macaques that were vaccinated and then underwent lymph node removal, splenectomy and BC depletion using the anti-CD20 reagent,

Rituximab, and were therefore unable to generate new PC, serum antibody half-lives against the vaccination as well as other antigens were stable for up to decades [81]. In patients, total Ig levels decreased slightly upon Rituximab treatment but were never ablated, indicating that to a large extent the PC pool does not require replenishment by newly differentiating BC [24,82]. In addition, antigenic re-challenge in BC depleted patients causes antibody titers to increase only slightly, thus the PC pool is hardly replenished in the absence of BC [83,84]. Thus, it is probable that PC can confer long-term immunity independently from BC.

Although the idea that PC can potentially persist for a very long time [13,14,85], possibly in the range of decades in humans, is not new, the mechanistic basis for this remains enigmatic. Landsverk et al. (2017) demonstrated in a small intestine (SI) transplant study that donor PC persist in the host for up to one year without proliferating [86]. They further show elegantly by cell birth dating through measurement of carbon-14 in genomic DNA that PC of the SI can be up to two decades old. Interestingly, they also provide evidence that different lifetimes are linked with the differential expression of CD19 and CD45 [86].

To explain durable humoral immune memory that is maintained by PC independently from memory BC and with the capacity to adapt to new pathogenic challenges, two models have been proposed: the PC niche competition concept [87] and the PC imprinted lifespan model [88]. In general, both models assume that PC can survive for long time periods and that the space for PC in the BM as the major storage site for PC is limited but they propose different approaches regarding the mechanisms by which their varying lifespans may be limited.

1.10.1. The plasma cell niche competition concept

The niche competition concept assumes that PC survival niches are limited, and that, upon antigenic challenge, pre-existing PC compete with newly generated PC for the niches. Thus, when new PC are generated, some old PC are displaced and die, which would explain the fading of pre-existing antibody titers and the accommodation of PC with new antigen-specificities. This model assumes that all antigen-specificities are affected to an equal extent by the displacement from the survival niches. Thus, all specificities of the memory repertoire would fade at the same rate. It is likely that this concept alone does not account for the varying half-lives of serological immunity [77]. Nevertheless, there is evidence that, upon vaccination, PC specific for vaccine-irrelevant antigen and with a mature PC phenotype are found in the peripheral blood [89]. Severe immune challenges such as a measles infection can even lead to loss of pre-existing specificities entirely [90].

1.10.2. The PC imprinted lifespan model

The imprinted lifespan model attempts to explain differential durations of humoral memory by assuming that LLPC which maintain serum antibody levels are imprinted with the capability to survive for a determined lifespan when their generation is induced [88]. This model is based on the proposition that PC are terminally differentiated, non-proliferative cells that continuously secrete antibody without further stimulation. The model assumes that PC cannot sense their antigenic microenvironment due to loss of MHC class II molecules, and thus, PC are likely to be imprinted with features determining differing lifespans when they are generated. A possible mechanism is that imprinting may be in part due to

properties of the antigen triggering the activation of BC [91]. It is discussed that the properties of antigens, i.e., monovalent (with only one epitope) versus multivalent (with repetitive epitopes) antigens, influence the strength and duration of interactions between a BC and a follicular helper TC. Increased BCR clustering, antigen presentation and duration of BC-TC interactions could imprint particularly long PC lifespans. In support of this idea, a multivalent antigen such as measles virus generates very long-lived immune memory, whereas monovalent antigens such as tetanus toxoid produce intermediate antibody responses [77]. Moreover, since niches for PC in the BM are likely to be limited [41,87], the imprinted lifespan model allows for the adaptation of the memory repertoire because old PC that die due to a shorter, imprinted lifespan liberate niches for new PC.

In addition to these models, it is becoming increasingly acknowledged that LLPC that mediate humoral immunity for up to a lifetime are not uniform regarding their phenotype and biology [33,86,92,93]. This heterogeneity may translate into a taxonomy of PC populations with different propensities to survive. Therefore, PC with variable levels of intrinsic stability in the BM could provide another explanation for the varying durations of humoral immunity immune memory.

1.11. Plasma cell heterogeneity and humoral immune memory

Variable antibody titers directed against common vaccines suggest differential regulation of BC memory at the level of terminally differentiated PC (see 1.10.). It is becoming increasingly acknowledged that PC are not uniform regarding their phenotypes and lifestyles. To date, a clear concept for differential regulation of humoral immune memory at the level of ASC has not yet been established. The surface molecule CD19 has been in the focus regarding the phenotype of LLPC. Hallileyet al. found that tetanus- and influenza-specific PC were predominant among but not restricted to $CD19^-$ BMPC and measles, mumps and rubella- (MMR) specific BMPC were found only in the $CD19^-$ PC compartment [93]. Mei and colleagues simultaneously showed that tetanus-specific BMPC were contained in both $CD19^+$ and $CD19^-$ BMPC compartments [92]. The work of Landsverk et al. revealed that $CD19^-$ $CD45^-$ SIPC were older than their $CD19^-$ $CD45^+$ counterparts [86]. Together, these findings are highly suggestive of a further diversification of $CD19^-$ BMPC that may explain the differential regulation of antigen-specific BMPC, and thus of variable durability of humoral immunity. The present study focuses on three differentially expressed surface markers of normal PC, CD19, CD45 and CD56, and aims to characterize this heterogeneity regarding features suggestive of differential regulation.

1.11.1. CD19 function and expression in plasma cells

The Ig superfamily member and transmembrane glycoprotein CD19 is a specific marker of the BC lineage [94]. It is first expressed at the stage of pro-BC when immunoglobulin gene rearrangement takes place, and CD19 expression is thought to be lost upon terminal differentiation into PC [95–97].

CD19 is a co-receptor of the BCR together with CD21, CD81 and CD225. In BCR signal transduction, CD19 lowers signaling thresholds and amplifies signaling because it recruits and activates Src protein tyrosine kinases such as Lyn as well as PI3K and Akt kinases [94]. The CD19/CD21 complex alone can bind to

complement fragment C3d, and is involved in the arrangement of BCR signaling molecules in lipid raft domains which are known to facilitate and prolong BCR signaling [98]. The function of CD19 as a modulator of BCR signaling affects BC maturation starting at early stages of pre-BC in the BM to peripheral, antigen-dependent BC differentiation [96]. CD19 was found to be crucial for normal BC responses as CD19 deficiency impaired humoral response and increased susceptibility to infection [99,100]. On the other hand, elevated expression of CD19 has been associated with autoimmunity [101,102].

Although the precise mechanism by which CD19 expression is lost in PC is not known, Pax5 has been implicated in its transcriptional activation [103] and loss of CD19 expression may therefore be a result of the suppression of the BC program. There are indications that $CD19^-$ PC may already emerge at early stages of PC differentiation, suggesting that CD19 loss is established in the course of commitment to the PC fate [104,105]. Nevertheless, this model does not exclude the possibility of gradual loss of CD19 due to aging in the BM.

The $CD19^-$ BMPC compartment appears to harbor large amounts of LLPC. $CD19^-$ BMPC have an expression profile indicating a pro-survival, mature phenotype compared to $CD19^+$ BMPC [92], and long-lived antigen-specific BMPC were found to be enriched among $CD19^-$ BMPC [93]. On the other hand, $CD19^+$ BMPC were also found to contribute to serum titers against tetanus and MMR [92]. Nevertheless, $CD19^-$ BMPC and associated antigen-specific IgG and IgA antibody responses were maintained independently of BC repopulation upon CD19-directed BC depletion [106]. Moreover, PC of the SI also contained virus-specific $CD19^-$ PC which were found to be decades old compared to $CD19^+$ SIPC which seemed to be a constantly renewed population [86]. Therefore, CD19-negativity seems to be a feature of a great part of LLPC although there are indications that this is not a determining criterion of PC longevity. It is also unknown whether other processes within the BM can influence the dynamics of CD19 expression by the BMPC pool, e.g., the differentiation of antigen-specific memory BC into PC *in situ*, or CD19-re-expression.

1.11.2. CD45 function and expression in plasma cells

CD45, originally named leukocyte common antigen (LCA), was initially thought to be expressed on all nucleated hematopoietic cells [107]. Later, it was revealed that CD45 is downregulated in terminally differentiated PC although a fraction of them retain CD45 expression and it is unclear whether its loss is a result of maturation [108,109]. MM cells can also express high or low levels of CD45, thereby distinguishing proliferative from quiescent cells, respectively [108].

CD45 is a protein tyrosine kinase which is important for lymphocyte activation and maturation. Src family kinase (SFK) activation is the first step of antigen receptor signaling in TC and BC. CD45 modulates antigen-receptor signaling by dephosphorylation of inhibitory tyrosine of SFKs leading to activation of SFKs and thus enhancement of signaling [110,111]. Recently, Szodoray et al. showed that T helper cell signals enhanced CD45 phosphatase activity in memory BC and thereby increased their efficiency to different into ASC [112]. In contrast, in cytokine signaling, CD45 was also found to negatively regulate JAK-STAT signaling by dephosphorylating JAK and thus reducing phosphorylation of STATs [113]. Although IL-6, a cytokine that targets the JAK-STAT pathway, is not an essential PC survival factor, it has been shown to have a positive effect on PC survival *in vitro* [45]. Therefore, it is intriguing to speculate that this inflammatory cytokine preferentially stabilizes the $CD45^-$ BMPC compartment under certain conditions, i.e., an inflammatory setting.

As mentioned in the prior chapter (see 1.11.1.), SIPC were found to display a phenotypic heterogeneity not only in their differential expression of CD19 but also of CD45. Landsverk et al. found that $CD19^-$ $CD45^+$ SIPC were on average 11 years old and $CD19^-$ $CD45^-$ SIPC were on average 22 years old. Moreover, $CD45^+$ SIPC showed a higher variability in the inferred age in between the examined subjects because in 2 of 6 individuals, CD45+ SIPC were on average 0 years old [86]. Therefore, CD45 expression seems to distinguish differentially regulated PC populations in the SI, and loss of CD45 may mark the entry into the LLPC pool.

1.11.3. CD56 function and expression in plasma cells

CD56, or neural cell adhesion molecule 1 (NCAM1), is a glycoprotein originally known for its role in the development of the nervous system as a regulator of neurite outgrowth and neural cell motility [114]. CD56 is also expressed by natural killer (NK) cells and is used as a phenotypic marker for their identification together with CD3-negativity. CD56 expression on NK cells can be high or dim, the latter being an indication of advanced maturity. Although the degree of CD56 expression has been linked to different NK cell functions, the precise role for CD56 expression on these immune cells has not been clarified [115]. CD56 was found to be involved in the cell contact and motility of NK cells on stromal cells, thereby forming a developmental synapse shaping NK cell maturation [116].

CD56 is expressed on MM and monoclonal gammopathy of undetermined significance (MGUS) PC, and originally was thought to be absent or only weakly expressed on normal PC [117]. Elevated serum levels of CD56 is considered a marker of tumor progression in myeloma patients [118]. In normal cancellous bone, CD56 is expressed in osteoblasts. Work with MM cell lines co-cultured with osteoblasts has demonstrated that these cell types directly interact through CD56, and that this interaction induced IL-6 production by osteoblasts, suggesting a role in modulation of the BM environment by MM cells [119]. More recently, $CD56^+$ PC have been identified in BM of healthy donors [120], and in the SI where they were enriched among $CD19^-$ SIPC [86], although the role of CD56 expression in PC remains unclear to date. CD56 is known to mediate homotypic interactions [121], and therefore, potential interaction partners for $CD56^+$ BMPC may be BM mesenchymal stromal cells and afore mentioned osteoblasts [122,123].

1.12. Aims of this work

To this day, it is unclear how humoral immune memory is regulated at the level of long-lived plasma cells. Plasma cells provide humoral immune memory by secreting antibodies against previously encountered antigens. The duration of humoral protection against common vaccinations and infections is variable depending on the antigen-specificity, but the reason for this variability is not known so far. This is not only relevant in the context of vaccination strategies, but also in the therapy of autoimmune diseases. Current therapeutic approaches either fail to deplete pathogenic long-lived plasma cells or deplete pathogenic and protective plasma cells alike.

The current understanding of the regulation of immune memory on the level of plasma cells is based on two types of factors that confer survival potential onto plasma cells: first, there are intrinsic survival factors which may be imprinted in plasma cells through signals possibly received during their generation; second, there are extrinsic factors provided to plasma cells once they are embedded in a cellular microenvironment, which are conceptually integrated in the plasma cell survival niche. Currently, a concept of how these factors influence the survival of plasma cells in the context of homeostasis of humoral immune memory is still missing. An aspect that has not been included in this discussion is the role of plasma cell heterogeneity as well as the possibility, that plasma cells embed in heterogenous microenvironments with potentially different qualities in terms of plasma cell maintenance.

Therefore, the major aim of this study is to provide a basic scaffold of plasma cells in human bone marrow incorporating their phenotypical heterogeneity and microanatomical distribution.

Specifically, the following questions will be addressed:

- Do the surface markers CD19, CD45 and CD56 distinguish transcriptionally distinct human bone marrow plasma cell populations regarding plasma cell maintenance and immunoglobulin genes?

- Do plasma cells localize to specific microanatomical sites in human bone marrow *in situ*, and how does this relate to plasma cell heterogeneity?

Together this work will provide profound insights into the biology of plasma cells with potential impacts on the understanding of the regulation of humoral memory in the context of infections, the development of vaccination strategies, and therapeutic approaches against autoimmune diseases.

2. Materials and Methods

2.1. Materials

2.1.1. Bone marrow samples

There are fundamental factors that must be taken into account when conducting analyses of PC in human BM. While we assume that the analyzed patients undergo hip replacement surgery only when they are in an otherwise good state of health, i.e. not experiencing acute infections, allergic reactions or other conditions compromising the immune system, we do not know if any of them recently received a vaccination or are experiencing an immune response. In that case, their BMPC pool may therefore be subject to very recent or ongoing adaptation. Moreover, especially when analyzing BM samples from hip replacement surgeries, we cannot fully rule out hematological systemic disorders because this information is not accessible to us due to anonymization, in contrast to iliac crest trephine biopsy samples obtained for diagnostic purposes. To obtain data as representative of healthy individuals as possible, we analyzed BM from 19 donors. In addition, our immunohistochemical analyses substantiate the findings in flow cytometry as they show that fractions of $CD19^-$ and $CD45^-$ BMPC occur regularly in individuals with normal BM.

BM samples for ex vivo analyses

For ex vivo analyses, BM samples were obtained from patients undergoing hip endoprosthesis surgery. During this procedure, the femoral head and, often, cancellous bone from inside the femoral shaft is removed and normally discarded as waste. With the patients' consent, this material is collected upon removal and distributed for research purposes by Dr. Simon Reinke and Antje Blankenstein the Core Unit Cell & Tissue Harvesting (Berlin Institute of Health Center for Regenerative Therapies) or collected by the medical staff at the department for orthopedics and emergency surgery at the Bundeswehrkrankenhaus Berlin. The patients included in this study were regarded as healthy based on their own information regarding immunological diseases. Furthermore, cancer patients or patients having received cancer medication one year prior to surgery, as well as patients with local necrosis were excluded from this study.

Table 1 of materials and methods: List of donors for FACS analyses, Fluorospot and RNA sequencing experiments indicating age and gender.

Donor #	**Gender**	**Age (years)**
Samples for FACS analyses:		
1	Female	77
2	Female	74
3	Male	76
4	Male	59
5	Female	47
6	Male	50
7	Female	78
8	Female	68
9	Female	75

10	Female	77
11	Male	67
12	Female	54
13	Male	63
14	Female	68
15	Female	60
16	Female	59
17	Female	71
18	Female	72
19	n.a.	n.a.
Samples for Fluorospot assays:		
1	Female	77
1357	Female	78
Samples for RNA sequencing (bulk)		
1	Male	70
2	Female	72
3	Male	45
4	Female	57
Samples for RNA sequencing (single cell)		
1	Male	75
2	Male	50

FFPE BM samples for immunohistochemistry

For all immunohistochemical analyses, archival formalin-fixed paraffin-embedded (FFPE) BM samples were provided by the Institute of Pathology, Unfallkrankenhaus Berlin, Germany. The BM biopsies had been obtained for diagnostic purposes and were used for research purposes after completion of diagnoses. None of the BM specimens used for the present immunohistochemical analyses were collected for the purpose of this research study. The diagnoses of all patients included in this study were reviewed by Prof. Dr. Gerald Niedobitek to ensure that the BM samples included in this study showed no evidence of hematological systemic disorders, including plasma cell disorders.

Table 2 of materials and methods: List of donors analyzed in immunohistochemistry experiments indicating age and gender.

Donor #	**Gender**	**Age**
583/16	Male	59
1663/16	Male	68
1409/18	Male	59
7022/18	Male	66
228/19	Male	41
1082/19	Male	71
4420/19	Female	74

6751/19	Male	64
1409/20	Male	60
5642/20	Female	66

2.1.2. Buffers and media

Name	**Composition**	**Supplier**
Phosphate buffered saline (PBS)	1x PBS pH 7.2	Th. Geyer GmbH & Co. KG
PBS/BSA	1x PBS	Th. Geyer GmbH & Co. KG
	0.2% BSA	PAN Biotech GmbH
PBS/BSA/EDTA	1x PBS	Th. Geyer GmbH & Co. KG
	0.2% BSA	PAN Biotech GmbH
	5 mM EDTA	Invitrogen by Life technologies
Standard RPMI	RPMI 1640	Gibco
	10% FCS	Gibco
	100 U/mL Penicillin-Streptomycin	Gibco
	50µM 2-mercaptoethanol	Gibco
CSM	1x PBS	Th. Geyer GmbH & Co. KG
	0.5% BSA	PAN Biotech GmbH
	0.02% sodium azide	Sigma Aldrich

2.1.3. Chemicals

Name	**Composition**	**Supplier**
4',6-Diamidin-2-phenylindol (DAPI)	1 mg/ml in 1x PBS	Thermo Fisher Scientific
Xylene	Pure (isomeric mixture)	WALTER CMP
Ethanol	99%, denatured with about 1% methyl ethyl ketone	WALTER CMP
Methanol	Methanol ≥99,5 %, Ph. Eur., extra pure	Carl Roth
Hydrogen peroxide (H_2O_2)	30% hydrogen peroxide, stabilized	Carl Roth
Paraformaldehyde (PFA)	EM grade	Electron Microscopy Sciences

2.1.4. Consumbles, MACS beads

Name	**Supplier**
Whole Blood Column Kit	Miltenyi Biotec B.V. & Co. KG
StraightFrom® Whole Blood and Bone Marrow CD138 MicroBeads, human	Miltenyi Biotec B.V. & Co. KG
Falcon™ Cell Strainers 70 µm	Corning B.V.
MACS® Separation Filter, 30 µm	Miltenyi Biotec B.V. & Co. KG
EQ Four Element Calibration Beads	Fluidigm

2.1.5. Kits and reagents

Name	Supplier
ZYTOMED Systems Wash Buffer (20 X)	Zytomed Systems
ZytoChem Plus HRP Polymer Kit	Zytomed Systems
ZytoChem Plus AP Polymer Kit	Zytomed Systems
Antibody Diluent	DAKO Agilent
DAB Substrate Kit	Zytomed Systems
PermaBlue Plus/AP	Diagnostic BioSystems
Permanent AP Red Kit	Zytomed Systems
Glycergel Mounting Medium, Aqueous	DAKO Agilent
Tofaticinib (CP-690550)	Selleckchem
Recombinant Human IL-6	Peprotech
Smart Tube proteomic stabilizer	Smart Tube Inc.
Thaw-lyse buffer	Smart Tube Inc.
Beriglobin	CSL Behring
Heparin	Ratiopharm

2.1.6. Immunohistochemistry antibodies

Specificity	Clone	Supplier	Catalogue no.
Anti-human MUM1	BC5	Biocare medical	CRM 352 B
Anti-human CD138	SP152	Zytomed Systems	503-4522
Anti-human SLAMF7	E5C4M	Cell signaling technology	98611S
Anti-human CD19	BT51E	Novocastra	NCL-L-CD19-163
Anti-human CD45	PD7/26+2B11	Zytomed Systems	MSK054
Anti-human CD56	RCD56	Zytomed Systems	RBK050-05
Anti-human CD34	QBEnd 10	Dako	GA632
Anti-human Ki67	SP6	Zytomed Systems	RBK027
Anti-human CD3	Polyclonal	DakoCytomation	GA503

2.1.7. Flow cytometry antibodies

Specificity	Clone	conjugate	Supplier	Catalogue no.
Anti-human CD3	BW264/56	VioBlue	Miltenyi	130-113-133
Anti-human CD10	HI10a	APC-FIRE 750	BioLegend	312230
Anti-human CD14	M5E2	APC-FIRE 750	BioLegend	301854
Anti-human CD14	TÜK4	VioBlue	Miltenyi	130-113-152
Anti-human CD16	REA423	VioBlue	Miltenyi	130-113-396
Anti-human CD38	HIT2	BV510	BioLegend	303540
Anti-human CD38	HIT2	APC	BioLegend	303510
Anti-human CD138	44F9	FITC	Miltenyi	130-119-839
Anti-human CD138	44F9	PE	Miltenyi	130-119-840
Anti-human CD45	HI30	PE	BioLegend	304008
Anti-human HLA-DR	L243	PerCP	BioLegend	307628

Anti-human CD19	HIB19	Pe-Cy7	BioLegend	302216
Anti-human CD56	AF12-7H3	APC	Miltenyi	130-113-305

2.1.8. CITE-Seq antibodies

Specificity	**Clone**	**barcode**	**Supplier**	**Catalogue no.**
TotalSeq™-C0050 anti-human CD19	HIB19	CTGGGCAATTACTCG	Biolegend	302265
TotalSeq™-C0084 anti-human CD56 (NCAM) Recombinant	QA17A16	TTCGCCGCATTGAGT	Biolegend	392425
TotalSeq™-C0391 anti-human CD45	HI30	TGCAATTACCCGGAT	Biolegend	304068
TotalSeq™-C0386 anti-human CD28	CD28.2	TGAGAACGACCCTAA	Biolegend	302963

2.1.9. Technical equipment

Name	**Supplier**
BD FACSAria	BD Biosciences
Sony cell sorter MA900	Sony Biotechnology
MACS® Separator and MultiStand	Miltenyi Biotech
Centrifuge Heraeus Fresco 21	Thermo Fisher Scientific
Centrifuge 5810 R	Thermo Fisher Scientific
Multifuge X1R centrifgue	Thermo Fisher Scientific
Clean bench Hera Safe HS18	Heraeus Instruments
Helios CyTOF system	Fluidigm
IKA® Vortex Genius 2	Sigma-Aldrich
Philips Ultra Fast Scanner	Philips
MACSQuant Analyzer	Miltenyi Biotech
AID ISPOT Elispot/Fluorospot Reader	AID Autoimmun Diagnostika
Bone mill	USTOMED INSTRUMENTS

2.1.10. Software

Name	**Supplier**
Loupe Browser v5.0	10x Genomics
FlowJo10 v7.1	FlowJo LLC
GraphPad Prism 9	GraphPad Software
OMIQ	OMIQ
Helios instrument control software v6.7.1014	Fluidigm
Microsoft Office	Microsoft Corporation
Philips image management system	Philips
AID EliSpot Software Version 7.0	AID Autoimmun Diagnostika

2.2. Methods

In order to address the aims of this study, a spectrum of methodological approaches was used. We employed flow cytometry for the phenotypic analysis of *ex vivo* BMPC, for the purpose of quantifying

BMPC populations. In order to further study BMPC populations, we performed magnetic enrichment of *ex vivo* CD138-expressing BM cells prior to fluorescence activated cell sorting (FACS) to extract selected BMPC based on their phenotype from total BM cells. The obtained populations were processed for the sequencing of their RNA transcripts, with the objective of performing global gene expression analysis. In a separate, single cell-based approach, we enriched *ex vivo* BMPC by magnetic enrichment of CD138-expressing cells prior to fluorescence activated cell sorting (FACS) for sequencing of RNA transcripts and immunoglobulin genes at the single cell level. In addition, we used a stimulation assay followed by mass cytometric analysis in order to study the induction of cytokine signaling in BMPC populations. For the study of PC localization in the human BM, we used immunohistochemical staining methods allowing for the chromogen-based detection of two or three different epitopes. This is facilitated by sequential staining and detection employing different enzymes and substrates which produce precipitates visible under normal light.

2.2.1. Isolation of BM cells

Immediately upon receipt, BM tissue samples were immersed in chilled PBS/BSA/5 mM EDTA, rinsed and filtered using 70 µm cell strainers to separate any solid components such as fragments of trabecules from the cell suspension. Whenever necessary, larger bone fragments were disintegrated using pliers or a bone mill (USTOMED INTSTRUMENTS) before rinsing and filtering in order to release as much BM as possible. During the entire procedure, tissue samples, cell suspensions and buffers were chilled at 4°C or stored on ice.

2.2.2. Magnetic enrichment of $CD138^+$ BM cells

BM cell suspensions were spun down (300 x g, 4°C, 10min) to achieve cell pellets, and supernatant was reduced to approximately the initial volume of the BM sample before isolation of BM cells. From this point, magnetic enrichment using StraightFrom® Whole Blood and Bone Marrow CD138 MicroBeads (Miltenyi, Bergisch-Gladbach, Germany) was performed according to the suppliers manual. In brief, cell suspensions were mixed and incubated with StraightFrom® Whole Blood and Bone Marrow CD138 MicroBeads, unbound microbeads were removed by washing and centrifuging, and labeled cells were separated from unlabeled cells over Whole Blood columns (Miltenyi) located in a magnetic field of a MACS® Separator (Miltenyi). $CD138^-$ fractions were obtained by collecting the flow-through of the labeled cell suspensions with the magnetic column located within the magnetic field of a MACS® Separator. $CD138^+$ fractions were obtained by removing the magnetic column from the magnetic field and elution with elution buffer. To determine cell counts, cells were stained with DAPI (1:1000 dilution) and live lymphocyte counts were determined by volumetric measurement on a MACS Quant flow cytometer.

2.2.3. Flow cytometry staining

Viable ex vivo PC were counted using the MACSQuant Analyzer. Cells were spun down (300 x g, 4°C, 10min), supernatant was removed, and up to $2x10^7$ cells were resuspended in 100 µl PBE. Prior to antibody staining, cells were incubated with FcR blocking reagent (Miltenyi Biotech) for 10 min on ice. Then,

antibodies were added and cells were incubated for 15 min at 4 – 8°C in the dark. To remove unbound antibodies, 1 ml PBE was added to the stained cells, cells were spun down (300 x g, 4°C, 10min), supernatant was removed and cells were resuspended in 200 µl PBE for analysis with the MACSQuant Analyzer. Immediately before analysis, cells were stained with DAPI (1:1000) for exclusion of dead cells.

Table 3 of materials and methods: Antibody staining panel for flow cytometry analysis and FACS-sorting of ex vivo BMPC subpopulations for bulk RNA sequencing.

Specificity	Clone	conjugate	dilution
Anti-human CD3	BW264/56	VioBlue	1:20
Anti-human CD16	REA423	VioBlue	1:10
Anti-human CD38	HIT2	BV 510	1:50
Anti-human CD138	44F9	FITC	1:20
Anti-human CD45	HI30	PE	1:20
Anti-human HLA-DR	L243	PerCP	1:20
Anti-human CD19	HIB19	Pe-Cy7	1:100
Anti-human CD56	AF12-7H3	APC	1:50
Anti-human CD10	97C5	VioBlue	1:11
Anti-human CD14	TÜK4	VioBlue	1:200

2.2.4. Fluorescence-activated cell sorting

$CD138^+$ MACS-enriched BM cells were sorted on either a BD FACSAria or Sony MA900. For bulk RNA sequencing, target cells were directly sorted into Eppendorf tubes containing 350µl Qiagen RLT buffer and stored at -80°C until RNA isolation. For Fluorospot experiments, target cells were sorted into Eppendorf tubes coated with standard RPMI medium. FACS sorting strategy generally started with a lymphocyte gate and exclusion of cell doublets, followed by gating of $CD138^+$and $CD38^{high}$ cells. Then followed gating onto $CD3^-$ $CD10^-$ $CD14^-$ $CD16^-$ $DAPI^-$ cells to exclude unwanted lymphocytes and dead cells. This BMPC population was then further divided by gating onto $CD19^{+/-}$, $CD45^{+/-}$ and $CD56^{+/-}$ BMPC subpopulations. For bulk RNA sequencing and Fluorospot experiments, the following subpopulations were sorted: $CD19^+$ $CD45^+$ $CD56^-$ (A), $CD19^-$ $CD45^+$ $CD56^-$ (B), $CD19^-$ $CD45^-$ $CD56^-$ (C), $CD19^-$ $CD45^-$ $CD56^+$ BMPC (D). For Fluorospot assays, $CD138^-$ $CD38^-$ cells were sorted in addition to serve as controls as non-ASC.

2.2.5. Stimulation assay

Total BM cells were acquired as described in 2.1.1. To identify live nucleated cells, $B2M^+$ $DAPI^-$ cells were counted on a MACS Quant Analyzer and the suspension was adjusted to $5x10^4$ to $9.6x10^4$ cells per sample (400 µl BM cells). Cells were then aliquoted appropriately and treated with combinations of Tofaticinib (50 nM) and IL-6 (50 ng/ml) for 15 min. The samples were then cryo-conserved by mixing with Smart Tube proteomic stabilizer (Smart Tube Inc.) (sample:stabilizer = 1:1.4), incubating for 12 min at room temperature and immediately freezing at -80 °C.

2.2.6. Mass cytometry analysis of stimulated BM cells

Cryo-preserved samples from the stimulation assay were thawed in a water bath (10 – 15 °C). The samples were then mixed with 5 ml 1x Thaw-Lyse Buffer (Smart Tube Inc.), incubated at room temperature for 10 min and centrifuged for 5 min at 700 x g. The cell pellet was resuspended in 10 ml 1x Thaw-Lyse Buffer, incubated at room temperature for 5 min and centrifuged for 5 min at 700 x g. Cells were then washed with CSM buffer twice by resuspending and centrifuging (5 min at 700 x g). Cells were counted on a MACS Quant analyzer. Cells were spun down (5 min at 700 x g), resuspended in a barcode antibody mix and incubated for 30 min at room temperature. Barcoding was used in order to be able to analyze multiple samples simultaneously in one CyTOF run. Each sample was labeled with a combination of B2M conjugated to two different metal isotopes, allowing for the separation of the samples as double positive cells in the analysis. Barcode staining was stopped by adding 3 ml CSM and centrifuging (5 min at 700 x g). This step was repeated with 2 ml CSM. Barcoded cells were resuspended in 300 µl CSM and pooled. For cell surface stainings, cells were spun down (5 min at 700 x g), blocked with Beriglobin (0.2 mg/ml) (10 min at room temperature), washed with 2 ml CSM (5 min at 700 x g), and incubated with 100 U/ml Heparin for 15 min at room temperature. Then the antibody mixture was added, the cell suspension was mixed and incubated for 30 min at room temperature. Cells were washed with 2 ml CSM twice, then cells were washed in 2 ml PBS twice and spun down (5 min at 700 x g). Stained cells were fixed with 4% formaldehyde solution by incubating for 10 min at room temperature. Cells were then spun down (5 min at 700 x g), resuspended in 100 % Methanol and incubated overnight at -80 °C. On the next day, cells were spun down, washed with 2 ml CSM and incubated with 100 U/ml Heparin for 15 min at room temperature. Intracellular staining antibody mixture was added to the cells and incubated for 60 min at room temperature. The cells were then washed with 2 ml CSM and again washed with 2 ml PBS (5 min at 700 x g). Stained cells were fixated with 2% formaldehyde solution for 10 min at room temperature. Cells were washed twice with PBS (5 min at 700 x g) and then stained with Iridium intercalator (1:500) for nuclear staining (20 min at room temperature). Cells were washed with CSM and washed twice with deionized water. Cells were filtered using a cell strainer (35 µm) and then counted using a MACS Quant Analyzer. Cell concentration was adjusted to 7.5 x 105 cells/ml in deionized water and supplemented with 10% EQ Four Element Calibration Beads. Cells were then acquired on a Helios instrument using a super sampler.

Table 4 of materials and methods: Metal-conjugated antibodies used for sample barcoding, surface and intracellular stainings. In house antibodies were kindly provided by Marie Burns, Axel Schulz, Heike Hirseland, Iiris Virta and Eva Holzhäuser.

Metal isotope conjugate	Specificity	clone	Supplier (catalogue no.)	dilution
Barcoding antibodies:				
104Pd	Anti-human B2M	2M2	In house	1:25
105Pd				
106Pd				
108Pd				
Surface antibodies:				
115In	Anti-human CD3	UCHT1	In house	1:100

140Ce	Anti-human CD14	RMO52		1:200
116Cd	Anti-human CD15	W6D3		1:25
195Pt	Anti-human CD20	2H7		1:100
209Bi	Anti-human CD38	HIT2		1:100
171Yb	Anti-human CD319	162,1		1:50
198Pt	Anti-human CD45	Hi30		1:100
Intracellular antibodies:				
155Gd	IRF4	3E4	Fluidigm (3155014B)	1:100
153Eu	pStat1	4a	Fluidigm (3153005A)	1:100
153Gd	pStat3	4/P-STAT3	Fluidigm (3158005A)	1:100
150Nd	pStat5	47	Fluidigm (3150005A)	1:100

2.2.7. Fluorospot assays

FACS-sorted cells obtained from FACS-sorting as described in 2.2.4 were applied in Fluorospot assays using the human IgG/IgA/IgM Fluorospot Kit (Mabtech). The obtained cell fractions were diluted in standard RPMI. One day prior to the assay, IPFL plates were coated with capture antigen solution and incubated at 4°C in a refrigerator overnight. The next day, plates were washed and blocked with RPMI + 10% FCS before incubation of the freshly obtained FACS-sorted cell fractions for 3 h at 37°C and 5% CO_2. Maximum 1000 cells per well were used as input for PC populations; for negative controls, $50x10^3$ $CD138^-$ $CD38^-$ cells were applied. Cells were then removed by washing, and immunoglobulin spots were detected using fluorescently labeled anti-IgG/-IgA/-IgM antibodies and analyzed using a Fluorospot reader (AID Autoimmun Diagnostika).

2.2.8. Bulk RNA sequencing

Ribonucleic acid (RNA) was isolated from FACS-sorted BMPC subpopulations (see 2.2.3 and 2.2.4) using RNeasy Plus Micro Kit (Qiagen, Hilden, Germany) and according to the provided manual. In brief, cells are lysed, genomic Deoxyribonucleic acid (DNA) is removed, and the RNA is purified and enriched. The obtained RNA was then analyzed regarding its quality using the Fragment Analyzer System and HS RNA 15nt Kit (Agilent Technologies, Germany), which determined RQN (RNA quality number), 28S/18S ratio and total concentration.

RNA sequencing was performed by Gitta Heinz (Mashreghi lab, DRFZ Berlin) and Katrin Lehmann (lab manager, DRFZ Berlin). Gene expression library preparation was performed with the Smart-Seq v4 mRNA Ultra Low Input RNA Kit (Takara Bio USA, USA) according to the manufacturer's instructions and using 9.5 µl of total RNA (up to 5 ng) as input. Following quality control using the HS NGS Fragment Kit (1-6000bp) (Agilent Technologies, Germany) and determining concentrations with the Qubit dsDNA HS Assay Kit (Invitrogen, USA), 1 ng of purified complementary DNA (cDNA) was used for library completion using the

Nextera XT library preparation kit (Illumina, USA). Paired-end sequencing (2x75nt) was performed using a High Output flow cell (150 cycles) on a NextSeq500 device (Illumina, USA).

Differential gene expression analysis was performed by Pawel Durek, Frederik Heinrich and René Riedel (DRFZ Berlin). In brief, Reads were mapped using HTseq [124], immunoglobulin genes were removed, and differential gene expression analysis was performed using DESeq2 [125].

2.2.9. Single cell RNA sequencing

Single cell sequencing experiments were performed in collaboration with Marta Ferreira Gomes, Gabriela Guerra and Mir-Farzin Mashreghi (all DRFZ Berlin).

Similar to the procedures described in 2.2.1 and 2.2.2, BM cells were isolated and magnetically enriched for $CD138^+$ cells, although in the first step of cell isolation, BM material was rinsed with chilled PBS/BSA/5 mM EDTA containing 2 µg/mL Actinomycin D which prevents dissociation-induced gene expression. Following magnetic enrichment, the buffering solution was changed from PBS/BSA/EDTA to PBS/BSA, thus avoiding EDTA in the final cell suspension because it may interfere with sequencing reagents. The cells were sorted on a Sony MA900 sorter using a Sony Sorting Chip LE-C32 Series-100um (Sony Biotechnology), and $CD138^+$ $CD38^{hi}$, $CD3^-$ $CD10^-$ $CD14^-$ $CD16^-$ single lymphocytes were sorted (see Table 5). After cell counting on a MACSQuant, cell concentrations were adjusted to the required concentrations for the 10x Genomics workflow (10x Genomics). The obtained cell suspensions were then captured for scRNA gene expression (GEX) and BCR/CiteSeq library preparation using the Chromium Single Cell 5' Library & Gel Bead Kit as well as the Single Cell 5' Feature Barcode Library Kit (10x Genomics) according to the manufacturer's instructions. Following cDNA amplication, CiteSeq libraries were generated separately using the Single Index Kit N Set A (10x Genomics). BCR target enrichment was performed using Chromium Single Cell V(D)J Enrichment Kit for Human BC (10x Genomics). Library quantification was performed using Qubit HS DNA assay kit (Life Technologies). Fragment sizes were determined with the Fragment Analyzer with the HS NGS Fragment Kit (1-6000bp) (Agilent). Sequencing was performed on a NextSeq2000 device (Illumina) applying the sequencing conditions recommended by 10x Genomics for libraries prepared with Next Gem Reagent Kits v2. NEXTSeq 1000/2000 P3 reagent kits (200 Cycles, Illumina) were used for 5' GEX and Cite-Seq libraries (read1: 26nt, read2: 90nt, index1: 10nt, index2: 10) and NEXTSeq 1000/2000 P3 reagent kits (300 Cycles, Illumina) were used for BCR libraries (read1: 151nt, read2: 151nt, index1: 10nt, index2: 10nt., 2% PhiX spike-in).

The single-cell transcriptome, isotype and somatic hypermutation bioinformatic analysis was kindly provided by Pawel Durek and Frederik Heinrich (Mashreghi research group, DRFZ Berlin). The data were analyzed using Loupe Browser v5.0 (10x Genomics).

Table 5 of materials and methods: Antibody staining panel used for enrichment of ex vivo BMPC for single cell sequencing.

Specificity	**Clone**	**conjugate**	**dilution**
Anti-human CD3	BW264/56	VioBlue	1:400
Anti-human CD10	97C5	VioBlue	1:11
Anti-human CD14	TÜK4	VioBlue	1:200

Anti-human CD16	VEP13	VioBlue	1:50
Anti-human CD38	HIT2	APC	1:25
Anti-human CD138	44F9	PE	1:50

2.2.10. Immunohistochemistry

2.2.10.1. FFPE BM specimens

BM biopsies, i.e., iliac crest trephine biopsy samples, were formalin-fixed and paraffin-embedded in the laboratory at the Institute of Pathology of the Unfallkrankenhaus Berlin, Germany. In brief, samples were immersed in 4% formaldehyde solution immediately after extraction and fixed for 24h at room temperature, followed by decalcification in 0.5M EDTA solution for 24h at 37°C. The further preparation, i.e., dehydration, paraffin-embedding and sectioning, followed standard histological procedures.

2.2.10.2. Pretreatment of BM sections for immunohistochemistry

Approximately 3 µm FFPE tissue sections were dewaxed and rehydrated by incubation in Xylene (2 x 5 min), followed by incubation in absolute ethanol (2 x 3 min), and 3 min in washing buffer. Antigen retrieval was performed with EDTA buffer (pH 9) in a pressure cooker (120°C for 1 min), and then sections were cooled down to approximately 85°C. After washing for 2 min in wash buffer, peroxidase block was performed (3% H_2O_2 in methanol) for 5 min. Then sections were washed in distilled water for 2 min before creating a hydrophobic barrier with a PAP pen (DAKO) and subsequently washing sections in wash buffer for 5 min.

2.2.10.3. Multiplex immunohistochemistry

Multiplex immunohistochemical stainings were performed by sequential rounds of immunohistochemistry using either ZytoChem Plus HRP Polymer Kit or ZytoChem Plus AP Polymer Kit (Zytomed systems, Germany). The first immunohistochemical staining was generally detected via horse radish peroxidase (HRP) which catalyzes the oxidation of DAB, resulting in a brown precipitate where the primary antibody had bound. The second and, if applicable, third immunohistochemical stainings were detected using alkaline phosphatase (AP) which reacts with chromogens, i.e., Permanent Blue (supplier) or FastRed (supplier), to yield blue or red precipitates, respectively, at the location of primary antibody binding. The staining procedure was performed according to the manufacturer's instructions. In brief, pretreated sections were treated at room temperature as follows:

- blocking solution (1 x 5 min)
- washing buffer (1 x 2 min)
- primary antibody (45 min in a humidity chamber)
- washing buffer (3 x 5 min)
- Postblock solution (20 min)
- washing buffer (3 x 5 min)

- respective enzyme-labelled Polymer (30 min)
- washing buffer (3 x 2 min)
- detection of antibody binding via a color-producing reaction

For washing steps, the cuvettes containing the sections were placed on a rocker. The first antibody staining was finalized by stopping the HRP reaction by immersion in distilled water once the desired staining intensity was obtained. Before continuing to the second antibody staining with the AP Polymer Kit, sections were washed in wash buffer for 2 min. After finalizing the second antibody staining by stopping the AP reaction by immersion in distilled water, sections were mounted using Glycergel Mounting Medium, Aqueous (DAKO Agilent). Sections were scanned using a Philips Ultra Fast Scanner and examined employing the Philips image management system (Philips, Netherlands).

2.2.11. Statistical analyses

Statistical analyses were performed using GraphPad Prism. Data were tested for normality, and the according test for parametric or non-parametric data was employed. Statistical analysis is specified individually in the figure legends.

3. Results

3.1. Plasma cells lacking surface expression of CD45 and expressing CD56 are part of the normal bone marrow plasma cell pool

The indications are increasing that LLPC that mediate humoral immunity for up to a lifetime are not uniform regarding their phenotype and biology [33,86,92]. PC heterogeneity may be relevant for understanding the basis of variable durabilities of immune memory in response to vaccination as well as for the development of therapies against autoreactive or malignant PC. We therefore aimed to further delineate phenotypic heterogeneity of PC of the human BM regarding CD19, CD45 and CD56 expression.

BM cells enriched for $CD138^+$ cells were analyzed by flow cytometry using the gating strategy illustrated in Figure 1. Since PC have particular light scatter and background fluorescence properties, the $CD138^+$ $CD38^{high}$ population was gated first to avoid that PC were mistakenly excluded from the analysis. Then, unwanted cells, dead cells and cell aggregates were excluded, and light scatter gating was applied [126]. Mature PC identity was ensured by exclusion of minor fractions of remaining $HLA\text{-}DR^+$ cells [127]. Staining of CD19, CD45 and CD56 detected populations with high and low expression of the three markers (henceforth termed $CD19^+$, $CD19^-$, $CD45^+$, $CD45^-$, $CD56^+$, $CD56^-$) (Figure 1).

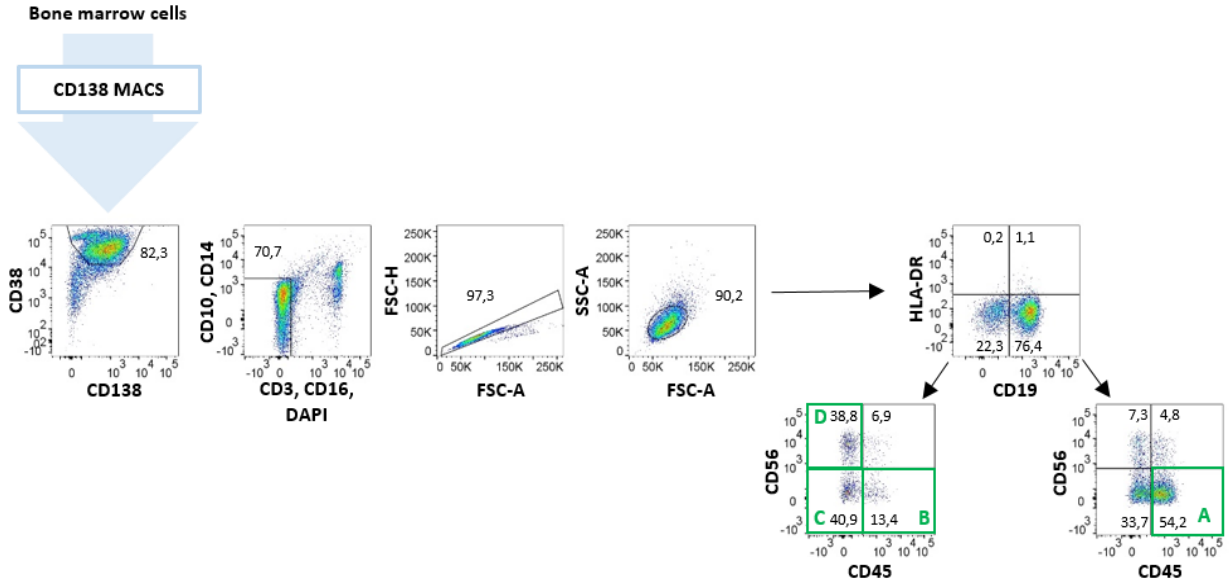

Figure 1: Flow cytometric analysis of heterogeneous *ex vivo* BMPC. Exemplary illustration of the gating strategy revealing heterogeneity of BMPC for one representative donor is shown. After magnetic enrichment for $CD138^+$ BM cells, $CD138^+$ $CD38^{hi}$ cells were gated, followed by removal of unwanted cells by exclusion of $CD3^+$, $CD16^+$, $CD10^+$, $CD14^+$ and $DAPI^+$ cells; then doublets were excluded and, lastly, a light scatter gate was applied. $CD19^+$ and $CD19^-$ BMPC further divided onto eight $CD45^{+/-}$ and $CD56^{+/-}$ combinatorial populations. Numbers indicate frequencies of parent populations. Green boxes indicate FACS-sorted populations used in Fluorospot assays and bulk RNA sequencing.

BMPC consistently showed bimodal expression of CD19, CD45 and CD56 in all analyzed donors (N=19) albeit numbers of the populations varied (Figure 2A). On average, 40% of human BMPC were $CD19^-$, while frequencies ranged from 9% to 98%. On average 38% were $CD45^-$, ranging from 9% to 55%, and 19% were $CD56^+$, ranging from 1% to 79% (Figure 2A). Therefore, we find a heterogeneity of BMPC which consistently occurs in normal human BM.

3.2. Non-canonical human bone marrow plasma cells lacking CD45 and expressing CD56 are significantly enriched among CD19$^-$ bone marrow plasma cells

Given that CD19-negativity is associated with PC longevity and conferral of systemic immune memory, and CD45-negativity was also associated with a longer lifetime of SIPC [86,93], we were interested in how the heterogeneity regarding CD45 and CD56 was within CD19$^+$ and CD19$^-$ populations, respectively. We detected CD45$^{+/-}$ and CD56$^{+/-}$ BMPC among both CD19$^+$ and CD19$^-$ populations. With average frequencies of 61% ± 22 and 37% ± 19, respectively, CD45$^-$ BMPC and CD56$^+$ BMPC were both significantly enriched among CD19$^-$ BMPC compared to CD19$^+$ BMPC (Figure 2B).

When analyzing the distribution of combinatorial subpopulations differentially expressing CD45 and CD56 among CD19$^+$ BMPC compared to CD19$^-$ BMPC, we identified eight distinct populations (Figure 2C). With regard to CD19$^+$ subpopulations, the majority of BMPC were CD45$^+$ CD56$^-$ with 64% ± 20 of CD19$^+$ BMPC. Thus, the majority of CD19$^+$ BMPC had the canonical PC phenotype. Of the remaining CD19$^+$ BPMC, 23% ± 10 were CD45$^-$ CD56$^-$, 9% ± 16 were CD45$^-$ CD56$^+$, and 5% ± 3 were triple positive, i.e. CD45$^+$ CD56$^+$.

The distribution was quite different within the CD19$^-$ BMPC compartment. With 36% ± 16, CD45$^-$ CD56$^-$ BMPC represented the largest fraction among CD19$^-$ BMPC. 26% ± 13 were CD45$^-$ CD56$^+$, and 11% ± 15 were CD45$^+$ CD56$^+$. Thus, non-canonical phenotypes prevailed among CD19$^-$ BMPC, and the remaining 28% ± 20 were CD45$^+$ CD56$^-$, resembling the canonical CD19$^+$ counterpart.

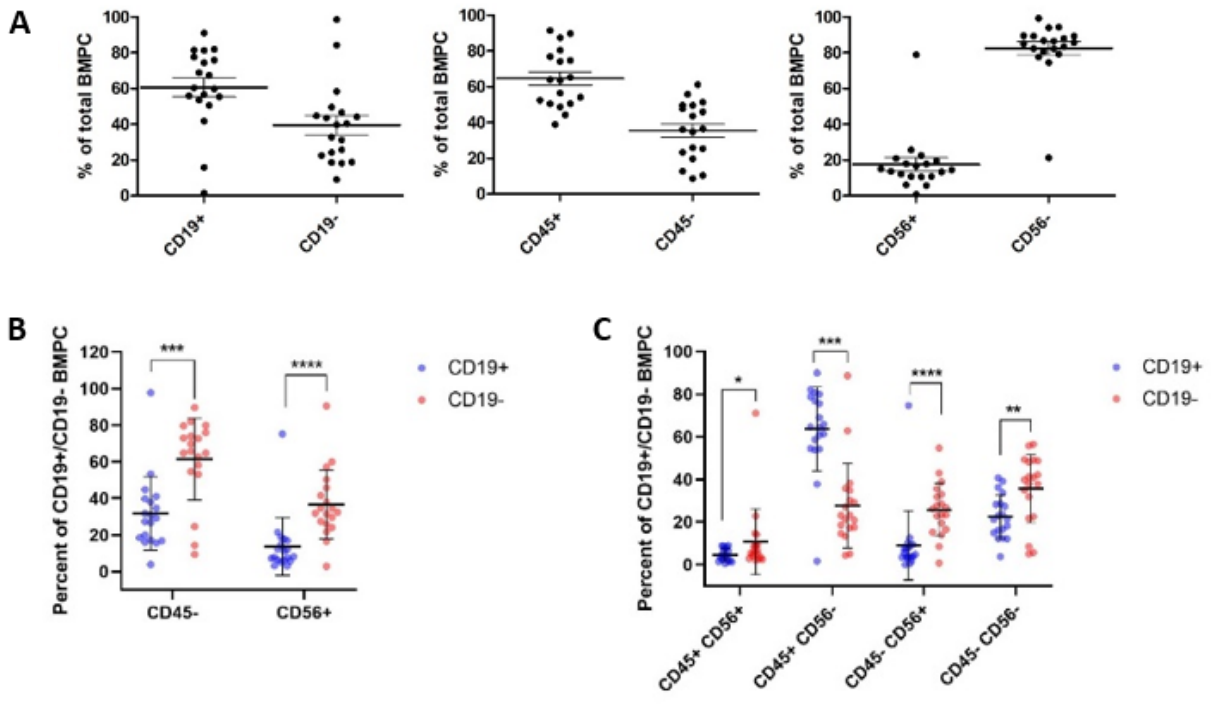

Figure 2: Newly identified, non-canonical human BMPC subsets lacking CD45 and expressing CD56 are significantly enriched among CD19- BMPC. A: Distributions of BMPC from 19 donors undergoing hip replacement surgery on to CD19$^{+/-}$, CD45$^{+/-}$ and CD56$^{+/-}$ subsets are shown as frequencies of total BMPC. On average, 1,8 x 10^4 BMPC were analyzed (cells analyzed: lowest value: 200; highest value: 2,6 x 10^5). B and C: Distributions of CD19$^+$ (blue) and CD19$^-$ (red) BMPC on to CD45$^{+/-}$ and CD56$^{+/-}$ phenotypes.

Statistical differences between $CD19^+$ and $CD19^-$ subpopulations were determined by Mann-Whitney U test (* $p<0.05$; ** $p<0.005$; *** $p<0.001$).

We conclude that, in addition to $CD19^+$ $CD45^+$ $CD56^-$ PC, PC with reduced CD45 expression, as well as gain of CD56 expression are constituents of the normal human PC pool in the BM. Furthermore, this analysis reveals that, compared to $CD19^+$ BMPC, the $CD19^-$ BMPC compartment contains a relatively higher heterogeneity regarding the analyzed surface markers. This is suggestive of functional heterogeneity within the two compartments.

3.3. Non-canonical $CD38^{hi}$ $CD138^+$ cell populations contain Ig secreting plasma cells

To verify that the newly described subpopulations of $CD38^{hi}$ $CD138^+$ $CD19^-$ BM cells lacking expression of CD45 as well as those expressing CD56 are functional ASC, we performed Fluorospot experiments of FACS-sorted, representative subpopulations from two donors as indicated by the green boxes in Figure 1 (Figure 3). The analyzed subpopulations were of the following phenotypes: **A**: $CD19^+$ $CD45^+$ $CD56^-$ BMPC; **B**: $CD19^-$ $CD45^+$ $CD56^-$ BMPC; **C**: $CD19^-$ $CD45^-$ $CD56^-$ BMPC; **D**: $CD19^-$ $CD45^-$ $CD56^+$ BMPC. The Fluorospot assay allows simultaneous detection of IgA, IgM and IgG secretion by single cells, and results in one detected spot per secreting cell.

Although overall spot counts varied between the two analyzed donors, spots were detected in all four FACS-sorted populations. While spot counts were fairly comparable in between the analyzed groups in donor #1, in donor #2 these numbers varied considerably in between the analyzed subpopulations (Figure 3). For donor #1, on average 16% of sorted cells, and for donor #2, on average 44% of sorted cells were spot forming cells. FACS sorting efficiencies were on average approximately 60%, thus frequencies of spot forming units probably represent an underestimate of the true PC frequencies. We conclude that all FACS-sorted populations analyzed here contain ASC. Moreover, we found that all Ig isotypes appear to be present in all BMPC phenotypes although, interestingly, our data also indicate that $CD56^+$ BMPC are enriched for IgG expressing cells.

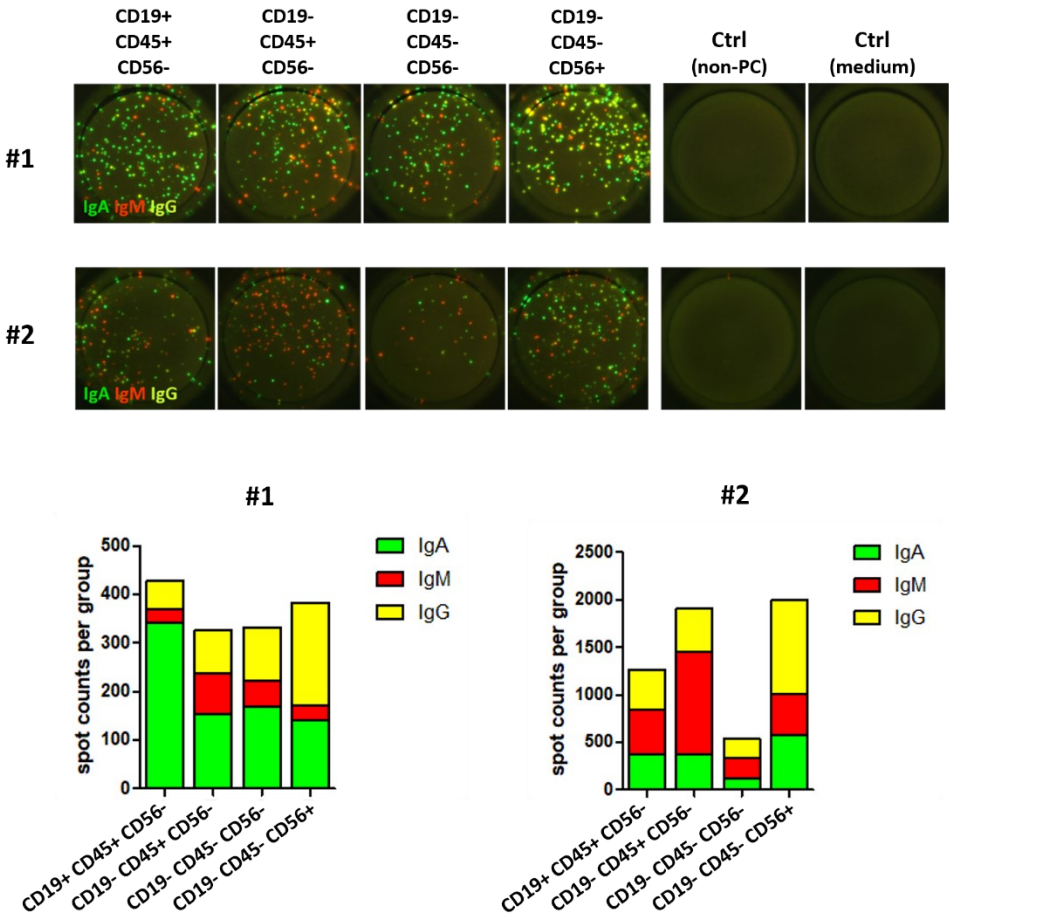

Figure 3: CD38hi CD138^{+} BM cells lacking expression of CD19 and CD45 and expressing CD56 are functional ASC. Upper panel: Representative images of detected IgA (green), IgM (red) and IgG (yellow) spots as overlay images. As controls, FACS-sorted CD138^{-} CD38^{low} cells (non-PC) or medium only were used. Lower panel: IgA, IgM and IgG spots are shown as spot counts per group.

3.4. Characterization of bone marrow plasma cell distribution *in situ* by histology

The finding of a heterogeneity of human BMPC raised the question how the different BMPC phenotypes were distributed in the BM *in situ*, and whether BMPC may have different microenvironments depending on their phenotype. To this end, we performed immunohistochemical analyses of FFPE BM sections to analyze the microenvironments of the newly described BMPC populations.

3.4.1. MUM1/IRF4 identifies bone marrow plasma cells

In order to study the distribution and environment of BMPC using immunohistochemical staining, we first analyzed whether the PC transcription factor MUM1/IRF4 reliably identifies BMPC. Double labeling immunohistochemistry combining the detection of MUM1/IRF4 with either CD138, a surface marker for PC [128], or CD319 [63,129], were performed, and MUM1/IRF4-positive cells were analyzed regarding positivity or negativity of the two surface PC markers (Figure 4). 87% ± 4 of MUM1/IRF4-positive cells were

CD138-positive, and 90% ± 11 were CD319-positive, demonstrating that the vast majority of MUM1/IRF4^{+} cells in the BM identify as PC. Moreover, double positive cells displayed morphological features of PC, i.e., often ovoid in shape and with eccentrical nuclei. We further showed that MUM1/IRF4 does not detect other BC and TC by analyzing MUM1/IRF4 co-staining with CD20 and CD3. 98% ± 2 and 99% ± 1 of MUM1/IRF4^{+} cells were negative for CD20 and CD3, respectively (Figure 4). In conclusion, this confirms that MUM1/IRF4 is a specific marker for BMPC.

We further examined the expression of Ki67 on BMPC as an indicator of proliferation. We co-stained Ki67 with the surface PC markers CD138 and CD319, and quantification of Ki67-positive and negative cells referring to CD138^{+} and CD319^{+} cells demonstrated that 98% (SD=1) and 99% (SD=1), respectively, were Ki67^{-}. We thus conclude that the majority of BMPC are resting in terms of proliferation and, therefore, represent mature BMPC.

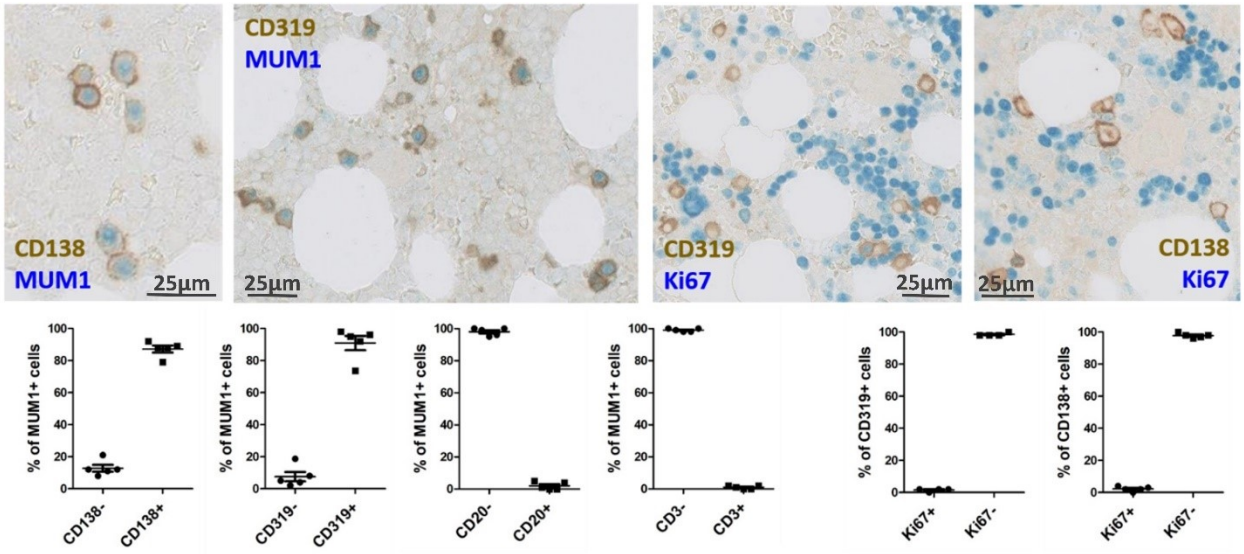

Figure 4: MUM1/IRF4 identifies BMPC via immunohistochemistry. Images show double immunohistochemistry of PC markers co-stained with validation markers. Top panel: representative images of co-staining of nuclear MUM1 (blue) with and surface CD138 or CD319 (brown), or co-staining of Ki67 (blue) with CD319 and CD138 (brown). Lower panel: quantification of single- and double-positive cells using combinations of PC markers with CD20, CD3 and Ki67 to validate that the majority of MUM1+ cells is CD138+, CD319+, CD20-, CD3-, Ki67- and thus reliably identifies mature PC. FFPE BM sections from 5 patients with normal BM were analyzed, 100 cells per section were quantified.

3.4.2. Immunohistochemistry identifies non-canonical BMPC *in situ*

We next co-stained MUM1/IRF4 with CD19 and CD45 in order to examine the relation between BMPC phenotypes and localization in the BM. We found that 75% ± 11 of BMPC were CD19^{-} and 68% ± 7 were CD45^{-} (Figure 5).

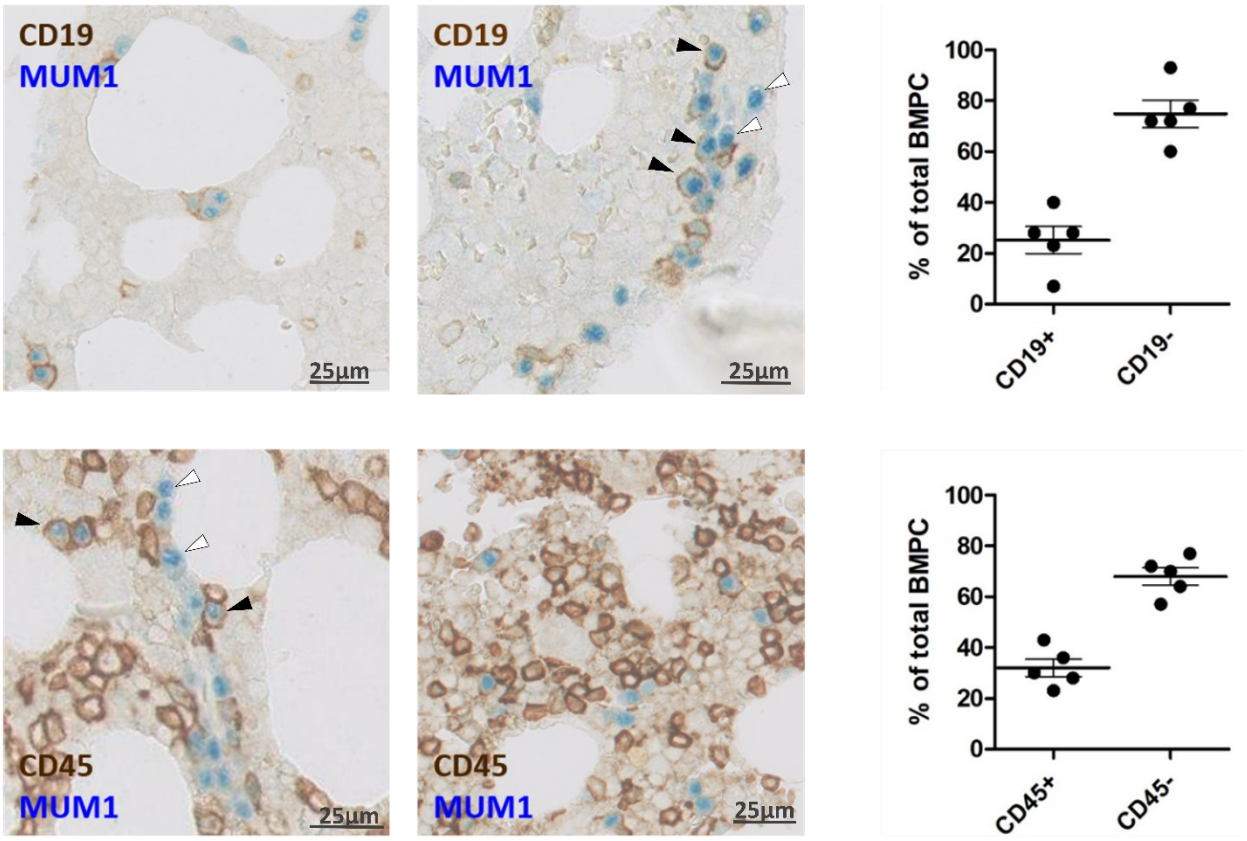

Figure 5: Immunohistochemistry detects differential expression of CD19 and CD45 on BMPC *in situ*. Upper panel: Representative images of double immunohistochemistry of MUM1 (blue) and surface CD19 expression (brown). Two images showing different areas from one section from one BM donor. Black arrows: Double positive cells. White arrows: $MUM1^+$ $CD19^-$ or $CD45^-$ cells. Lower panel: Representative images of double immunohistochemistry of MUM1 (blue) and surface CD45 expression (brown). The two images show areas of sections from two different BM donors. On the far right of each panel, the quantification of positive and negative BMPC for each marker are shown. FFPE BM sections from 5 patients with normal BM were analyzed, 100 cells per section were quantified.

Co-staining of MUM1/IRF4 and CD56 surface expression did not identify $CD56^+$ BMPC to similar extents as observed in flow cytometry (Figure 6; also see Figure 2). Only very few, if any, BMPC displayed visible CD56 signals (on average 2%), and these, in turn, were very weakly positive (Figure 6). Thus, they could not be sensitively identified for a reliable analysis. The clearly $CD56^+$ osteoblasts lining BM trabecula served as positive staining control. An example of one of few weakly $CD56^+$ BMPC in comparison to $CD56^-$ BMPC is illustrated in Figure 6.

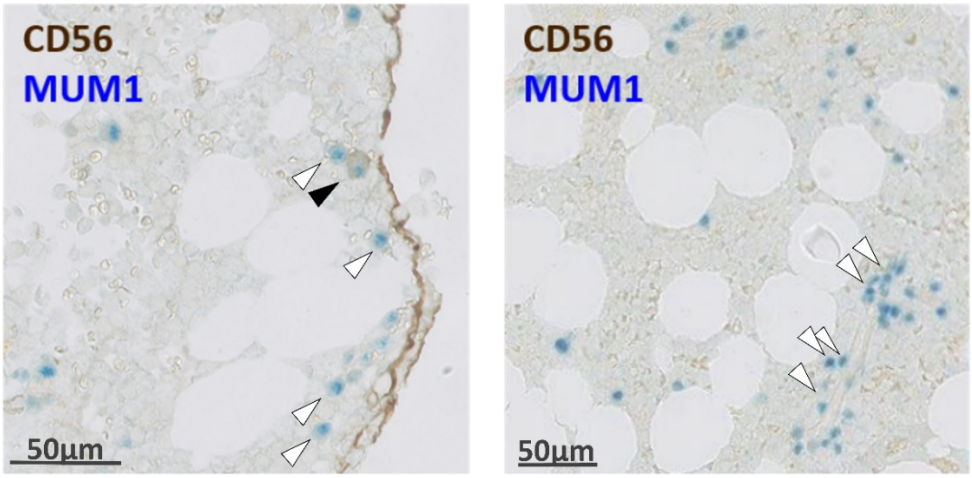

Figure 6: CD56 expression is not sensitively detected on BMPC by immunohistochemistry. Representative images of double immunohistochemistry of MUM1 (blue) and surface CD56 expression (brown). Black arrow: MUM1$^+$ with weak CD56 staining. White arrows: MUM1$^+$ CD56$^-$ cells. Two images showing areas from sections from two BM donors. FFPE BM sections from 5 patients with normal BM were analyzed.

3.4.3. A large fraction of bone marrow plasma cells co-localizes to blood vessels and perivascular bone marrow plasma cells are significantly enriched for CD45$^-$ cells

During the previous analyses, it became apparent that BMPC are not evenly distributed throughout the BM. We regularly observed not only solitary BMPC but also accumulations of BMPC, suggestive of association with vascular structures (see Figure 5). To investigate whether BMPC indeed localize to the perivascular area, we co-stained MUM1/IRF4 with CD34, a marker for vascular endothelial cells, and quantified frequencies of BMPC in direct vicinity of blood vessels. For standardization, only BMPC immediately proximate to CD34-positive structures, i.e., without space or another cell between BMPC and vessel, were considered perivascular. On average, 41% ± 8 of all BMPC were perivascular (Figure 7A and C).

Next, we analyzed expression of CD19 and CD45 in perivascular and non-perivascular BMPC by staining MUM1/IRF4 and CD34 combined with either CD19 or CD45 (Figure 7B and 7D). We found that frequencies of CD19$^+$ and CD19$^-$ BMPC did not vary between the two locations, with 83% ± 5 CD19$^-$ perivascular BMPC and 84% ± 9 CD19$^-$ non-perivascular BMPC. On the other hand, CD45$^-$ BMPC were significantly enriched among perivascular BMPC, with on average 88% ± 7 CD45$^-$ perivascular BMPC compared to 66% ± 14 non-perivascular BMPC. Based on these data, we conclude that there is an association between perivascular localization and CD45-negativity of BMPC.

Although we were not able to identify sufficient numbers of CD56$^+$ BMPC by immunohistochemistry, the very few weakly positive CD56$^+$ BMPC we did find did not localize to perivascular sites (Figure 6). Instead, perivascular BMPC appeared to be CD56$^-$ (Figure 6, left image), suggesting that CD56$^+$ BMPC reside in a different anatomical site of the BM with a putatively different microenvironment.

In summary, these findings document a relation between CD45 expression on BMPC and localization in BM compartments, supporting the notion that distinct PC subsets may inhabit different BM environments.

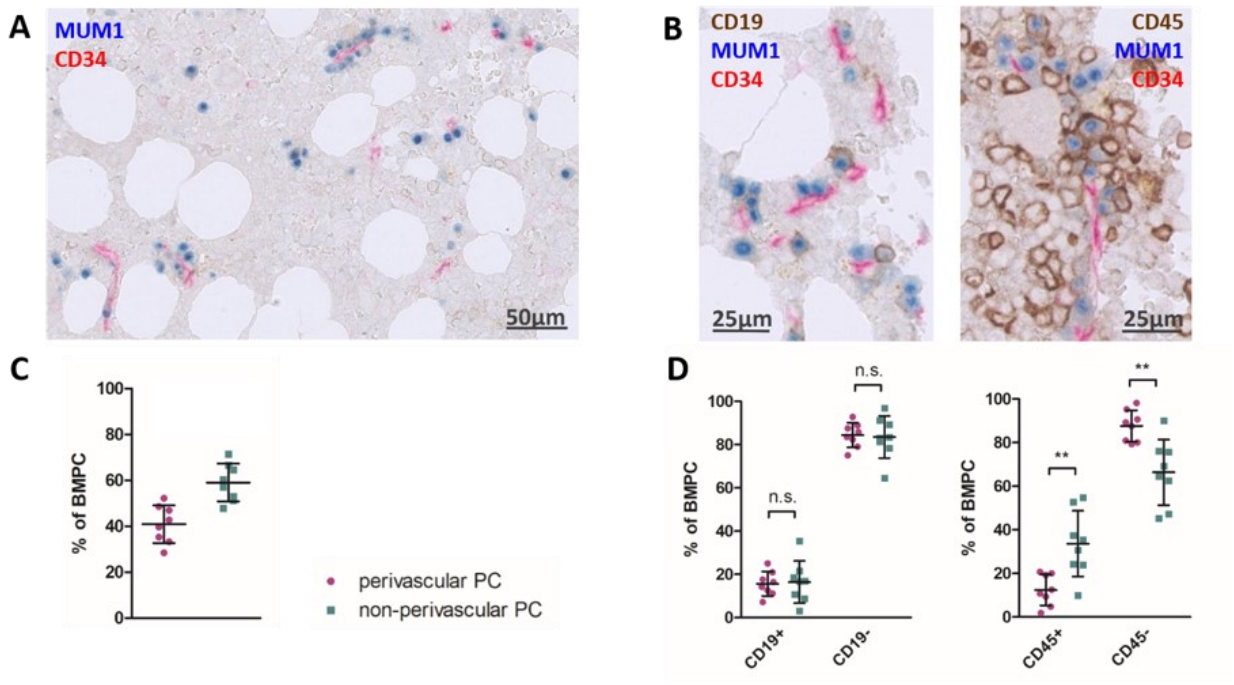

Figure 7: 40% of BMPC co-localize to blood vessels and perivascular BMPC are significantly enriched for CD45⁻ BMPC. A: Representative image of double-immunohistochemical staining on FFPE BM section. MUM1⁺ BMPC (blue) and CD34+ endothelium of blood vessels (red) in human BM. B: Representative images of triple immunohistochemical staining of MUM1⁺ BMPC (blue), CD34⁺ endothelium of blood vessels (red) and CD19⁺ or CD45⁺ cells (brown) in human BM. C. In average, 41% of BMPC co-localized to blood vessels. N = 8 patients with normal BM (≥300 cells per section) were analyzed. D. N = 8 patients with normal BM (≥300 cells per section) were analyzed. In average, 88% of perivascular BMPC were CD45⁻ and 66% non-perivascular BMPC were CD45⁻. Statistical differences were determined using Mann-Whitney U test (** p=0.0011).

3.5. Correlation of pSTAT1 with CD45-negativity upon stimulation with IL-6

It has been described that CD45 can act as an inhibitor of JAK-STAT signaling [113]. Therefore, we analyzed whether CD45⁻ BMPC showed higher responsiveness to IL-6, a pro-inflammatory cytokine that is known to signal via the JAK-STAT signaling pathway [130]. IL-6 has positive effect on PC survival and antibody production [45], and endothelial cells were shown to be capable of producing IL-6 [131,132]. We hypothesized that CD45-negativity may provide a survival advantage to BMPC and that their accumulation close to BM vasculature may act as a stabilizing factor of this BMPC subpopulation.

Ex vivo total BM cell suspensions were incubated with or without IL-6 ("+IL6" or "-IL6") as well as the JAK-inhibitor Tofaticinib and were analyzed by mass cytometry (Figure 8). PC were gated as CD38^{hi} CD319⁺ IRF4⁺ CD3⁻ CD20⁻ CD14⁻ CD15⁻ cells (Figure 8A). IL-6 stimulation induced pSTAT1 and pSTAT3 in BPMC, and Tofaticinib clearly inhibited induction of these pSTATs (Figure 8B). No effect of IL-6 or Tofaticinib was seen for pSTAT5. Spearman correlation of BMPC pooled from five donors revealed a significant but minute negative correlation between pSTAT1 and CD45 expression in both unstimulated and stimulated samples. Additionally, this negative correlation increased slightly in stimulated compared to unstimulated pools. pSTAT3 did not correlate with CD45.

In sum, IL-6 stimulation expectedly induced pSTAT1 and pSTAT3 although CD45-negativity correlated only with pSTAT1 induction.

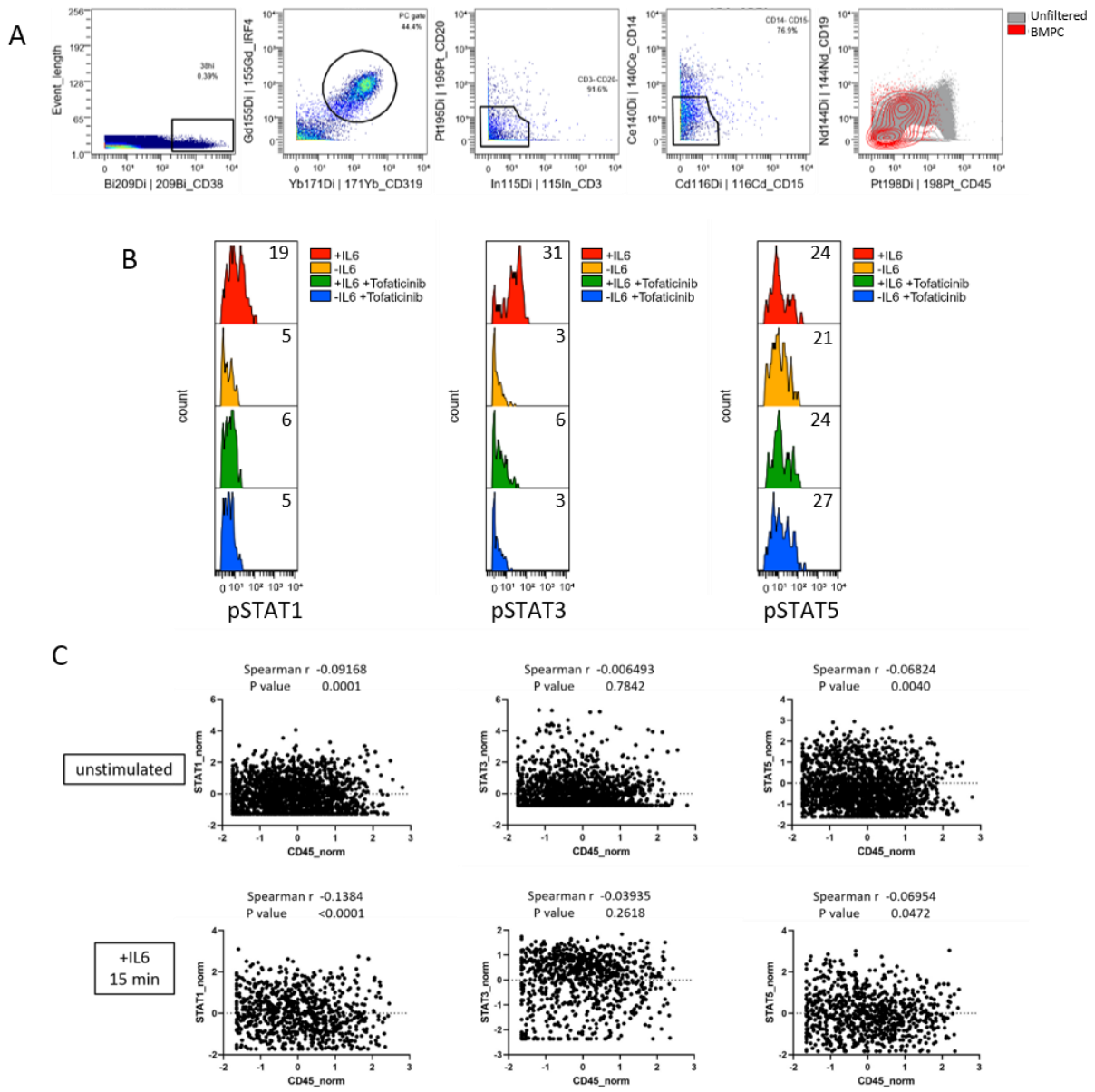

Figure 8: Stimulation with IL-6 induced pSTAT1 and pSTAT3, and pSTAT1 induction correlated negatively with CD45 expression. A: Stimulated BMPC were analyzed via CyTOF and gated as $CD38^{+}$ $CD319^{+}$ IRF-4^{+} $CD3^{-}$ $CD20^{-}$ $CD14^{-}$ $CD15^{-}$ cells. Data are concatenated from five donors. B: pSTAT1 and pSTAT3 protein levels were elevated upon IL-6 stimulation and inhibited by Tofaticinib. Numbers indicate mean signal intensities. Representative data from one donor are shown. C: Spearman correlation analysis of CD45 and pSTAT1/3/5 in unstimulated and stimulated BMPC. Data from five donors were concatenated and z-normalized. The total cell count available for analysis was 1781 (unstimulated) and 815 (stimulated) cells.

3.6. Transcriptional analysis of representative bone marrow plasma cell subsets

We next addressed the question whether the newly described BMPC phenotypes defined transcriptionally different, and therefore putatively functionally different, subpopulations. To this end, we FACS-sorted CD138-enriched BM cells into $CD19^{+}$ $CD45^{+}$ $CD56^{-}$ and $CD19^{-}$ $CD45^{+/-}$ $CD56^{+/-}$ BMPC populations as indicated in (Figure 1). This was done for four donors undergoing hip replacement surgery, and the obtained cells were then sequenced and differential gene expression analysis was performed. Due to very low RNA concentration in one sample of one donor (group D), this data point is missing in this analysis.

3.6.1. Transcriptional profiles of bone marrow plasma cell populations confirm their PC identity

In order to verify the identity of the FACS-sorted PC populations, we examined their gene expression levels of several PC identity genes as well as genes encoding for surface markers that had been used for FACS-sorting (Figure 9). As expected for PC, expression levels for *SDC1* (CD138), *SLAMF7* (CD319), *PRDM1* (Blimp-1), *IRF4*, *XBP1* and *CD38* were relatively high and comparable in all groups. Interestingly, *SDC1* expression was significantly higher in groups C ($CD19^{-}$ $CD45^{-}$ $CD56^{-}$) and D ($CD19^{-}$ $CD45^{-}$ $CD56^{+}$) compared to A ($CD19^{+}$ $CD45^{+}$ $CD56^{-}$), and in group D compared to B ($CD19^{-}$ $CD45^{+}$ $CD56^{-}$), and overall highest in group D. CD138 has been shown to enhace pro-survival cytokine signaling and is required for PC survival [47]. Furthermore, we found that expression levels of *MKI67* were mostly very low, indicating that the cells included in the analysis were resting in terms of proliferation. Expression levels for the BC transcription factor *PAX5*, as well as *CD3D* (CD3 delta chain), *MME* (CD10), *CD14* and *FCGR3* (CD16) which encode for the surface markers used for exclusion of unwanted lymphocytes were generally relatively low and comparable in all groups. Expression levels of *CD19*, *PTPRC* and *NCAM1* confirmed the identity of the FACS-sorted BMPC subpopulations on the transcriptional level. Taken together, the examined gene expression reflected BMPC identity as well as FACS-sorted phenotypes.

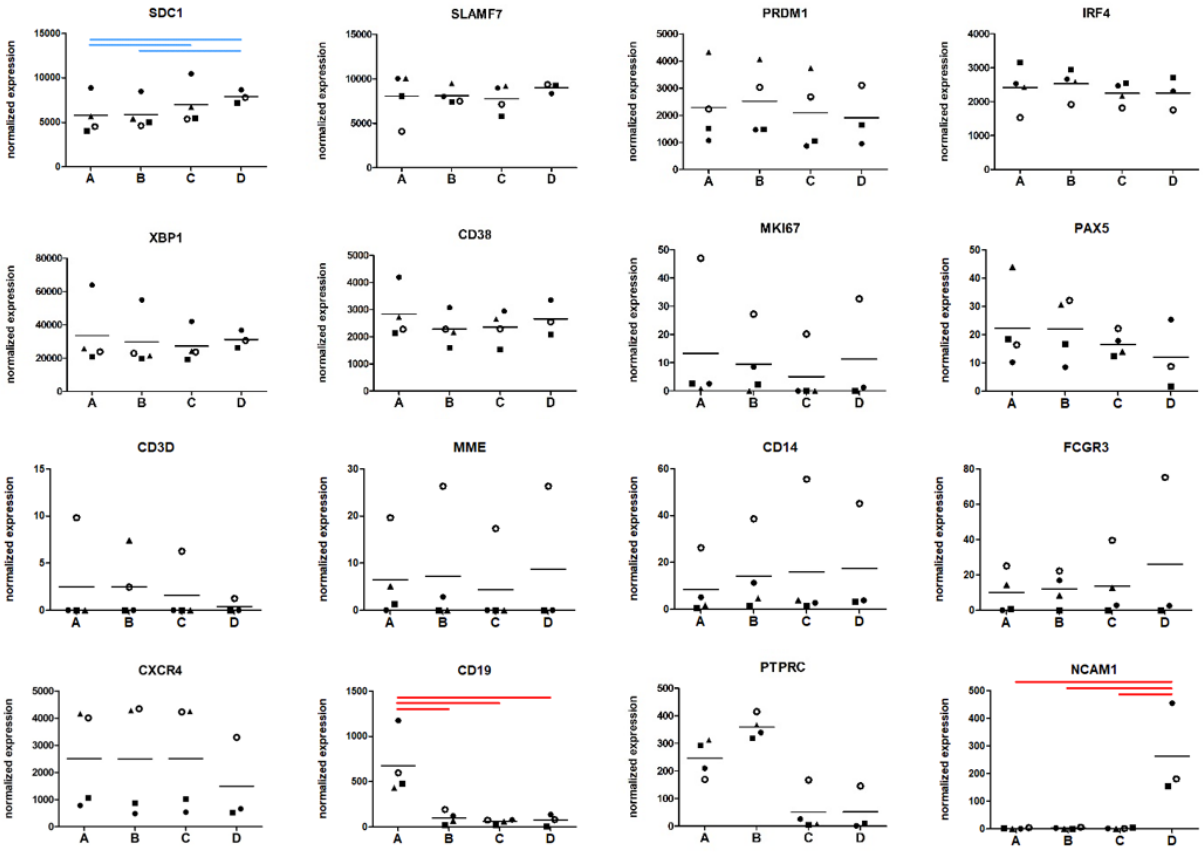

Figure 9: Gene expression profiles confirm general PC and subpopulation identity. Plots show gene expression for individual donors (indicated by different symbols) as well as averages (horizontal lines). A: CD19^{+} CD45^{+} CD56^{-}; B: CD19^{-} CD45^{+} CD56^{-}; C: CD19^{-} CD45^{-} CD56^{-}; D: CD19^{-} CD45^{-} CD56^{+}. Colored lines indicate significant (adjusted p-Value < 0.05) and differential gene expression (blue: fold change > 1.3; red: fold change > 2).

3.6.2. Transcriptional diversity of bone marrow plasma cells is largely associated with CD19 expression

Differential gene expression analysis comparing all four groups with one another revealed 802 differentially expressed genes (DEG) (FC>2; padj < 0.05). The majority of DEG were upregulated in the CD19^{-} groups (B, C, and D) (Figure 10). Regarding the numbers of DEG upregulated in CD19^{-} groups (B, C and D) vs. CD19^{+} group (A), transcriptional diversity increased from the CD19^{-} CD45^{+} CD56^{-} BMPC group (417 DEG), over the CD19^{-} CD45^{-} CD56^{-} group (481 DEG), to the CD19^{-} CD45^{-} CD56+ group (485 DEG), indicating that transcriptional diversity slightly increased from B to D in a gradual manner (Figure 10A). Similarly, the numbers of DEG that were upregulated in group A (CD19^{+} CD45^{+} CD56^{-}) compared to groups B, C and D also increased, again illustrating a small but consistent, gradual increase of diversity between CD19^{+} and CD19^{-} PC populations. Nevertheless, CD19 status seemed to be the major parameter for transcriptional BMPC diversity in the present analysis, and transcriptional heterogeneity among the three CD19^{-} BMPC groups was relatively low.

A

	A	B	C	D
A	0	178	205	278
B	417	0	79	173
C	481	190	0	145
D	485	273	152	0

B

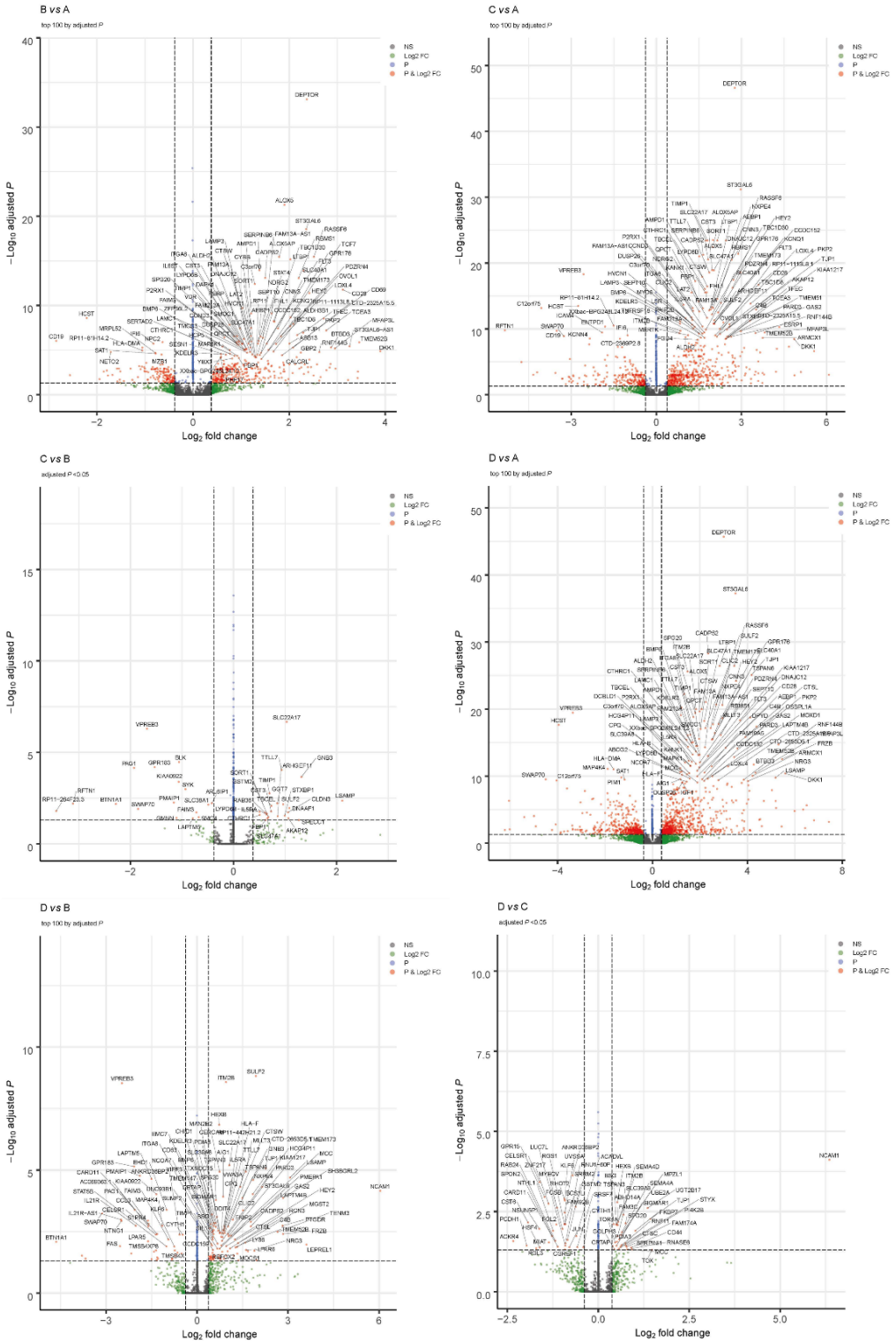

Figure 10: Transcriptional diversity of BMPC subpopulations is largely determined by CD19 surface expression. A: Numbers of genes upregulated in the group on x-axis compared to the group on the y-axis. A: $CD19^+$ $CD45^+$ $CD56^-$; B: $CD19^-$ $CD45^+$ $CD56^-$; C: $CD19^-$ $CD45^-$ $CD56^-$; D: $CD19^-$ $CD45^-$ $CD56^+$. B: Volcano plots of $\log_2$ fold change versus inverted $\log_{10}$ adjusted p-value for each pairwise comparison between the four analyzed BMPC groups.

3.6.3. Gene expression levels of intrinsic maintenance factors of plasma cells

We next examined the transcriptome data for gene expression levels of known intrinsic factors of PC maintenance and survival. The expression data was filtered for fold changes greater than 1.3, 1.7 and 2 individually, as well as significance (adjusted p-value smaller than 0.05).

3.6.3.1. Survival and chemotaxis receptors

TACI and BCMA are the receptors for BAFF and APRIL on PC, and binding of APRIL to either of them induces the anti-apoptotic factor Mcl-1 while downregulating the pro-apoptotic factor Bim, therefore promoting PC survival [18,46,48]. *TNFRSF13B* which encodes for TACI was significantly upregulated in $CD19^-$ $CD45^+$ $CD56^-$ (B) and $CD19^-$ $CD45^-$ $CD56^-$ (C) BMPC compared to $CD19^+$ $CD45^+$ $CD56^-$ (A) (FC > 1.3) (Figure 11).

Furthermore, the chemokine receptor CXCR3, implicated in recruitment of PC to inflammatory niches via its ligand CXCL9, CXCL10 and CXCL11, was transcriptionally significantly downregulated in the CD45-negative groups (C and D) (Figure 11). Considering that it was published that PC lose chemotactic responsiveness towards ligands for CXCR3 and CXCR4 when they arrive in the BM [16], one can speculate that expression is lower in $CD45^-$ as a consequence of downregulation of this chemotactic receptor due to advanced maturity, or that these groups are less likely to home to inflammatory niches than their $CD45^+$ counterparts.

CD28 is a survival factor of long-lived PC [70,133] and was recently shown to support their survival through modulation of their metabolic program by upregulating IRF4 [72]. *CD28* transcript levels were significantly increased in $CD19^-$ BMPC groups, with highest levels in $CD45^-$ BMPC (C and D) (Figure 11). This finding is in line with previously reported higher CD28 protein levels in $CD19^-$ BMPC [92]. Elevated *CD28* expression may be interpreted as an indication of advanced maturity [69].

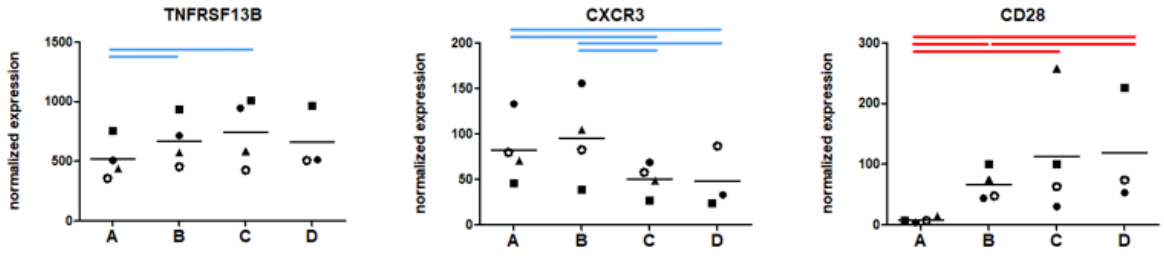

Figure 11: Gene expression levels of *TNFRSF13B*, *CXCR3* and *CD28* differentially expressed on BMPC. Plots show gene expression for individual donors (indicated by different symbols) as well as averages (horizontal lines). A: $CD19^+$ $CD45^+$ $CD56^-$; B: $CD19^-$ $CD45^+$ $CD56^-$; C: $CD19^-$ $CD45^-$ $CD56^-$; D: $CD19^-$ $CD45^-$ $CD56^+$. Colored lines indicate significant (adjusted p-Value > 0.05) and differential gene expression (blue: fold change > 1.3; red: fold change > 2).

3.6.3.2. Transcription factors

Zinc finger and BTB domain-containing protein 20 (Zbtb20), a transcriptional repressor promoted by IRF4, is presumed to play a role in long-term antibody responses by influencing PC survival by supporting anti-apoptotic Mcl-1 levels, and is expressed at its highest levels in mature, long-lived PC [63,74,75]. *ZBTB20* transcript levels were significantly increased in all $CD19^-$ BMPC populations (B, C and D) compared to the $CD19^+$ group (A) (Figure 12). The increased expression of *ZBTB20* may be due to a putative enhanced activity of IRF4, although, at the transcriptional level, it is expressed at comparable levels in all examined groups (see Figure 9).

Zinc finger and BTB domain-containing protein 32 (Zbtb32) is induced upon BC activation and was implicated in the regulation of memory BC recall responses [134]. In mice, secondary PC originating from *ZBTB32*-deficient memory BC have higher expression levels of cell cycle and mitochondrial genes, indicating that Zbtb32 restricts the extents of secondary responses. Zbtb32 is also implicated in PC differentiation due to its involvement in the silencing of crucial genes, such as MHC class II genes [135]. In our analysis, *ZBTB32* transcript levels are significantly decreased in $CD19^-$ BMPC populations compared to $CD19^+$ BMPC (Figure 12). The observed decrease in *ZBTB32* expression may be a feature of advanced maturity, as Zbtb32 has been implicated in PC differentiation and may not be of functional importance in mature PC.

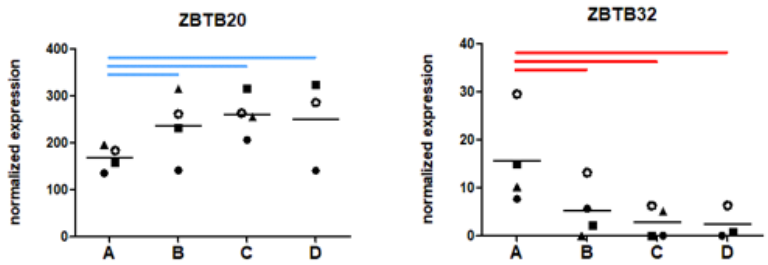

Figure 12: Transcription factors implicated in PC generation and maintenance. Plots show gene expression for individual donors (indicated by different symbols) as well as averages (horizontal lines). A: $CD19^+$ $CD45^+$ $CD56^-$; B: $CD19^-$ $CD45^+$ $CD56^-$; C: $CD19^-$ $CD45^-$ $CD56^-$; D: $CD19^-$ $CD45^-$ $CD56^+$. Colored lines indicate significant (adjusted p-Value > 0.05) and differential gene expression (blue: fold change > 1.3; red: fold change > 2).

3.6.3.3. Adhesion molecules

Since the expression of adhesion molecules is important for the embedding of BMPC in their niche, we examined the expression of known PC adhesion molecules (Figure 13). Some of the following genes are known for their involvment in BMPC positioning.

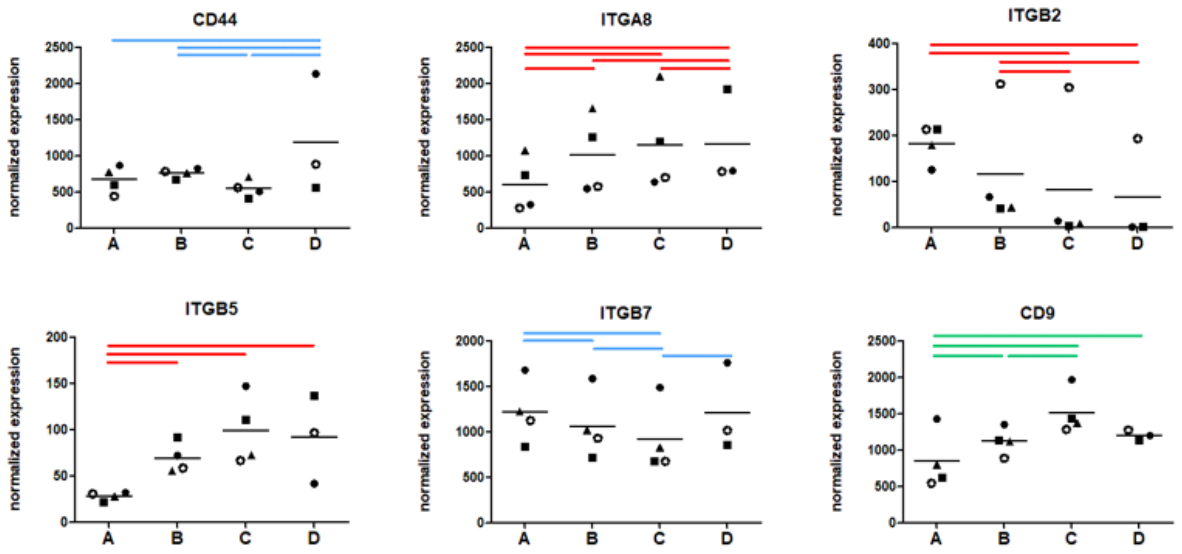

Figure 13: Gene expression levels of cell adhesion molecules. Plots show gene expression for individual donors (indicated by different symbols) as well as averages (horizontal lines). A: CD19$^+$ CD45$^+$ CD56$^-$; B: CD19$^-$ CD45$^+$ CD56$^-$; C: CD19$^-$ CD45$^-$ CD56$^-$; D: CD19$^-$ CD45$^-$ CD56$^+$. Colored lines indicate significant (adjusted p-Value > 0.05) and differential gene expression (blue: fold change > 1.3; green: fold change > 1.7; red: fold change > 2).

CD44 was significantly upregulated in CD19$^-$ CD45$^-$ CD56$^+$ BMPC (D) compared to CD19$^+$ CD45$^+$ CD56-(A), CD19$^-$ CD45$^+$ CD56$^-$ (B) and CD19$^-$ CD45$^-$ CD56$^-$ (C) BMPC (Figure 13). CD44 was implicated as a factor mediating survival of BMPC [45] and can interact with extracellular matrix proteins [136]. CD44 is a glycoprotein with several splice variants, of which CD44v3, v6 and v9 are known to be expressed on PC. Ligation of CD44v9 isoform to SC has been shown to induce IL-6 production by SC in the BM, indicating a putative modulation of the SC niche by PC [76].

CD9 gene expression was found to be upregulated in CD19$^-$ BMPC with highest expression in CD19$^-$ CD45$^-$ CD56$^-$ BMPC (C) (Figure 13). The member of the tetraspanin family, CD9, has been implicated in a wide range of cellular functions such as motility and adhesion, and is involved in so called tetraspanin-enriched microdomains by its ability to associate with a plethora of molecules, such as e.g. the integrin heterodimers VLA-4 (α4 β1), LFA-1 (αL β2), and CD44 [137]. CD9 may also be involved in supporting CD9$^+$ BC through the VLA-4/VCAM-1 axis in human tonsillar BC [138]. Therefore, the involvement of CD9 in supporting PC adhesion to its survival niche seems likely.

SC provide survival niches for PC in the BM which, in mice, is mediated by direct cell-cell contact and binding of VLA-4 (integrin α4β1) and LFA-1 (integrin αLβ2) to the stromal cell binding partners VCAM and ICAM, respectively [15,37]. In the present transcriptome analysis, four genes encoding for integrin αβ subunits were differentially expressed among BMPC groups (Figure 13). *ITGA8* and *ITGB5*, which both encode for integrins that recognize the tripeptide sequence RGD [139], were significantly upregulated in CD19$^-$ BMPC, and *ITGB7* was decreased in CD19$^-$ CD45$^+$ CD56$^-$ (B) and CD19$^-$ CD45$^-$ CD56$^-$ (C) BMPC but at comparable levels in CD19$^+$ CD45$^+$ CD56$^-$ (A) and CD19$^-$ CD45$^-$ CD56$^+$ BMPC (D). Although these three integrins are not known to be associated with a specific function in PC, they are generally able to mediate binding to fibronectin and extracellular matrix components [140], and thereby may convey overall stronger

retention properties. *ITGB2*, encoding for the β2 subunit of LFA-1, significantly decreased from group A ($CD19^+$ $CD45^+$ $CD56^-$) to D ($CD19^-$ $CD45^-$ $CD56^+$) in a gradual manner.

Overall, this modulation of integrin expression is suggestive of the residence of different BMPC populations in distinct microenvironments. These results also imply that the integrin expression in human PC may be different from those implicated in murine PC-stromal cell contact [15,37]. Whether these transcriptional differences between different BMPC phenotypes are the prerequisites for the inhabitation of possibly different BM microenvironments, or whether these are adaptations of the settling in such, remains to be elucidated.

3.6.3.4. Pro- and anti-apoptotic factors

Programmed cell death, or apoptosis, is controlled by an array of interactions between pro- and anti-apoptotic proteins of the Bcl-2 family. Apoptosis can be induced via an extrinsic pathway, i.e., in response to death stimuli via Fas, or via the intrinsic pathway, e.g., in response to endoplasmic reticulum stress. Both pathways ultimately intersect at the mitochondria where mitochondrial outer membrane permeabilization marks the tipping point upon which cytochrome c is released into the cytoplasm. From there, activated caspases exert their functions, resulting in elimination of the cell [65]. Differentially expressed gene for factors involved in the regulation of apoptosis are shown in Figure 14.

BIRC3, encoding for cellular inhibitor of apoptosis 2 (cIAP2) which can inhibit caspase activity [141], was upregulated in all $CD19^-$ BMPC groups. The gene encoding for effector caspase 3 (*CASP3*) was slightly downregulated in group C compared to A and D. *HRK*, encoding for activator of apoptosis harakiri which interacts with anti-apoptotic Bcl-2 members, was significantly downregulated in all $CD19^-$ BMPC and lowest expressed in group D [141,142]. The Bcl-2 family member *BCL2L1* which through alternative splicing can encode anti-apoptotic Bcl-XL or pro-apoptotic Bcl-XS was slightly downregulated in $CD19^-$ BMPC. The anti-apoptotic factor *MCL1* was also downregulated to rather small extent in $CD19^-$ BMPC, while pro-apoptotic *PMAIP1* (encoding for Noxa) was significantly decreased in $CD19^-$ $CD45^-$ groups. Although Mcl-1, implicated as an essential factor for PC survival [46], was decreased in $CD19^-$ BMPC, its only pro-apoptotic antagonist, Noxa, was also downregulated [142]. This indicates that downregulation of *MCL1* may not necessarily lead to a higher propensity to apoptosis. Overall, the stability of the different BMPC populations may ultimately be determined by protein expression and a complex balance of these and other factors. Yet, the observed differences are in sum suggestive of a differential regulation of apoptosis in which, dependent on the context, $CD19^-$ BMPC may be more resilient towards apoptosis based on, e.g., decreased expression of pro-apoptotic Casp3, Noxa and HRK, and elevated anti-apoptotic cIAP2.

The transcriptional downregulation of the death receptor *Fas* as well as its overall relatively low expression levels are in line with work showing that, in PC, apoptosis mainly occurs via the intrinsic pathway and the extrinsic pathway induced by engagement of Fas may not substantially contribute to PC death [64].

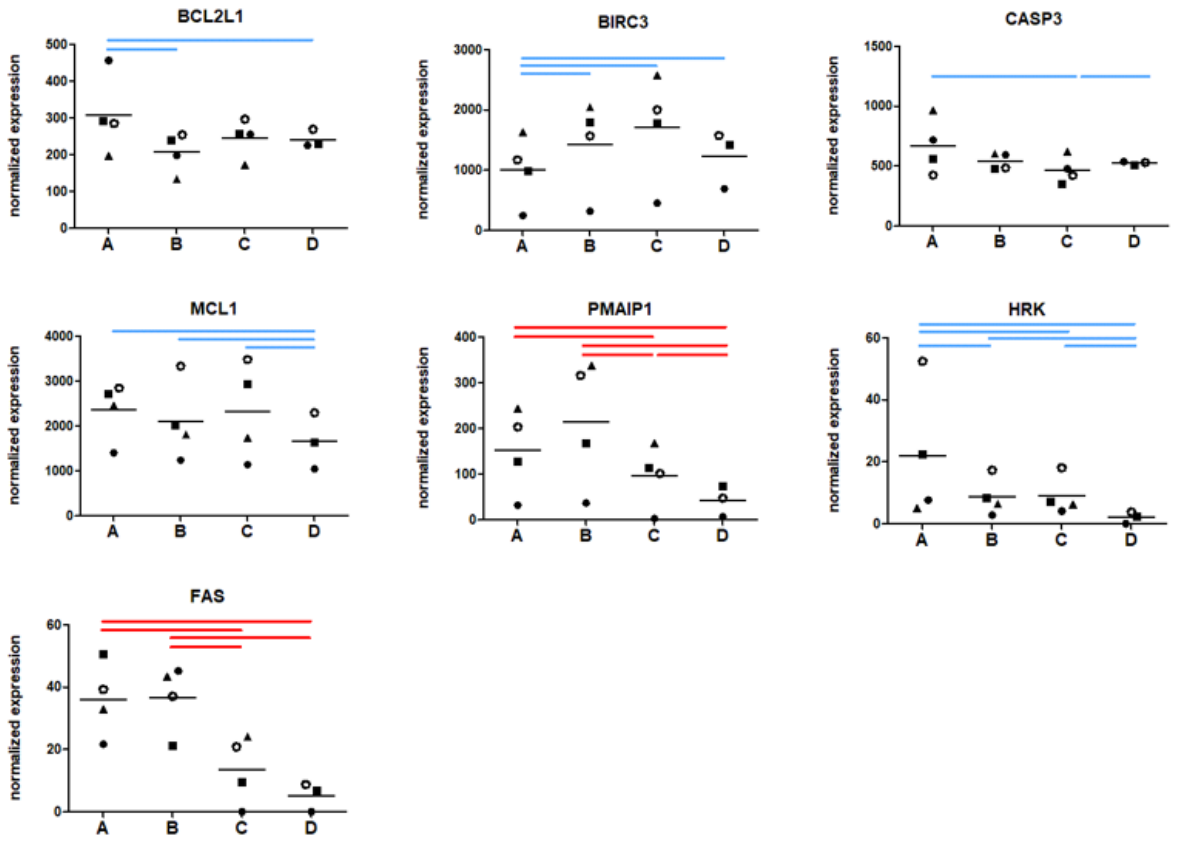

Figure 14: Gene expression levels of pro- and anti-apoptotic factors. Plots show gene expression of *BCL2L1*, *BIRC3*, *CASP3*, *MCL1*, *PMAIP1*, *HRK* and *FAS* for individual donors (indicated by different symbols) as well as averages (horizontal lines). A: $CD19^+$ $CD45^+$ $CD56^-$; B: $CD19^-$ $CD45^+$ $CD56^-$; C: $CD19^-$ $CD45^-$ $CD56^-$; D: $CD19^-$ $CD45^-$ $CD56^+$. Colored lines indicate significant (adjusted p-Value > 0.05) and differential gene expression (blue: fold change > 1.3; red: fold change > 2).

3.6.3.5. Solute carriers

Murine LLPPC have higher demands for glucose and it was published that this demand coincides with elevated surface expression of the glucose transporter Glut1 although transcript levels were similar [33,62]. Indeed, transcription of *SLC2A1* gene which encodes for Glut1 appeared to be at comparable levels among BMPC subsets (data not shown). We examined other members of the SLC2A family and found three of them to be significantly upregulated with a gradual increase from group A to D: *SLC2A5*, a fructose transporter, *SLC2A10*, a glucose/galactose transporter, and *SLC2A13*, a myo-inositol transporter [143] (Figure 15). Although it is not clear whether PC metabolize fructose, galactose and inositol, these findings are suggestive of metabolic adaptations to distinct anabolic or catabolic requirements. Whether human BMPC show differential glucose uptake and whether upregulation of *SLC2A10* may be linked with this process remains to be investigated.

We also found that the solute carrier gene *SLC7A1* was upregulated in $CD19^-$ BMPC (Figure 15). *SLC7A1* encodes for the amino acid transporter CAT-1, and its expression was shown to be induced by amino acid deprivation in rat C6 glioma cells and the human hepatoma cell line Huh7 [144]. A role for this amino acid

transporter in PC is not known, yet PC generally have high demands for amino acids as building blocks for antibodies.

Together, these data suggest that $CD19^+$ and $CD19^-$ BMPC differ in their available carriers for the uptake of nutrients and amino acids. Whether these carriers indeed lead to increased uptake of, e.g., glucose or amino acids, and whether this functional consequences for BMPC, e.g., higher rates of antibody secretion, remains to be investigated.

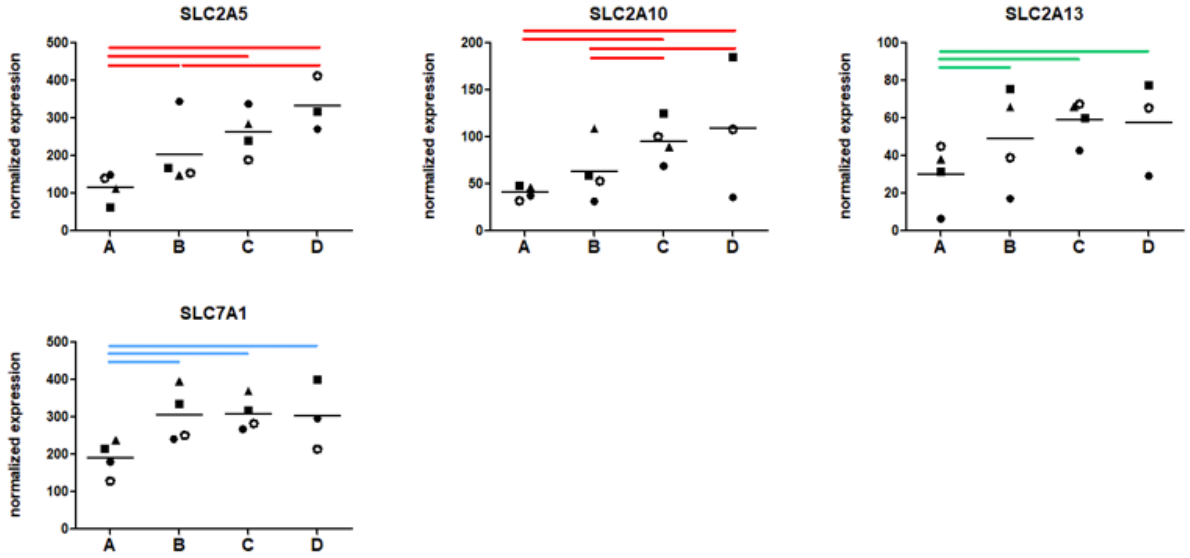

Figure 15: Gene expression levels of significantly, differentially regulated solute carriers in BMPC. Plots show gene expression of *SLC2A5*, *SLC2A10*, *SLC2A13* and *SLC7A1* for individual donors (indicated by different symbols) as well as averages (horizontal lines). A: $CD19^+$ $CD45^+$ $CD56^-$; B: $CD19^-$ $CD45^+$ $CD56^-$; C: $CD19^-$ $CD45^-$ $CD56^-$; D: $CD19^-$ $CD45^-$ $CD56^+$. Colored lines indicate significant (adjusted p-Value > 0.05) and differential gene expression (blue: fold change > 1.3; green: fold change > 1.7; red: fold change > 2).

3.6.3.6. Sphingosine-1 phosphate receptor 1 gene expression is downregulated in $CD45^-$ bone marrow plasma cells

We analyzed the present transcriptome data regarding further indications of the stage of maturity of the predominantly $CD45^-$, perivascular BMPC observed in our immunohistochemical study (see 3.4.3.). We examined gene expression levels of *AICDA*, encoding for activation induced deaminase, and *S1PR1*, encoding for the sphingosine-1 phosphate receptor 1. These factors are involved in CSR and SHM, and the emigration of ASC from secondary lymphoid organs, respectively, and, therefore, would be indicative of recent generation and immigration of BMPC into the BM [145,146]. *AICDA* was generally expressed at very low levels. *S1PR1* was expressed at relatively low levels overall, and, moreover, was significantly decreased in the $CD45^-$ groups C and D (Figure 16). Based on these observations, we reason that the predominantly perivascular $CD45^-$ BMPC are likely mature and not recently immigrated PC.

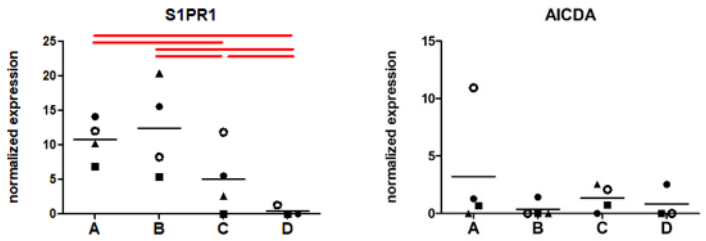

Figure 16: **Gene expression levels of *S1PR1* and *AICDA* in BMPC.** Plots show gene expression of *S1PR1* and *AICDA* for individual donors (indicated by different symbols) as well as averages (horizontal lines). A: $CD19^+$ $CD45^+$ $CD56^-$; B: $CD19^-$ $CD45^+$ $CD56^-$; C: $CD19^-$ $CD45^-$ $CD56^-$; D: $CD19^-$ $CD45^-$ $CD56^+$. Colored lines indicate significant (adjusted p-Value > 0.05) and differential gene expression (red: fold change > 2).

3.7. Single cell RNA and BCR sequencing of *ex vivo* bone marrow plasma cells

In addition to bulk RNA sequencing of selected $CD19^+$ and $CD19^-$ BMPC subpopulations (see chapter 3.6.), we examined the transcriptional diversity of the entirety of *ex vivo* BMPC in connection with Ig isotypes and somatic hypermutation rates of BCRs. To this end, *ex vivo* CD138-enriched BM cells from two donors (A: male, 75, and B: male, 50) were FACS-sorted for purification of $CD3^-$, $CD10^-$, $CD14^-$, $CD16^-$, $CD138^+$ $CD38^{hi}$ lymphocytes, and their transcriptomes and BCR repertoires were sequenced via 10X Genomics-based droplet sequencing.

3.7.1. Confirmation of plasma cell identity

Based on gene expression, BMPC clustered into 14 populations (Figure 17A). When split onto the two individual donors, we found that cluster 10 appeared to be enriched in donor A and few cells from donor B pertained to this cluster (Figure 17B). Clusters 11 and 12, on the other hand, seemed to be specific for donor B because only few cells from donor A clustered here. In general, all other clusters were present to comparable extents in both donors.

We next examined gene expression of PC identity markers and found that *PRDM1* was expressed in the majority of cells, and *SDC1* was also expressed at relatively high levels except for clusters 4 and 12 (Figure 17C). *MKI67* expression was absent in all clusters except from cluster 14, indicating that this cluster contains proliferative cells. The expression of BC genes *PAX5* and *MS4A1* was generally low but enriched in cluster 13. Furthermore, gene *MME* (CD10), which is expressed in BC precursors, was enriched in cluster 13 and 14. In sum, this indicated that cluster 0 to 12 represent BMPC, and cluster 13 and 14 showed traits of plasma blasts and BC precursors. Thus, we excluded cluster 13 and 14 from the further analysis.

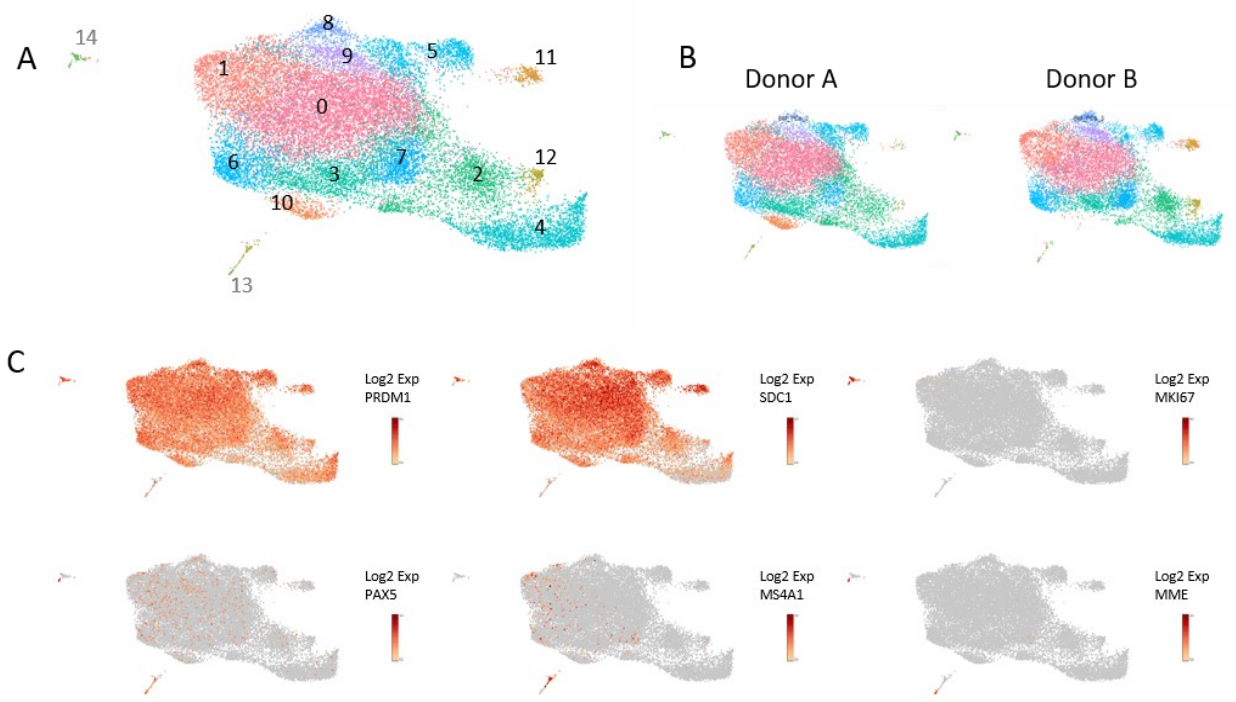

Figure 17: Single cell sequencing of BMPC from two donors. *Ex vivo* BMPC from two donors were FACS-sorted as $CD3^-$ $CD10^-$ $CD14^-$ $CD16^-$ $DAPI^-$ $CD138^+$ $CD38^{hi}$ cells and then sequenced with the 10x Genomics droplet sequencing. Figure shows data of both donors combined. A: Analyzed BMPC clustered onto 14 clusters as determined by clustering according to transcriptional data. B: Clusters split by donors reveal few donor-specific clusters. C: Gene expression of PC and BC identity genes. Figure shows data of both donors combined.

3.7.2. Identification of BMPC heterogeneity by single cell sequencing

Single cell RNA sequencing was combined with CITE-Seq technology for simultaneous cell surface protein phenotyping (Figure 18). While *CD19* gene expression levels revealed differences in transcript levels between the clusters, the lowest being in cluster 2, 3, 7 and 10, CITE-seq did not confirm this at the protein level. CD19 protein expression was noticeably low in cluster 7 but comparable in all other clusters. Transcript levels of *PTPRC*, encoding for CD45, were overall very low, apart for cluster 1 where cells with higher expression levels of this gene appeared to be enriched. On the protein level, CD45 was slightly reduced in cluster 0 and 2, and markedly lowest in cluster 7. Expression of *NCAM1*, encoding for CD56, was overall hardly detected, while CITE-seq identified cluster 7 as clearly enriched for CD56-expressing cells, and cluster 11 was also found slightly elevated for CD56 expression.

Overall, the non-canonical phenotypes observed by flow cytometry were in part confirmed in this independent approach using single cell sequencing combined with CITE-seq. We identified clusters enriched for cells with low *CD19* expression of which some also showed lower expression levels of CD45. Cluster 7 most strikingly resembled the non-canonical $CD19^-$ $CD45^-$ $CD56^+$ BMPC phenotype.

Regarding technical aspects, CD19 and CD45 CITE-Seq signals were unable to resolve differential expression as expected based on gene expression. This is probably due to technical issues as CITE-Seq

antibodies were not validated and titrated prior to analysis, thus antibody clones or titers may have been suboptimal.

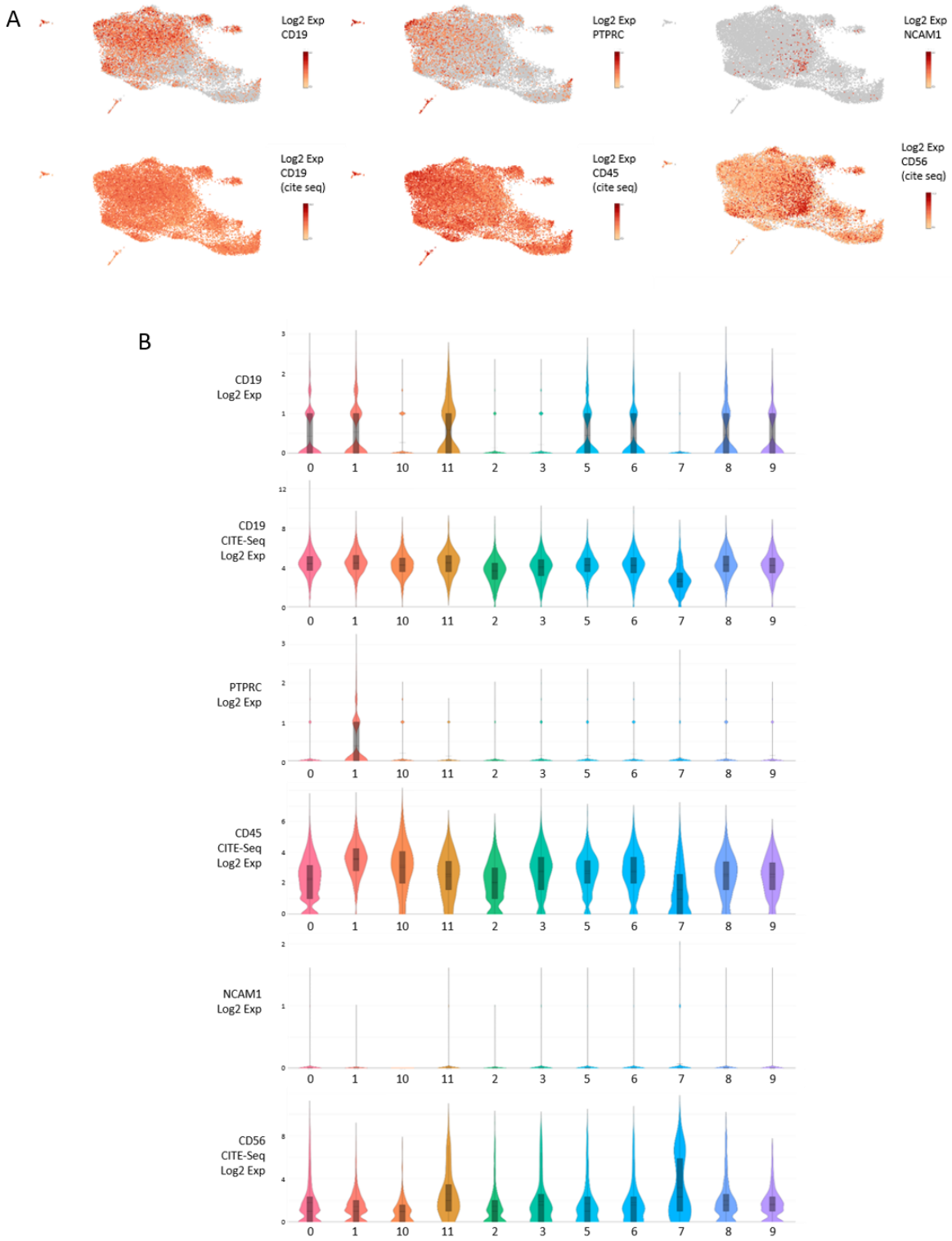

Figure 18: Transcript and protein expression levels of CD19, CD45 and CD56 detected by single cell RNA sequencing and combined CITE-Seq in BMPC clusters. A: Expression of *CD19*/CD19, *PTPRC*/CD45 and *NCAM1*/CD56 mapped onto BMPC clusters.

B: Violin plots display relative expression levels of transcripts for *CD19*, *PTPRC* and *NCAM1* genes as well as expression levels of the corresponding encoded proteins detected by CITE-Seq.

3.7.3. Isotype distribution

We examined the distribution of isotype subclass expression in the BMPC clusters. We found that clusters 4 and 12 predominantly contained cells which were not assigned (NA) to any isotype (Figure 19). These two clusters also displayed lower *SDC1* expression levels (see Figure 17), thus their PC identity is questionable. Based on these observations, we excluded these clusters from the further analysis.

Moreover, we found that cluster 3 seemed enriched for IgD^+ and IgM^+ BMPC compared to the other clusters. Interestingly, we also found that clusters 5 and 7 predominantly consisted of $IgG1^+$ BMPC, with cluster 7, the cluster previously identified as $CD19^-$ $CD45^-$ $CD56^+$, containing the overall largest fraction of IgG1+ BMPC. Moreover, the clear majority of cells in cluster 9 were $IgG2^+$ BMPC (Figure 19B).

When examining the Ig isotype distribution overall in the two donors individually, we found that donor A had approximately 5% IgD^+ BMPC while in the cells analyzed from donor B there were no IgD^+ cells at all. Apart from this, all other isotype classes were present in both donors, although to slightly different extents which can be considered a regular variation between human donors (Figure 19C).

In summary, this data confirms previous findings that $CD19^-$ BMPC are enriched for IgG^+ cells [92]. In addition, these data reveal that BMPC clusters based on transcriptional differences are in part linked with the enrichment of certain Ig isotypes, indicating that, to some extent, BMPC heterogeneity may be imprinted during their generation, e.g., through the instruction by cytokines leading to the expression of certain Ig isotypes. However, as not all BMPC clusters correlated with certain Ig isotypes, additional regulation of PC subset identity beyond cytokine instruction appears to exist.

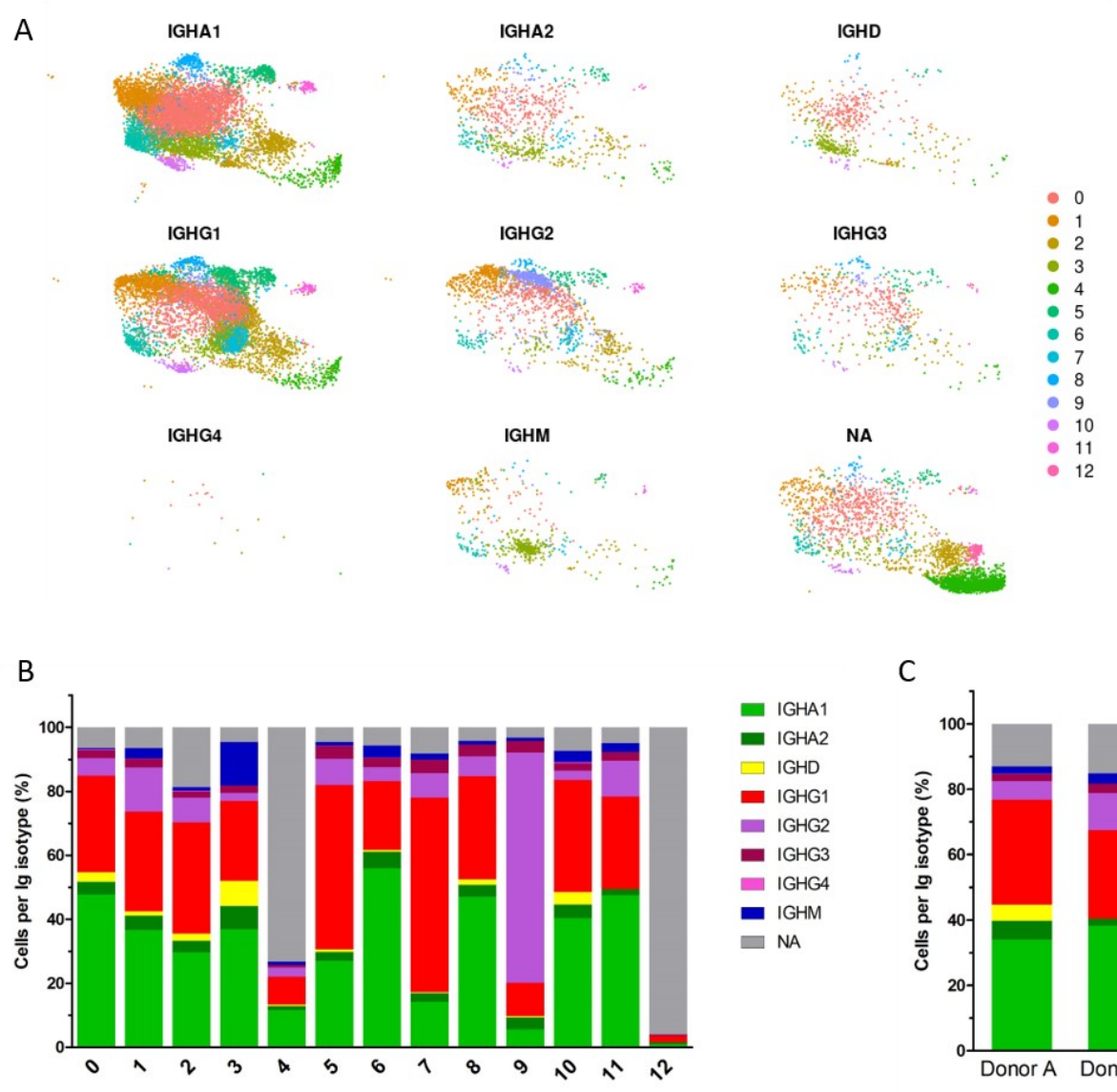

Figure 19: Distribution of immunoglobulin isotype subclasses. (A) Expression of immunoglobulin isotypes was determined by BCR sequencing and mapped onto clusters obtained from the analysis of single cell transcriptomes. NA: not assigned. (B) Isotype frequencies were calculated as percent of cells per cluster. (C) Ig isotype distribution are shown individually for the two donors as percent of cells per total cells analyzed.

3.7.4. Decreased somatic hypermutation rates are associated with CD56^{+} bone marrow plasma cells

The extent of SHM in PC may provide information on the conditions under which they were generated, for example, whether they may result from primary versus repeated immune response or even from responses in different points of an individual's lifetime as SHM rates may accumulate in memory BC successively [147,148]. Therefore, we compared SHM rates of the CDR-H3 and framework regions in the

identified BMPC clusters (Figure 20). We found that in both donors, BMPC in cluster 7 clearly had the lowest SHM rates in both CDR-H3 and framework region. BMPC in the remaining clusters displayed higher SHM rates, and there was a notable divergence in between the donors. In most clusters, donor B had higher SHM rates than donor A. This data confirm previous findings that $CD19^-$ BMPC have less mutated Ig genes [92], and they extend this data by identifying that CD56 expression is linked with lower SHM.

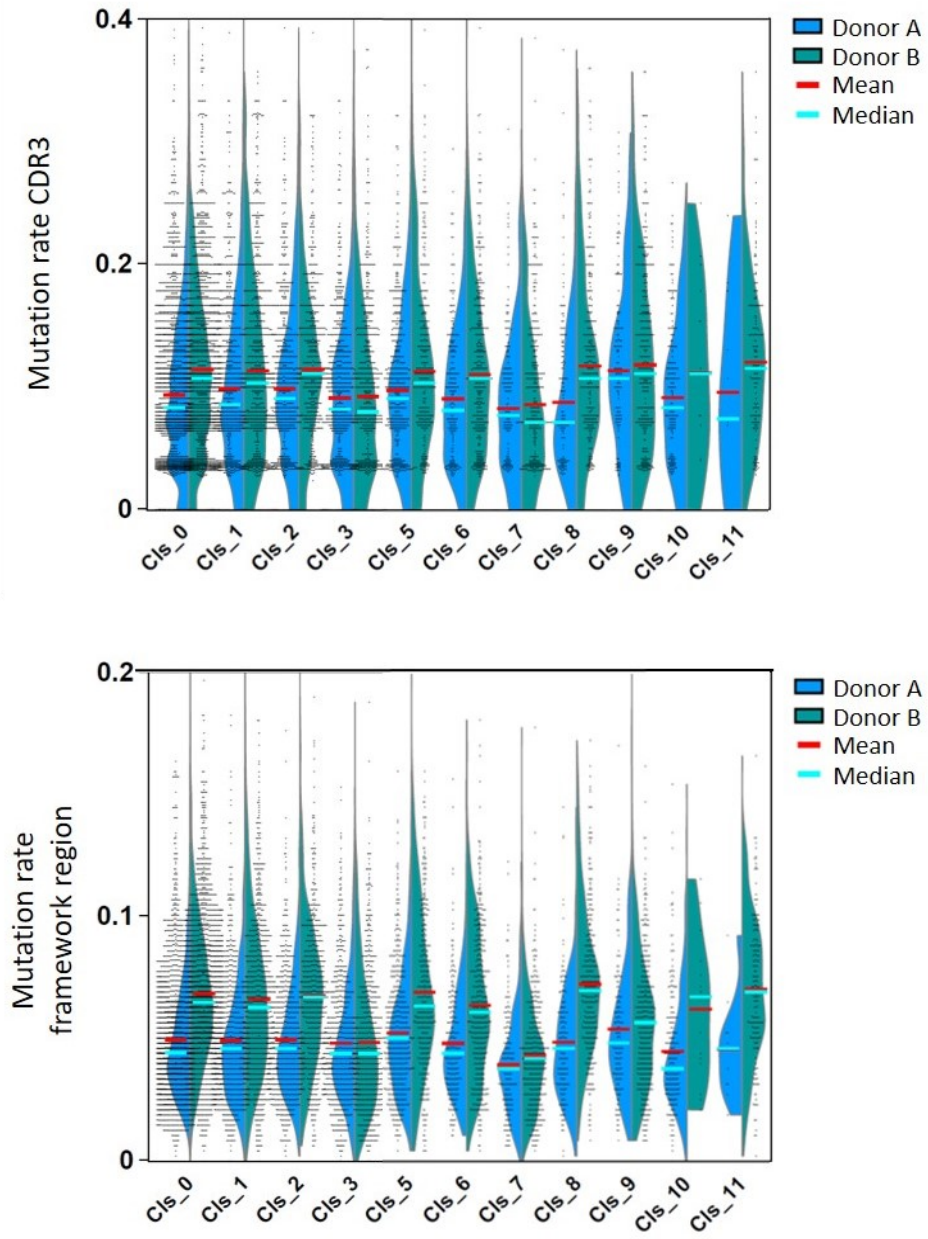

Figure 20: Somatic hypermutation rates in BMPC clusters ("Cls"). Somatic hypermutation rates are plotted per donor as the number of mutations by the length of the nucleotide sequence of the given region in heavy and light chain. The number of mutations was calculated by comparison to germline sequences. Data were kindly provided by Pawel Durek (DRFZ Berlin).

3.7.5. Metabolic genes define transcriptional heterogeneity of bone marrow plasma cells

Differential gene expression analysis was performed using cell loupe browser 5.1.0 (10X Genomics). Cluster 6 was transcriptionally the most diverse with 11 differentially expressed genes, followed by cluster 10 (seven DEG), cluster 11 (six DEG) and cluster 8 (five DEG) (Figure 21). Information on the function and putative relevance for BMPC is given in Table 6.

Cluster 1, which was found to be enriched for BMPC with elevated *PTPRC* expression, appeared to be enriched for cells at rather early stages of plasmablast to PC transition. This cluster showed elevated levels of *HLA-DPA1* and *CD74*, two MHC class II molecules, and *CD79A,* the signal transducing portion of the BCR, all of which are thought to be lost during BC differentiation into PC [127,149,150]. Due to the absence of *KI67* expression as well as enrichment of analyzed cells for *SDC1* expressing BMPC (Figure 17), we reason that these are terminal PC.

The highest number of transcriptionally upregulated genes appeared in cluster 6. Various genes with putative relevance for PC metabolism were upregulated in this cluster. *SLC3A2,* encoding for the heavy subunit of CD98, an amino acid transporter that has been shown to be elevated in long-lived PC [33], as well as *SLC1A5*, encoding for ASCT2, a Na^+-dependent amino acid transporter that mainly transports glutamine [151], were elevated here. PC can utilize glutamine not only for antibody synthesis but also for mitochondrial respiration [33]. Cells in this cluster upregulated *ERN1*, encoding for IRE1, one of the three ER stress sensors which, upon activation by accumulation of misfolded proteins, leads to expansion of ER size and function, and throttles entry of newly translated proteins through regulated IRE1alpha-dependent decay (RIDD) [152]. *WARS* encodes for tryptophanyl tRNA synthase (WRS), an enzyme that is essential during translation [153]. *ASS1* encodes for Argininosuccinate synthetase 1, an enzyme crucial for *de novo* synthesis of arginine [154]. *MTHFD2*, *SHMT2*, *PSAT1* and *PHGDH* encode for enzymes implicated in one carbon metabolism, a pathway that generates various molecules needed for protein biosynthesis as well as redox reactions [155]. *PSAT1* (phosphoserine aminotransferase) and *PHGDH* (phosphoglycerate dehydrogenase) carry out serine synthesis from glucose, *SHMT2* (mitochondrial serine hydroxymethyltransferase) converts serine into glycine, thereby providing amino acids as well as substrates for the folate cycle [156], and *MTHFD2* (mitochondrial methylenetetrahydrofolate dehydrogenase/cyclohydrolase) is involved in the mitochondrial formate cycle [157]. Although it is not known which role one carbon metabolism plays in PC, this observation is interesting because one carbon metabolism is discussed as a pathway integrating nutrient availability and biosynthetic capacity [158], and upregulation of its enzymes may represent a metabolic adaptation of PC with especially high nutrient or energy demands. Taken together, these upregulated genes highlight cluster 6 as a particularly specialized BMPC cluster which may be capable of producing elevated amounts of Ig molecules compared to other BMPC.

In cluster 7 which was enriched for $CD19^-$ and $CD56^+$ BMPC, *IL6ST* which encodes for glycoprotein 130, the common signal transducing receptor chain of IL-6 family receptors [130], was significantly upregulated. Moreover, the gene encoding for the cysteine protease cathepsin W, *CSTW*, was upregulated in this cluster. Cathepsins are important in autophagy, a process that is vital for PC [34,159]. The gene encoding for fructose-1,6-bisphosphatase 1 (FBP1), FBP1, was also upregulated in cluster 7. This enzyme is involved in glycogen synthesis and seems to negatively regulate glycolysis and glucose uptake in cancer cells [160,161]. Transcript levels of *CD9*, which encodes for the tetraspanin CD9, were also elevated. CD9 is a tetraspanin which can associate with adhesion molecules such as LFA-1, VLA-4 and CD44 in so-called tetraspanin-

enriched microdomains [137]. In addition, CD9 was found to be physically linked to CD19 and CD81 in BC at different points of differentiation, and it induced tyrosine phosphorylation in different proteins such as CD19, indicating a functional role in signal transduction [162,163]. CD9 was further implicated in promoting $CD9^+$ GC BC survival by interaction with follicular DC through the VLA-4/VCAM-1 axis [138]. In addition, CD9 is a common exosome marker [164]. *QPCT* encodes for glutaminyl-peptide cyclotransferase, an enzyme that catalyzes the formation of pyroglutamate from glutamine or glutamate of some peptides and proteins, a post-transcriptional modification that occurs on in secretory proteins such as immunoglobulins. It appears to have a stabilizing effect on proteins against degradation [165]. On the transcriptional level, cluster 7 shows adaptations in line with functions important for PC, such as autophagy and energy metabolism, and, moreover, the elevation of CD9 in this cluster may equip this BMPC group with additional means of adhesive contacts for the habitation of customized BM niches.

Various interferon-inducible antiviral genes were upregulated in cluster 8 (*OAS1, MX1, ISG15, IFITM1*) [166–169]. It is tempting to speculate that these BMPC derive from antiviral responses.

The elevated transcript levels of methallothionein genes (*MT1G, MT2A, MT1H, MT1X, MT1E*) and heat shock protein genes (*HSPA1A, HSPA1B, HSPA6, HSP90AA1, HSPB1*) indicates that cluster 10 and 11 contained cells that were adapting to high levels of metabolic stress. These factors are induced by ER stress as a coping mechanism, and heat shock proteins lead to degradation or salvation of damaged or misfolded proteins [170,171]. In general, the expression of these types of genes can be considered as a corollary of immense stress levels intrinsically tied to mass antibody secretion.

In summary, single cell sequencing of BMPC especially highlights the role for metabolic adaptations to the role of PCs as heavy-duty antibody secretors, and these also distinguish BMPC subpopulations.

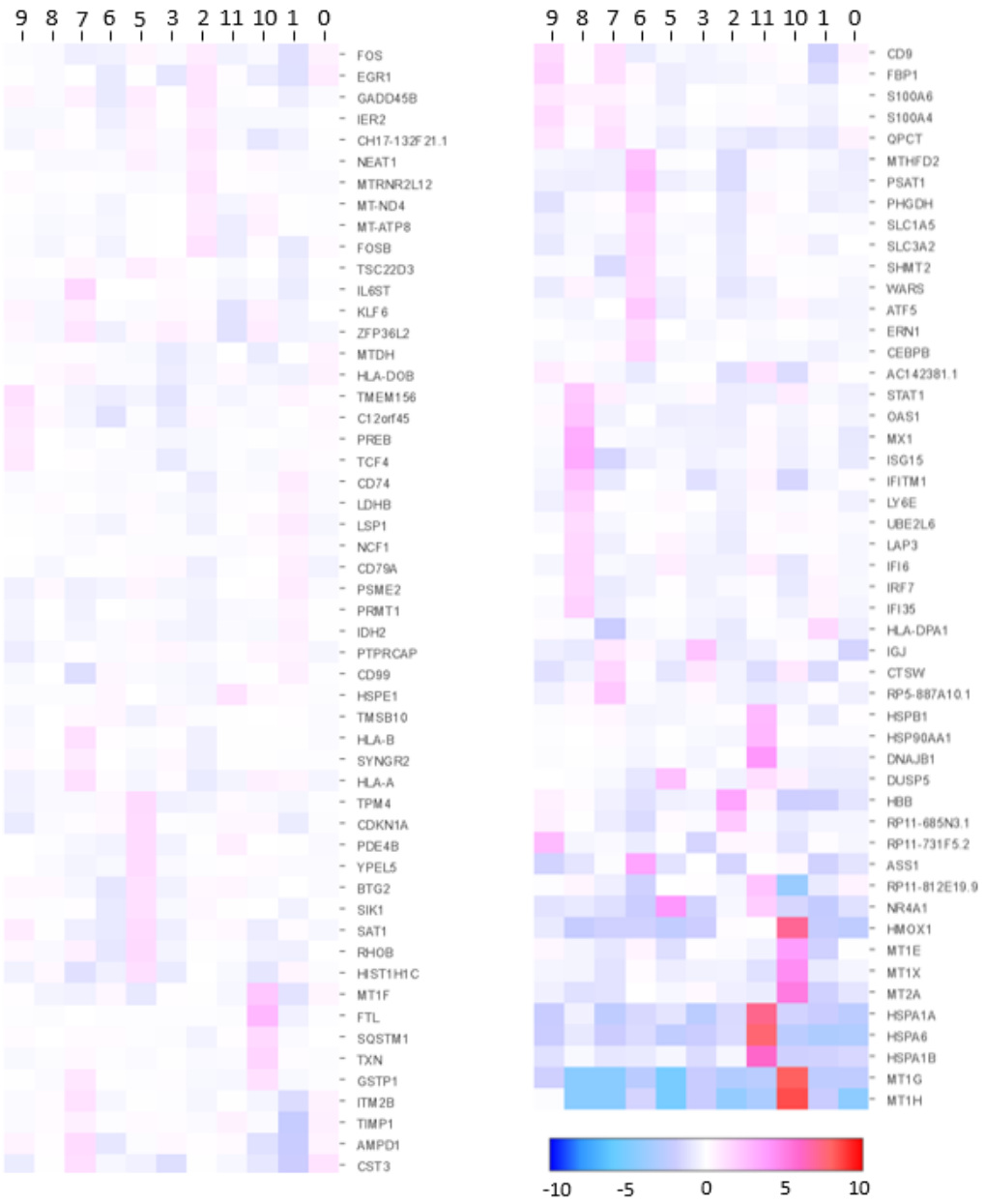

Figure 21: Differential gene expression determined by single-cell transcriptome analysis in BMPC clusters. Top upregulated genes per cluster are shown. The scale bar indicates Log_2 fold changes. Heatmap was generated using the 10X Genomics cell loupe browser.

Table 6: Selected upregulated genes identified by differential gene expression analysis of BMPC single-cell transcriptomes.

Symbol	Name	Known functions or relevant information	Literature
CST3	Cystatin C	extracellular cysteine proteinase inhibitor; induction of cytokines (e.g., IL-6) in BM DC; *(Upregulated in cluster 7)* induction autophagy through suppression of mTOR in neuronal cells	172–174
HLA-DPA1	Major Histocompatibility Complex, Class II, DP Alpha 1	Antigen presentation *(Upregulated in cluster 1)*	175
RP11-685N3.1	-	Uncharacterized transcript *(Upregulated in cluster 2)*	-
HBB	Hemoglobulin subunit beta	Oxygen transport *(Upregulated in cluster 2)*	176
FOS; FOSB	Fos Proto-Oncogene; FosB Proto-Oncogene	Subunits of AP-1 transcriptional complex *(Upregulated in cluster 2)*	177
EGR1	Early growth response 1	Transcriptional regulation in response to hypoxia *(Upregulated in cluster 2)*	178,179
GADD45B	Growth arrest and DNA-damage-inducible, beta	Cell cycle control and apoptosis *(Upregulated in cluster 2)*	180
MT-ND4; MT-ATP8	Mitochondrial transcripts	Energy metabolism *(Upregulated in cluster 2)*	181
IGJ	J-chain	Multimerization of secretory IgM and IgA; Transport of IgM and IgA across mucosal membranes *(Upregulated in cluster 3)*	182
DUSP5	Dual Specificity Phosphatase 5	Negative regulator of MAPK/Erk signaling *(Upregulated in cluster 5)*	183
NR4A1	Nur77	Modulates BC function in artherosclerosis; Bcl-2 mediated induction of apoptosis *(Upregulated in cluster 5)*	184,185
SLC3A2	Heavy subunit of CD98	Amino acid transporter; elevated in LLPC *(Upregulated in cluster 6)*	33
SLC1A5	ASCT2	Na+-dependent amino acid transporter that mainly transports glutamine *(Upregulated in cluster 6)*	151
ERN1	IRE1	Endoplasmic reticulum stress sensor *(Upregulated in cluster 6)*	152
WARS	Tryptophanyl tRNA synthase	Translation *(Upregulated in cluster 6)*	153
ASS1	Argininosuccinate synthetase 1	De novo synthesis of arginine *(Upregulated in cluster 6)*	154
PHGDH	Phosphoglycerate dehydrogenase	Serine synthesis from glucose (conversion of 3-PG to 3-hydroxypyruvate) *(Upregulated in cluster 6)*	156
PSAT1	Phosphoserine aminotransferase 1	Serine synthesis from glucose (conversion of 3-hydroxypyruvate to phosphoserine) *(Upregulated in cluster 6)*	156
SHMT2	Mitochondrial serine hydroxymethyltransferase	Conversion of serine to glycine; fueling of folate cycle *(Upregulated in cluster 6)*	156
MTHFD2	mitochondrial methylenetetrahydrofolate dehydrogenase /cyclohydrolase	Mitochondrial formate cycle *(Upregulated in cluster 6)*	157

RP5-887A10.1	long intergenic non-protein coding RNA 1781	differential expression in MM subgroups; Upregulated in memory BC compared to naive BC *(Upregulated in cluster 7)*	[186,187]
IL6ST	glycoprotein 130	common signal transducing receptor chain of IL-6 family receptors *(Upregulated in cluster 7)*	[130]
CSTW	cathepsin W	Cysteine protease involved in autophagy *(Upregulated in cluster 7)*	[34,159]
FBP1	Fructose-1,6-bisphosphatase 1	glycogen synthesis; negative regulation of glycolysis and glucose uptake in cancer cells *(Upregulated in cluster 7 and 9)*	[160,161]
CD9	Tetraspanin CD9	association with adhesion molecules in tetraspanin-enriched microdomains; association with CD19 and CD81; mediates interactions via VLA-4/VCAM-1 axis in GC BC *(Upregulated in cluster 7 and 9)*	[137,138,162,163]
QPCT	Glutaminyl-peptide cyclotransferase	Catalyzes post-transcriptional modification of secretory proteins, e.g., immunoglobulins *(Upregulated in cluster 7 and 9)*	[165]
KLF6	Krueppel-like factor 6	Regulation of hypoxia-induced transcriptional changes via HIF1α in macrophages *(Upregulated in cluster 7)*	[188,189]
STAT1	Signal transducer and activator of transcription 1	Phosphorylation of STAT1 upon induction of JAK-STAT-signaling by cytokines, e.g., IL-6 *(Upregulated in cluster 8)*	[45,190]
OAS1	2'-5'-oligoadenylate synthetase 1	Immune response to viral infection; interferon-inducible genes *(Upregulated in cluster 8)*	[166–169]
MX1	Myxovirus resistance 1		
ISG15	Interferon-stimulated gene 15		
IFITM1	Interferon-inducible transmembrane protein 1		
RP11-731F5.2	-	long non-coding RNA with unknown function *(Upregulated in cluster 9)*	-

4. Discussion

PC provide protective humoral immunity as long-lived antibody secretors. Common vaccines and infections lead to antigen-specific serum antibody titers with variable half-lives [77]. This observation suggests a differential regulation of PC pools which are stored in peripheral organs such as the spleen or the gut, and also to large extent in the BM. In this context, it has become increasingly apparent that PC are not uniform regarding their phenotypes and their biology [10,33,86,92,93]. CD19-negativity has been associated with a more stable PC population enriched in the BM [92]. In line with this work, Halliley et al. (2015) showed that long-lived tetanus-, mumps- and measles-specific PC were contained predominantly in the $CD19^-$ BMPC pool [93]. Furthermore, it has been shown that LLPC can survive in the SI for decades, as predicted 30 years earlier [14], and these populations displayed the $CD19^-$ $CD45^-$ phenotype [86]. On the other hand, vaccinia-specific long-lived BMPC were found to be $CD19^+$ or $CD19^-$ [105]. Overall, a surrogate phenotype for LLPC has not been unambiguously identified. Vaccines are still developed based on empirical observations, and a selective depletion of pathogenic PC still is not possible unless their antigen-specificity is known [25]. In addition, although putative components of the PC survival niche have been identified, the current model of the PC niche does not account for the differential regulation of humoral immune memory. This may be due to the fact that the possibility of heterogeneity of the PC niche itself has not been regarded. This discrepancy illustrates the need for studies delineating phenotypic heterogeneity of PC as this may elucidate the differential regulation of distinct PC populations.

4.1. $CD45^-$ and $CD56^+$ PC are part of the normal human BMPC pool, and are significantly enriched among $CD19^-$ BMPC

There are indications of PC populations with different lifetimes within the $CD19^-$ PC compartment, as has been shown for SI PC [86], and there is evidence of the accumulation of certain, but not all, antigen-specific LLPC in this compartment [92,93,105,191]. Therefore, we aimed to further delineate the heterogeneity of BMPC among $CD19^+$ versus $CD19^-$ BMPC. We found that in addition to $CD19^-$ PC, $CD45^-$ and $CD56^+$ PC constitute fractions of the normal BMPC pool and are not necessarily indications of an underlying PC malignancy (see 3.1.). Based on flow cytometric analyses, we found that on average 40% of BMPC were $CD19^-$, 38% were $CD45^-$ and 19% were $CD56^+$, revealing that major fractions of BMPC differentially express these surface markers in normal BM. Moreover, the distribution of combinatorial CD45 and CD56 phenotypes among $CD19^+$ and $CD19^-$ BMPC does not appear to be random, therefore suggesting that BMPC are differentially selected into $CD19^+$ and $CD19^-$ subpopulations. The fraction of $CD45^-$ BMPC was significantly larger among $CD19^-$ BMPC compared to $CD19^+$ BMPC. Similarly, $CD56^+$ BMPC were observed significantly more frequent in the $CD19^-$ BMPC compartment. The enrichment for the $CD45^-$ and $CD56^+$ BMPC within $CD19^-$ BMPC suggests a connection to the pro-survival, mature profile found in $CD19^-$ BMPC compared to $CD19^+$ BMPC [92]. In support of this, CD45-negativity was linked to increased longevity in SI PC [86]. The loss of CD19 and CD45 has been considered to be a normal feature of terminally differentiated PC [97,192], while the preserved expression of these surface antigens continues to be unexplained to date.

Our results suggest that BMPC subpopulations can pertain to any of the major Ig subclasses, IgG, IgA and IgM, with the exception of $CD56^+$ BMPC. $CD56^+$ BMPC were enriched for IgG^+ cells in fluorospot assays (see 3.3.) as well as for $IgG1^+$ cells in single cell RNA sequencing (see 3.7.3.). Therefore, the mechanisms for CSR to IgG may be connected to the signals that lead to CD56 expression in BMPC. Research on adhesion molecules in connection with Ig isotypes has previously suggested that the tetraspanin CD37,

which is essential for PC by the regulation of integrin α4β1 localization on PC [37,193], had a promotive effect on IgG1 production [194] but an inhibitory effect on IgA responses [193]. Therefore, a connection between CD56 expression and CSR is plausible, although this remains to be investigated.

While PAX5 is implicated in the transcriptional induction of *CD19* [103], to date no mechanism is known which could explain the differential expression of CD19 in terminal PC which have downregulated PAX5. As a co-receptor of the BCR, CD19 modulates BCR signaling throughout BC differentiation [94,96,97]. It would be consistent to assume that loss of CD19 expression is concomitant with the loss of BCR expression as a consequence of PC differentiation. There is, however, increasing evidence that only IgG^+ PC lose surface BCR expression, and IgA^+ and IgM^+ PC can respond to BCR stimulation [10,11]. Surface IgA expression is retained on BMPC regardless of their CD19 expression status, while surface IgG is downregulated [105]. Wiedemann et al. (2021) showed that surface IgA^+ BMPC were predominantly $CD19^+$ but a substantial fraction was also $CD19^-$. These authors found that IgA^+ BMPC responded to BCR stimulation while CD19 expression seemed to be independent of BCR engagement and, importantly, did not influence the levels of responsiveness to BCR stimulation [10]. This indicates that either other factors can substitute for CD19 in BCR signaling in $CD19^-$ PC or that CD19 may not function as a BCR co-stimulator in PC and may have an additional, to date unknown function.

The CD19 molecule consists of an ectodomain, a transmembrane part and a cytoplasmic tail, of which the latter contains tyrosines that mediate cytoplasmic signaling. It has not been sytematically investigated whether in $CD19^-$ PC, the expression is lost or only the ectodomain is shed. Our results show that FACS-sorted $CD19^-$ BMPC have significantly reduced *CD19* mRNA levels (see 3.6.1.), indicating that surface CD19 expression and transcription correlate, and that CD19 expression is regulated at the transcriptional level.

Similar to CD19, CD45 expression can be absent or preserved in PC, while the reason for this is elusive to this day. While CD45 positively regulates antigen receptor signaling by activating SFKs [110,111], it can also negatively regulate JAK-STAT signaling in cytokine signaling [113], thus its function is context-dependent. In IgA^+ PC which were found to have functional BCRs [10], CD45 expression may positively modulate BCR signaling. Our Fluorospot data show that IgA^+ BMPC were found among both $CD45^+$ and $CD45^-$ BMPC subsets (see 3.3.). Therefore, it would be informative to assess the response to BCR stimulation in $CD45^+$ and $CD45^-$ PC.

In MM cells, CD45 expression levels can be used to distinguish proliferative, immature $CD45^+$ cells, and quiescent, mature $CD45^-$ cells [108], suggesting that this may apply in a similar way to normal PC. From their finding of increasing age from $CD19^+$ $CD45^+$ over $CD19^-$ $CD45^+$ to $CD19^-$ $CD45^-$ PC in the human gut, Landsverk et al. (2017) deduct a developmental hierarchy from $CD45^+$ to $CD45^-$ PC [86]. While the evidence they present appears clear, they did not take into account the $CD19^+$ $CD45^-$ fraction in their analysis because they considered it negligible due to its low frequency, even though it appeared to be present. In the BM, over 30% of $CD19^+$ PC are $CD45^-$ (see Figure 2). Therefore, the model proposed by Landsverk et al. (2017) cannot be directly transferred to BMPC. While it is still possible that CD45 and CD19 distinguish PC with different ages in the BM, our data show that all possible combinations of $CD19^{+/-}$ and $CD45^{+/-}$ BMPC are present and, therefore, it is necessary to elaborate how $CD19^+$ $CD45^-$ PC fit into the hierarchy suggested by Landsverk and colleagues. Therefore, it would be important to elucidate whether CD19 and CD45 are downregulated at different timepoints during PC maturation and whether the molecules may be re-expressed.

CD56 expression is often used as a diagnostic marker for MM, although not all MM express CD56 and its value for MM prognosis is subject to current discussion [195]. Its expression on MGUS PC is long known [117]. Nevertheless, its expression on normal PC has hardly been studied to date. The expression of CD56, a marker associated with a prominent role in the regulation of adhesion of neural cells [114] as well as NK cells [116], on normal PC raises the question whether this marker distinguishes a discrete BMPC population in terms of function or regulation.

In sum, the present data point out that a substantial phenotypic heterogeneity must be accounted for when studying the regulation of humoral immune memory at the level of BMPC. For example, even very recent research has not regarded the presence of $CD19^-$ BMPC [196]. Moreover, only recently has it been revealed that CD45 expression distinguishes normal SIPC populations with different lifespans [86], although it remains unclear which functional role CD45 has in their differential regulation. Taken together, the to date underappreciated PC heterogeneity may explain why a surrogate marker for LLPC has not yet been identified, and, importantly, why a model for the differential regulation of humoral immune memory has to date not been established. The present data show that BMPC require a custom cytometric strategy for the accurate assessment of their heterogeneity which considers the presence of $CD19^-$, $CD45^-$ and $CD56^+$ among normal BMPC.

4.2. Perivascular association of BMPC

Contrary to findings in murine BM [17], we show that PC inhabit anatomically distinct compartments of the BM. While we found that 59% of BMPC localize as scattered cells distributed throughout the human BM, 41% were associated with $CD34^+$ blood vessels, and are therefore termed perivascular BMPC (see 3.4.3). In contrast, Zehentmeier et al. (2014) showed that, in mice that had been irradiated and reconstituted with Blimp1:GFP reporter BM cells, the distribution of PC appeared to be fairly even throughout the BM, without any perivascular accumulations [17]. It is not clear whether the experimental conditions, the age of the mice or fundamental differences between murine and human BMPC niches are the reason for these different observations. On the one hand, it has been shown that irradiation can manipulate the BM vasculature and disturb perivascular niches for mesenchymal stem cells [197]. Additionally, it has been shown that laboratory mice differ profoundly from free-living mice and humans in several aspects affecting the immune system [198], therefore suggesting that the cellular composition of the BM may also be affected by the housing conditions of laboratory mice. On the other hand, some anatomical differences between murine and human BM are known, such as higher adiposity of the human BM. Furthermore, the organization of adipose tissue changes during ageing and adipocytes may have effects on the regulation of vasculature [199,200]. Moreover, one could speculate that due to the short lifetime of mice and the limited time between reconstitution and analysis, possibly age-related accumulation of PC in the BM perivascular area is not observed. In our study, BM donors were on average 63 years old (see 2.1.) and, therefore, the BM in early life was not reflected. Analyses of donors of several younger age groups in comparison to older groups would be useful to clarify whether the accumulation of the $CD45^-$ BMPC phenotype at the perivascular site may be related to aging. It has been demonstrated that $CD19^-$ PC were absent in the BM of 5 to 7 month old infants [92]. This indicates that it is possible that $CD19^-$ BMPC may accumulate over time, and this is in line with the finding that long-lived, antigen-specific PC are contained in the $CD19^-$ BMPC compartment [93].

Based on the anatomy of the vascular structures we identified by immunohistochemical staining of FFPE BM, we reason that these are capillaries. As sinusoidal endothelial cells are $CD34^-$ [201], by using CD34 as a vascular marker, we exclude the possibility that perivascular BMPC localize to sinusoids, the main sites of cell trafficking and thus the putative entry points for PC [52]. In addition, the absence of Ki67 expression in the majority of BMPC as seen in immunohistochemistry (see 3.4.) as well as very low levels of *AICDA* and *S1PR1* (see 3.6.3.6.), indicate that $CD45^-$ BMPC are most likely mature PC that have not recently immigrated into the BM [145]. Furthermore, downregulation of chemotactic *CXCR3* in $CD45^-$ BMPC compared to $CD45^+$ BMPC (see 3.6.3.1.), which is known to be lost in PC upon arrival in the BM [16], further supports the notion that $CD45^-$ perivascular BMPC have settled in the BM temporally before their $CD45^+$ counterparts. In addition, it is tempting to speculate that PC actively migrate to perivascular niches due to optimal survival conditions at this site and accumulate at this site over a long time.

Although the BM is generally hypoxic, oxygen gradients have been found between the endosteum and different blood vessel types in mice [50]. Hypoxia was found to play a role in supporting ASC *in vitro* [38]. It also supported the *in vitro* differentiation of PC, which was associated with transcriptional changes involving genes such as *HIF1α* and *HIF2α* [202]. The transcription factor HIF-1α is considered as a marker of hypoxia that, together with its relative, HIF-2α, regulates a network of genes implemented in angiogenesis and oxygen transport [203,204]. In our bulk transcriptomes, *HIF1α* was significantly downregulated in $CD19^-$ $CD45^-$ $CD56^-$ BMPC (Supplemental figure 2), indicating that this BMPC subset might localize to compartments with elevated oxygen levels. Nevertheless, analysis of hypoxia-responsive factors in *ex vivo* samples may be problematic because the cells are removed from their physiological environment, which is not hypoxic, and this may hamper the stability of hypoxia-responsive transcripts. Thus, *in situ* study of hypoxia-inducible factors may be required for confirmation of these results, e.g., in immunohistochemistry with FFPE specimens which are fixated rapidly after extraction.

The expression of nestin by perivascular MSC can be used to distinguish different types of HSC niches. $Nestin^+$ perivascular MSC are found at the niches of quiescent HSCs, where oxygen levels are higher compared to vessels with $nestin^-$ MSCs. $Nestin^+$ MSC surrounding vessels are upstream of sinusoids, therefore they seem to be arterial vessels [50]. Thus, it would be interesting to assess whether perivascular BMPC may prefer blood vessels surrounded by $nestin^+$ over $nestin^-$ MSC. This would indicate a preference for arterial vessels with higher oxygen supply. Localization to arterial blood vessels would also suggest a better supply with other nutrients such as sugar. The elevated expression of genes encoding for solute carriers in $CD19^-$ BMPC (see 3.6.3.5.), and, in particular, significant upregulation of the glucose transporter gene *SLC2A10* in $CD45^-$ BMPC, may support that these subsets are in need of particularly high amounts of sugar, e.g. for energy supply or antibody glycosylation [62]. It is tempting to speculate that perivascular association may be a way of meeting these demands. Moreover, while the BM vasculature was found to be relatively dynamic rather than static by intravital imaging over short time periods in mice [36], it is not clear whether different types of vasculature in the human BM may differ in their range of plasticity, and whether perivascular BMPC are associated with rather stable blood vessels.

PC migrate to and are retained in the BM via responsiveness to the chemokine CXCL12 via the receptor CXCR4 and docking onto CXCL12-abundant reticular cells [35,43,205]. Perivascular CXCL12-abundant reticular (CAR) cells are not the only CXCL12 source at the perivascular niche. Endothelial cell themselves were found to express CXCL12, and endothelial cell-derived CXCL12 was found to support HSC maintenance [206,207]. Upon entry from the blood circulation into the BM, interaction between CXCL12 and CXCR4 on HSCs was found to induce integrin expression such as VLA-4 and LFA-1 by HSCs [208]. As in PC [37], the anchoring of

HSCs in a niche is based on interactions between VLA-4 and LFA-1, and their receptors VCAM-1 and ICAM-1 by vascular endothelial cells [209,210]. It is noteworthy that arterial endothelia express higher levels of VCAM-1 and ICAM-1 than sinusoidal endothelia in the BM [52], suggesting that the former may be more suitable as sites of retention for PC.

It is possible that there are further, so far unknown similarities between the niches of PC and HSC, as it has already been suggested by the mobilization of HSC and PC upon treatment with granulocyte colony-stimulating factor (G-CSF) [211]. The expression of stem cell antigen (Sca-1), a member of the lymphocyte antigen (Ly-6) family, is linked to primitive HSCs maintained in the BM, and is downregulated when they differentiate, and is also shared by PC, and interestingly also by arterial endothelial cells [212–214]. These findings are based on work in mice, and, although there is no direct homolog of Sca-1 in humans, the Ly6 proteins comprise a large family with diverse roles in humans [215].

In conclusion, these results provide new insights into the distribution of PC in the human BM and emphasizes the necessity to further characterize the perivascular microenvironment of human BMPC. The apparent avoidance of sinusoidal perivascular sites of BMPC suggests that perivascular BMPC are directed to the surroundings of blood vessels away from the entry sites into the BM. This raises the question whether a chemotactic mechanism in addition to the CXCR4-CXCL12 axis may steer BMPC to perivascular sites. The data also indicate that the perivascular location may differ from central BM sites in its oxygen levels and local nutrient supply.

4.3. The perivascular BM niche is enriched for CD45$^-$ BMPC

The accumulation of CD45$^-$ BMPC close to blood vessels raises two questions: What is the function of CD45 and loss thereof in PC? And: Is this function specifically supported at the perivascular site?

CD45 acts as a modulator of BCR signaling at early stages of BC development starting from the pre-BC stage in the BM [111,216] and appears to be involved up to terminal differentiation into ASC [112]. Even at the level of terminal PC, which were believed to lose their functional BCR, surface IgA can be expressed and mediate responsiveness to BCR stimulation [10]. Furthermore, CD45 has been implicated in the negative regulation of cytokine-mediated JAK-STAT signaling through the inhibition of JAK [113]. Thus, current evidence suggests two possible functions for CD45 in PC. Considering that IgA$^+$ BMPC can be CD45$^+$ or CD45$^-$ (see 3.3.), we reason that a connection between CD45 and BCR signaling is not likely.

In order to test whether CD45 has an inhibitory effect on JAK-STAT signaling in PC, we stimulated BMPC with IL-6, a cytokine that targets the JAK-STAT signaling pathway [130] and has a positive effect on PC survival in combination with other signals such as CD44 ligation [45]. It is intriguing to speculate that cytokine signaling via, e.g., IL-6 preferentially stabilizes CD45$^-$ BMPC in an inflammatory setting or when there may be competition of old BMPC and newly generated PC for BM niches. Our data show a significant yet very weak correlation of pSTAT1 levels with CD45-negativity (see 3.5.), indicating that either CD45 does not, or only to a very small extent, act as a negative regulator of JAK-STAT signaling in PC, or that there are additional factors, such as SOCS proteins [217], that substitute for CD45 in the negative regulation of JAK-STAT signaling. Transcripts of the SOCS family genes were detected in BMPC, and one of its members, *CISH*, was significantly upregulated in CD19$^-$ BMPC, with highest expression levels in CD45$^-$ BMPC (Supplemental figure 1). While IL-6 was shown to induce CISH and SOCS1 expression [218], our transcriptome

data suggest that a negative feedback loop mediated by SOCS proteins may have already been active in *ex vivo* BMPC. Our present study may therefore need to be extended to include the measurement of SOCS protein levels in order to provide conclusive results. Moreover, the assessment of CD45 phosphatase activity would be informative since it has been published that CD45 phosphatase activity is enhanced by binding of Galectin-1 [112], therefore adding to the complexity of the functional network around CD45. In summary, we cannot unambiguously establish a role for CD45 in JAK-STAT signaling in BMPC. Nevertheless, the hypothesis that CD45 downregulation may be a survival factor in perivascular BMPC remains interesting. Endothelial cells have been found to produce IL-6 in the peritoneum [131]. Moreover, in murine lymph nodes, perivascular DC were identified as major providers of IL-6 [219]. In addition, in co-culture experiments, PC induced IL-6 transcription in SC [220]. Even though the role of IL-6 in PC survival remains controversial, as PC persisted in its absence but stimulation with IL-6 had a positive effect on survival and antibody production [45], it is known that cytokine signaling via STAT3 is crucial for PC maintenance and function [221,222].

Our transcriptional analysis of $CD45^+$ vs. $CD45^-$ FACS-sorted BMPC subpopulations suggest that the loss of CD45 expression may be linked with advanced maturity based on decreased expression levels of *FAS* and *S1PR1* (see 3.6.3.4. and 3.6.3.6.). Moreover, chemotactic receptor *CXCR3* was downregulated in $CD45^-$ compared to $CD45^+$ BMPC, indicating that loss of chemotactic responsiveness occurred longer ago $CD45^-$ BMPC. Additionally, the knowledge on homing of PC to the BM so far does not regard how the precise localization of PC is determined, i.e., it does not explain the distribution throughout the BM with varying distances to the points of entry of newly immigration PC. The upregulation of the solute carrier *SLC2A10* in $CD45^-$ BMPC suggests that these PC may import more sugar compounds such as glucose, a function which has been linked to longevity of murine PC [33,62]. Therefore, a detailed analysis of glucose uptake and metabolism may provide insights as to whether metabolism and specific BM localization due to nutrient availability may be interconnected.

In sum, it remains to be investigated what the role for CD45 in PC is and how BM localization of PC is functionally linked to CD45. Nevertheless, it is possible that chemotactic and soluble factors organize BMPC around blood vessels, leading to the observed structures. Further characterization of perivascular SC in the BM in relation to PC organization will be required. To date, the taxonomy of SC in the human BM is poorly described, although recent work has shown that murine SC are highly diverse in their expression of factors which also affect PC maintenance, such as *TNFSF13B* (BAFF) [223]. Therefore, it is not known whether distinct subsets of human SC are specialized for the maintenance of BMPC, or for specific BMPC subpopulations, and may localize to specific sites such as the perivascular site.

4.4. Transcriptional features regarding survival, adhesion and nutrient supply distinguish bone marrow plasma cell subpopulations

Bulk RNA sequencing of FACS-sorted BMPC subpopulations not only showed that CD19 expression is a major determinant of transcriptionally different BMPC subsets. It also revealed a transcriptional diversity among $CD19^-$ BMPC defined by CD45 and CD56 expression, as well as differential expression of genes related to several aspects important for the maintenance of PC in the BM (see 0.).

$CD19^-$ BMPC subpopulations had elevated transcript levels of *SDC1*, *TNFRSF13B*, *ZBTB20* and *CD28*, (see 3.6.3.). Elevated levels of *SDC1* (CD138) and *TNFRSF13B* (TACI) might improve the availability of APRIL as

well as APRIL-mediated pro-survival signaling in CD19$^-$ BMPC [47,224]. In particular, the enhanced expression of TACI might be a way to adapt flexibly to lower surface expression of BCMA as an APRIL-binding receptor as BCMA surface protein has been shown to be shed by γ-secretase in BMPC [225]. *ZBTB20* transcripts, which were previously found to be expressed at highest levels in mature BMPC [75], were elevated in CD19$^-$ BMPC compared to CD19$^+$ BMPC. The transcription factor Zbtb20 was implicated in the maintenance of PCs in murine knock-out experiments [74,75]. Interestingly, Wang and Bhattacharya (2014) showed that the positive effect of Zbtb20 on PC survival depended on the adjuvant used in the immunization model, thus suggesting that the type of immune response may have implications for the capability of PC to become long-lived [74].

Furthermore, our analysis finds that CD56$^+$ BMPC had increased levels of *CD44*. CD44 has been implicated in the positive effect on PC survival in synergy with IL-6 [45]. In addition, BMPC express specific isoforms of CD44 which mediate adhesion to SC. Interestingly, the isoform CD44v9 on PC mediated induction of IL-6 by SC *in vitro* [76]. Therefore, the upregulation of *CD44* may be involved in the maintenance of CD56$^+$ PC, and CD44 upregulation may be survival advantage in an IL-6-rich setting, which might be a specific location in the BM or immunological condition such as inflammation.

The upregulation of *CD28*, a factor implicated in the maintenance of long-lived PC [70,72], in CD19$^-$ BMPC, with the highest expression in CD45$^-$ BMPC, supports the notion that this is a particularly stable population. Together with the accumulation of CD45- BMPC in perivascular areas seen in situ (see 3.4.3.), this suggests that the perivascular BM site may offer a particularly supportive environment. CD28 is most prominently known as a co-stimulatory molecule for TCR signaling as well as a receptor for CD80 and CD86. DC (DC) which express CD80 and CD86 were found to colocalize with BMPC, and this interaction induced IL-6 production in DC [219]. It is of note that CD28 can physically interact with CD45 on the surface of tumor infiltrating lymphocytes [226], and it has been suggested that CD45 and CD28 together play a role in TCR signaling [227]. In PC, CD28-mediated signaling supports the survival of long-lived PC through induction of Blimp-1, a master regulator of PC development [70], and it also modulates the metabolism of LLPC in favor of sustained survival [72].

In addition, *CD9* was upregulated in CD19$^-$ BMPC and expressed at highest levels in CD19$^-$ CD45$^-$ CD56$^-$ BMPC. CD9 is known to associate with various integrins and adhesion molecules such as VLA-4 and LFA-1 [137]. Therefore, it may be involved in the modulation of vital interactions between PC and SC through the VLA-4/VCAM-1 axis [37], similar to CD37 which organizes VLA-4 on the PC surface, thereby supporting their survival [228]. The upregulation of CD9 as a mediator of integrin interactions may benefit adhesion between PC and SC, thereby positively influencing the retention and survival of CD19$^-$ BMPC.

The differential expression of several integrin genes indicates that adhesion properties may diversify BMPC subpopulations (see 3.6.3.3.). Integrin α8 and integrin β5, which were upregulated in CD19$^-$ BMPC on the transcriptional level, can bind to fibronectin and extracellular matrix components [140], thus suggesting that CD19$^-$ BMPC may have improved adhesive properties in individualized BM niches. In this context, it is important to consider that the Ig isotype may influence adhesion molecule expression in PC. In mice, IgG$^+$ BMPC were specifically reduced upon infection with salmonella, and this was linked to interactions between an unknown adhesion molecule on PC and laminin β1 [229]. The tetraspanin CD37 was linked to an inhibition of IgA antibody responses [193] but was important for IgG1 production [194], and it was found to regulate the surface localization of integrin α4β1, an essential integrin for PC maintenance [37,228]. In addition, integrin β7-deficiency affected IgA but not IgG intestinal immune responses [230]. Taken

together, when examining adhesion molecules in PC, it appears important to take Ig isotypes into consideration, which was not the case in our bulk RNA sequencing analysis.

The upregulation of the anti-apoptotic factor *BIRC3* in CD19$^-$ BMPC and downregulation of the major effector caspase *CASP3* in CD19$^-$ CD45$^-$ CD56$^-$ BMPC is suggestive of a higher stress resilience in specific BMPC subsets (see 3.6.3.4.) [141,142]. On the other hand, the downregulation of anti-apoptotic *MCL1* in CD19$^-$ CD45$^-$ CD56$^+$ BMPC may appear contradictory at first sight [46], but it is of utmost importance to consider that apoptosis is dependent on a fine balance between several apoptosis factors. Noxa is the only pro-apoptotic antagonist for Mcl-1 [142], and its corresponding gene, *PMAIP1*, was also downregulated in CD19$^-$ CD45$^-$ BMPC, highlighting the necessity of further studies taking the apoptotic network into account and systematically evaluating apoptosis in CD19$^+$ and CD19$^-$ BMPC. All analyses at the transcriptional level require confirmation at the protein level, and taking into account their activation status, as, for example, in the case of caspases which require phosphorylation in order to be activated.

The role of solute carriers may be of relevance for PC biology due to recent findings that the level of glucose uptake distinguishes SLPC and LLPC in mice [33]. While in mice, the glucose transporter GLUT1, encoded by *SLC2A1*, was also elevated on the protein level in LLPC despite similar transcript levels, we found several other genes encoding for solute carriers were significantly upregulated in CD19$^-$ BMPC (see 3.6.3.5.). Especially, *SLC2A10*, which encodes for the glucose transporter Glut10 and was highly expressed in CD19$^-$ CD45$^-$ BMPC, may play a role for a similar enhanced uptake of glucose in human BMPC. Therefore, the comparison of glucose uptake in human BMPC subpopulations would elucidate whether previous findings apply in humans. Overall, the upregulation of several *SLC* family genes suggests a role for nutrient supply in the maintenance of CD19$^-$ BMPC subpopulations, potentially increasing their range of available metabolites.

In summary, the present transcriptional data suggest a putative hierarchy of advanced maturity and enhanced resilience from CD19$^+$ to CD19$^-$ BMPC based on the modulation of gene expression of survival factors such as *SDC1*, *ZBTB20* and *CD28*. The expression profiles of adhesion molecules are suggestive of the habitation of different BMPC subsets in different BM niches, in which the upregulation of, e.g., *CD9* or *CD44* may enable or enhance their anchoring. The differential expression of integrin genes, which have not yet been studied in the context of PC maintenance, suggests that BMPC subsets may diversify by differential adhesion properties, and this may relate to residence in different niches. Furthermore, this raises the question whether a different set of integrins may be of relevance in the study of the human PC niche compared to the murine PC niche. Moreover, the differential expression of genes related to apoptosis as well as solute carrier genes indicates that there may be an unknown diversity regarding PC resilience as well as nutrient and amino acid availability which require detailed functional analyses in order to fully elucidate the differences of BMPC subset lifestyles.

4.5. Single-cell transcriptome analysis of bone marrow plasma cells

In extension to our transcriptome analysis of FACS-sorted BMPC populations, single cell sequencing of BMPC allowed for a comprehensive transcriptional analysis in combination with isotype identification and mutational loads of BCRs. The analysis revealed that metabolic genes characterize BMPC subpopulations, and that CD19$^-$ CD45$^-$ CD56$^+$ BMPC are enriched for IgG1$^+$ cells with lower SHM rates compared to other BMPC (see 3.7.).

We found the upregulation of CD28*, ZBTB20* and *CD9* expression in CD19$^-$ CD45$^-$ CD56$^+$ BMPC (see 3.7.5. and Supplemental figure 3), thereby confirming our findings from bulk RNA transcriptomes. This expression profile may contribute to improved resilience and retention of this BMPC subset, as previously discussed in 4.4. The accumulation of IgG1$^+$ cells in this cluster suggests that they may derive from immune responses in which IL-21 has predominantly driven Ig class switching [6]. Moreover, lower SHM rates may further indicate that these BMPC were generated in distinct types of immune reactions compared to other BMPC. This will be discussed in detail in chapter 4.6.

The results from single-cell sequencing indicate that there may be links between BMPC phenotypes and the types of immune response from which BMPC derive. Various interferon-inducible genes were upregulated in cluster 8 which appeared to contain mostly CD56$^-$ BMPC (see Table 6), suggesting that these BMPC may have received a specific signature during their generation in viral immune responses. The elevation of *IGJ* transcripts in clusters 3, which was predominantly CD56$^-$, may suggest their generation at mucosal sites, as IGJ is important for the transport and multimerization of secretory IgA and IgM [182]. In line with this idea, cluster 3 was enriched for IgM$^+$ cells and also contained a large fraction of IgA$^+$ cells.

Cluster 6, which appeared to contain CD56$^-$ BMPC and which was enriched for IgA1$^+$ cells, was characterized by the upregulation of several metabolic genes suggestive of elevated antibody production and high energy consumption (see 3.7.5.). Upregulation of genes involved in amino acid transport (*SLC3A2, SLC1A5*) [33,151], amino acid biosynthesis (*ASS1, SAT1, PHGDH*) [154,156], protein translation (*WARS*) [153] and ER stress sensing (*ERN1*) [152] highly suggests that BMPC from this cluster were particularly dedicated to protein synthesis. Therefore, it is tempting to speculate that these BMPC may be high Ig secretors, and analysis of secretion rates may be informative [231]. It was shown that TC help during BC generation increased antibody production levels in PC progeny [232]. The amino acid transporter CD98, which is encoded by *SLC3A2* and *SCL7A5*, was shown to be elevated in murine LLPC [33]. Furthermore, the amino acid transporter ASCT2, encoded by *SLC1A5*, was found to associate with CD98 in a super-complex with CD147 regulated by mTOR [233]. The upregulation of several genes involved in one carbon metabolism suggests that this pathway may be a way of dual usage of glucose to generate substrates for Ig synthesis as well as for energy supply in professional antibody secretors [155]. Similarly, ^{13}C-glutamine tracing experiments showed that PC use glucose primarily for antibody glycosylation but can divert it to glycolysis and pyruvate-dependent respiration when energy levels run low [62]. These findings reveal candidate genes that may be useful in the elucidation of BMPC metabolism through additional functional studies. Future studies investigating the expression of these metabolic factors on the protein level in relation to the expression of CD19 and CD45 will elucidate whether BMPC subpopulations distinguish metabolically different BMPC.

Cluster 1 had features indicative of rather recent differentiation into PC as this cluster contained cells with elevated MHC class II genes as well as *CD79A*. Interestingly, this cluster was attributed with rather high *CD19* and *PTPRC* gene expression and CD56$^-$ phenotype, therefore linking this phenotype with PC that are possibly relatively newly generated.

Overall, the present single-cell transcriptomes of BMPC revealed a significantly smaller number differentially expressed genes. While the transcriptomic analysis of FACS-sorted BMPC subsets yielded over 800 differentially expressed genes (fold change ≥ 2; adjusted p-value < 0.05), transcriptomes from single-cell sequencing revealed only 36 (p-value < 0.1), even though criteria for significant differential

expression were less stringent than in the bulk RNA sequencing analysis. This is likely due to a major difference between the two types of analyses: the absolute amounts of transcripts per experimental unit. In bulk RNA sequencing, transcripts are highly concentrated, allowing for the detection even of low expression genes, while in single cell sequencing the number of transcripts is lower. Furthermore, one must take into account that PC are a particularly challenging cell type in transcriptome analysis based on the fact that a fraction as large as 50% of all transcripts present in these cells are Ig genes themselves [234]. To analyze PC transcriptomes, these Ig gene transcripts are subtracted from the dataset, thus at least halving the sequencing information. An individual sequencing run has a limited capacity of transcripts that can be sequenced, therefore especially low expression genes might not be detected.

Nevertheless, single-cell sequencing of BMPC offers a comprehensive view into the transcriptional heterogeneity of BMPC in combination with Ig isotypes. Importantly, the present results reveal a large set of genes related to protein synthesis and metabolism, which have not yet been studied in human PC, that provide the basis for future studies focusing on the metabolism of human PC. Future work may also elucidate the potential connection between the CD19 and CD45 expression and a BMPC subpopulation with an enhanced capacity of Ig production.

4.6. CD56$^+$ bone marrow plasma cells display low somatic hypermutation rates of their immunoglobulin genes

CD56 expression in normal PC has to date not been studied. Our findings identify CD56$^+$ PC as regular components in normal BM (see 3.1.), and, importantly, single-cell sequencing of BMPC clearly detects a CD56$^+$ BMPC population that is distinguished from other BMPC on the level of transcriptomes as well as in association with reduced mutational loads of antibody genes (see 3.7.).

CD56 expression is found in neural cells, NK cells, gamma delta TC, activated CD8$^+$ TC and DC [235–239]. It was also found to be expressed in some BM MSCs and was associated with HSC niches [240,241]. CD56 can engage in homotypic adhesion as well as heterophilic interactions with fibroblast growth factor receptor (FGFR) or extracellular matrix (ECM) components [242]. In addition to a role in adhesion, CD56 is implicated in promoting neurite growth and survival by activating phosphatidylinositol 3-kinase (PI3K) [243]. Similarly, the tetraspanin CD37-mediated maintenance of PC was also associated with activation of PI3K [228]. Importantly, PI3K signaling is implicated as an essential survival signal for BMPC [15]. Furthermore, CD56 has been implicated in the induction of IL-6 production in osteoblasts through CD56-mediated interaction with MM cells *in vitro* [119], indicating a role in the modulation of the BMPC environment. Taken together, the current knowledge on CD56 is suggestive of potential roles not only in stabilizing cell-cell adhesion but also providing signals promoting the survival of PC.

Our single-cell sequencing analysis revealed that *ZBTB20* transcripts, which were previously found to be expressed at highest levels in mature BMPC [75], were elevated in CD56$^+$ BMPC (Supplemental figure 3). The transcription factor Zbtb20 was found to be highly expressed in mature PC, and was implicated in the maintenance of PCs and expression of *MCL-1* in murine knock-out experiments [74,75]. Moreover, Wang et al. (2014) showed that Zbtb20 appeared to promote long-term antibody production resulting from immune reactions in which TLR-stimulating adjuvants were absent. Therefore, elevated *ZBTB20* expression in PC precursors may facilitate the generation of PC with the capability to become long-lived independent of the adjuvant used in vaccination. The upregulation of CD28 at protein levels in CD56$^+$

BMPC supports the notion that this BMPC subpopulation may be particularly stable [70,72], suggesting that this group contains BMPC with the capability of being particularly long-lived.

In addition, the present data show that $CD19^-$ $CD45^-$ $CD56^+$ BMPC comprised a population distinguished from other BMPC by their transcriptomes, an accumulation of $IgG1^+$ cells and reduced SHM rates of their immunoglobulin genes (see 3.7.). Several factors may affect the levels of SHM of BC. Regarding an isolated immune response, the rate of mutations of the Fv region and particularly of the CDRs accumulate as a consequence of ongoing affinity maturation. Moreover, there is a correlation between the stage of immunization, i.e. primary or secondary immunization, the degree of antibody specificity and the levels of SHM [148]. PC resulting from a primary immune response, e.g., in response to MMR vaccination once in early childhood, would be expected to have lower SHM loads than those resulting from repeated exposure as the latter would probably involve recruitment of memory BC to the response which would further mutate. In line with this, there are indications that, in mice, SHM rates increase with age [147]. Under this assumption, low SHM rates may point towards PC generation in early life, as it was already speculated for $CD19^-$ BMPC [92]. Mei et al. (2015) also found that frequencies of SHM were at comparable levels in $CD19^+$ IgG^+ BMPC and in blood tetanus-specific IgG^+ plasmablasts one week after tetanus-vaccination, which are likely the precursors of BMPC [89], but $CD19^-$ IgG^+ BMPC had markedly lower mutation frequencies. Additionally, while LLPC were commonly believed to derive primarily from GC, EF reactions are discussed as an alternative source of PC capable of entering the LLPC pool [29]. It is plausible that EF responses may differ from highly organized GC in their efficiency of affinity maturation, and, thus, may produce PC with less SHM.

In order to explain the reduced SHM rates seen in $CD56^+$ BMPC and, importantly, to assess the role for these BMPC in long-term humoral immunity, the identification of antigen specificities against model antigens or vaccinations such as MMR and tetanus would be highly informative. In addition, extension of the present analysis by the comparison of SHM rates according to Ig isotypes may be interesting, as it has been shown that lower SHM rates in $CD19^-$ BMPC were linked with IgG expression [92]. It may also be of interest to study adjuvant-related effects on the generation of $CD56^+$ BMPC, since the transcription factor Zbtb20, which we found to be transcriptionally upregulated in $CD56^+$ BMPC (see Supplemental figure 3), was implicated not only in the support of Mcl-1 expression but also in the regulation of PC survival after immunization without TLR stimulation [74]. This work suggests that the capability of PC to become long-lived may be imprinted during their differentiation into PC.

A major question that must be addressed in future work is that of a putative sequential maturation connected with the expression of CD56. At this point, there are two possible scenarios: CD56 may be upregulated upon arrival of the PC in its niche, where the cellular environment or the further maturation of the PC may induce CD56 expression, or it may be imprinted at an earlier timepoint, for example during BC differentiation into PC.

In addition to the present analysis, this data set offers further information regarding the interrelations of the novel BMPC subpopulations. Analysis of trajectory interference will provide insights on the transcriptional dynamics in between the BMPC clusters, which may indicate a possible sequential maturation hierarchy. Importantly, BCR sequencing also enables the analysis of clonal relationships across BMPC populations, i.e., clonal overlaps or other imprints derived from their generation, e.g., from TC-dependent generation.

In summary, our results from single cell transcriptional and BCR analysis highly suggest that $CD56^+$ BMPC comprise a subpopulation of BMPC which are more resistant to existential challenges, e.g., their displacement due to competing, newly immigrating BMPC. The elevation of CD28 as well as lower SHM rates in $CD56^+$ BMPC supports the notion that these BMPC may exist for extended time periods compared to $CD56^-$ BMPC and may even derive from events of PC generation early in life. Future functional studies will be useful to understand whether CD56 expression indeed is a factor that promotes BMPC retention or survival signaling.

5. Conclusion

The present work provides important insights into the heterogeneity of human BMPC defined by CD19, CD45 and CD56 expression, regarding transcriptional diversity and microanatomical distribution of PC in the BM.

We demonstrate that a substantial phenotypic heterogeneity, considering the presence of $CD19^-$, $CD45^-$ and $CD56^+$ BMPC, must be taken into account in the study of the regulation of humoral immune memory at the level of BMPC. Our transcriptional data suggest a putative hierarchy of advanced maturity and enhanced resilience from $CD19^+$ to $CD19^-$ BMPC. We identify candidate gene products which may potentially modulate adhesion properties, metabolism and resistance to apoptosis in $CD19^-$ BMPC, some of which have not yet been studied in PC. Importantly, our transcriptional analyses link $CD56^+$ BMPC with features indicative of a particularly strong resilience and, potentially, an extended durability compared to $CD56^-$ BMPC. This transcriptional diversity may translate into different degrees of capacities to survive for extended time periods. The assessment of antigen-specificities among $CD56^+$ BMPC will be crucial to elucidate whether lower SHM rates are indeed connected with BMPC age.

In addition, we reveal a so far unknown diversity of BMPC according to their distribution *in situ*. We find a large fraction of BMPC to localize to non-sinusoidal perivascular sites. This raises the question whether there are so far unidentified chemotactic mechanisms directing PC from the entry site into the BM to specific areas where vasculature or perivascular niche cells provide a favorable environment. Importantly, perivascular localization of BMPC was linked with CD45-negativity, which suggests that more resilient $CD45^-$ BMPC find a supportive environment at this specific site. To confirm this, it will be of relevance to assess whether the perivascular accumulation of $CD45^-$ BMPC is age-related, and what the functional consequences of the downregulation of CD45 expression are.

This work suggests, on one hand, a connection between CD56-expression and intrinsic survival factors, and, on the other hand, a link between $CD45^-$ BMPC and a specific BM microenvironment. This illustrates the ongoing discussion which suspects the key to the regulation of humoral memory in a balance between intrinsic survival factors and extrinsic regulation of PC maintenance in a survival niche. Therefore, to decipher how humoral immune memory is regulated at the level of BMPC, it will be fundamental to consider BMPC heterogeneity.

6. Literature

1. Murphy, K. & Weaver, C. *Janeway's Immunobiology 9th Edition*. (2017).
2. Robinson, M. J., Webster, R. H. & Tarlinton, D. M. How intrinsic and extrinsic regulators of plasma cell survival might intersect for durable humoral immunity. *Immunol. Rev.* **296**, 87–103 (2020).
3. Kovaltsuk, A. *et al.* How B-cell receptor repertoire sequencing can be enriched with structural antibody data. *Front. Immunol.* **8**, 1–11 (2017).
4. Cowell, L. G., Kim, H. J., Humaljoki, T., Berek, C. & Kepler, T. B. Enhanced evolvability in immunoglobulin V genes under somatic hypermutation. *J. Mol. Evol.* **49**, 23–26 (1999).
5. Vidarsson, G., Dekkers, G. & Rispens, T. IgG subclasses and allotypes: From structure to effector functions. *Front. Immunol.* **5**, 1–17 (2014).
6. Pène, J. *et al.* Cutting Edge: IL-21 Is a Switch Factor for the Production of IgG 1 and IgG 3 by Human B Cells . *J. Immunol.* **172**, 5154–5157 (2004).
7. Kitani, A. & Strober, W. Regulation of C gamma subclass germ-line transcripts in human peripheral blood B cells. *J. Immunol.* **151**, 3478–88 (1993).
8. Islam, K. B., Nilsson, L., Sideras, P., Hammarström, L. & Smith, C. I. E. TGF-β1 induces germ-line transcripts of both IgA subclasses in human B lymphocytes. *Int. Immunol.* **3**, 1099–1106 (1991).
9. Doherty, M. & Robertson, M. J. Some early Trends in Immunology. **25**, (2004).
10. Wiedemann, A. *et al.* Human IgA-Expressing Bone Marrow Plasma Cells Characteristically Upregulate Programmed Cell Death Protein-1 Upon B Cell Receptor Stimulation. *Front. Immunol.* **11**, 1–11 (2021).
11. Pinto, D. *et al.* A functional BCR in human IgA and IgM plasma cells. **121**, 4110–4114 (2013).
12. Chang, H. D. & Radbruch, A. Maintenance of quiescent immune memory in the bone marrow. *Eur. J. Immunol.* **51**, 1592–1601 (2021).
13. Manz, R. A., Löhning, M., Cassese, G., Thiel, A. & Radbruch, A. Survival of long-lived plasma cells is independent of antigen. *Int. Immunol.* **10**, 1703–1711 (1998).
14. Manz, R. A., Thiel, A. & Radbruch, A. Lifetime of plasma cells in the bone marrow. *Nature* **388**, 133–134 (1997).
15. Cornelis, R. *et al.* Stromal Cell-Contact Dependent PI3K and APRIL Induced NF-κB Signaling Prevent Mitochondrial- and ER Stress Induced Death of Memory Plasma Cells. *Cell Rep.* **32**, 107982 (2020).
16. Hauser, A. E. *et al.* Chemotactic Responsiveness Toward Ligands for CXCR3 and CXCR4 Is Regulated on Plasma Blasts During the Time Course of a Memory Immune Response. *J. Immunol.* **169**, 1277–1282 (2002).
17. Zehentmeier, S. *et al.* Static and dynamic components synergize to form a stable survival niche for bone marrow plasma cells. *Eur. J. Immunol.* **44**, 2306–2317 (2014).
18. Schuh, W., Mielenz, D. & Jäck, H. M. *Unraveling the mysteries of plasma cells*. *Advances in Immunology* vol. 146 (Elsevier Inc., 2020).

19. Lino, A. C. *et al.* LAG-3 Inhibitory Receptor Expression Identifies Immunosuppressive Natural Regulatory Plasma Cells Article LAG-3 Inhibitory Receptor Expression Identifies Immunosuppressive Natural Regulatory Plasma Cells. *Immunity* **49**, 120–133 (2018).

20. Castillo, J. J. Plasma Cell Disorders. *Prim. Care - Clin. Off. Pract.* **43**, 677–691 (2016).

21. Wang, L., Wang, F. S. & Gershwin, M. E. Human autoimmune diseases: A comprehensive update. *J. Intern. Med.* **278**, 369–395 (2015).

22. Hoyer, B. F. *et al.* Short-lived plasmablasts and long-lived plasma cells contribute to chronic humoral autoimmunity in NZB/W mice. *J. Exp. Med.* **199**, 1577–1584 (2004).

23. Cheng, Q. *et al.* Autoantibodies from long-lived 'memory' plasma cells of NZB/W mice drive immune complex nephritis. *Ann. Rheum. Dis.* **72**, 2011–2017 (2013).

24. Cambridge, G. *et al.* Circulating levels of B lymphocyte stimulator in patients with rheumatoid arthritis following rituximab treatment: Relationships with B cell depletion, circulating antibodies, and clinical relapse. *Arthritis Rheum.* **54**, 723–732 (2006).

25. Cheng, Q. *et al.* Selective depletion of plasma cells in vivo based on the specificity of their secreted antibodies. 284–291 (2020).

26. Bortnick, A. & Allman, D. What Is and What Should Always Have Been: Long-Lived Plasma Cells Induced by T Cell–Independent Antigens. *J. Immunol.* **190**, 5913–5918 (2013).

27. Bortnick, A. *et al.* Long-Lived Bone Marrow Plasma Cells Are Induced Early in Response to T Cell-Independent or T Cell-Dependent Antigens. *J. Immunol.* **188**, 5389–5396 (2012).

28. Elsner, R. A. & Shlomchik, M. J. Review Germinal Center and Extrafollicular B Cell Responses in Vaccination , Immunity , and Autoimmunity. *Immunity* **53**, 1136–1150 (2020).

29. Allman, D., Wilmore, J. R. & Gaudette, B. T. The continuing story of T-cell independent antibodies. *Immunol. Rev.* **288**, 128–135 (2019).

30. Tellier, J. *et al.* Blimp-1 controls plasma cell function through the regulation of immunoglobulin secretion and the unfolded protein response. *Nat. Immunol.* **17**, 323–330 (2016).

31. Shapiro-Shelef, M., Lin, K., Savitsky, D., Liao, J. & Calame, K. Blimp-1 is required for maintenance of long-lived plasma cells in the bone marrow. **202**, 1471–1476 (2005).

32. Hibi, T. & Dosch, H. -M. Limiting dilution analysis of the B cell compartment in human bone marrow. *Eur. J. Immunol.* **16**, 139–145 (1986).

33. Lam, W. Y. *et al.* Metabolic and Transcriptional Modules Independently Diversify Plasma Cell Lifespan and Function. *Cell Rep.* **24**, 2479-2492.e6 (2018).

34. Pengo, N. *et al.* Plasma cells require autophagy for sustainable immunoglobulin production. *Nat. Immunol.* **14**, 298–305 (2013).

35. Hargreaves, D. C. *et al.* A coordinated change in chemokine responsiveness guides plasma cell movements. *J. Exp. Med.* **194**, 45–56 (2001).

36. Reismann, D. *et al.* Longitudinal intravital imaging of the femoral bone marrow reveals plasticity within marrow vasculature. *Nat. Commun.* **8**, (2017).

37. DiLillo, D. J. *et al.* Maintenance of Long-Lived Plasma Cells and Serological Memory Despite Mature and Memory B Cell Depletion during CD20 Immunotherapy in Mice. *J. Immunol.* **180**, 361–371 (2008).

38. Nguyen, D. C. *et al.* Factors of the bone marrow microniche that support human plasma cell survival and immunoglobulin secretion. *Nat. Commun.* **9**, (2018).

39. Nie, Y. *et al.* The Role of CXCR4 in Maintaining Peripheral B Cell Compartments and Humoral Immunity. **200**, (2004).

40. Khodadadi, L., Cheng, Q., Radbruch, A. & Hiepe, F. The Maintenance of Memory Plasma. **10**, (2019).

41. Terstappen, L. W. M. M., Johnsen, S., Segers-Nolten, I. M. J. & Loken, M. R. Identification and characterization of plasma cells in normal human bone marrow by high-resolution flow cytometry. *Blood* **76**, 1739–1747 (1990).

42. Cheng, Q. *et al.* CXCR4–CXCL12 interaction is important for plasma cell homing and survival in NZB/W mice. *Eur. J. Immunol.* **48**, 1020–1029 (2018).

43. Belnoue, E. *et al.* Homing and Adhesion Patterns Determine the Cellular Composition of the Bone Marrow Plasma Cell Niche. *J. Immunol.* **188**, 1283–1291 (2012).

44. Lindquist, R. L., Niesner, R. A. & Hauser, A. E. In the Right Place, at the Right Time: Spatiotemporal Conditions Determining Plasma Cell Survival and Function. *Front. Immunol.* **10**, 788 (2019).

45. Cassese, G. *et al.* Plasma Cell Survival Is Mediated by Synergistic Effects of Cytokines and Adhesion-Dependent Signals. *J. Immunol.* **171**, 1684–1690 (2003).

46. Peperzak, V. *et al.* Mcl-1 is essential for the survival of plasma cells. *Nat. Immunol.* **14**, 290–297 (2013).

47. McCarron, M. J., Park, P. W. & Fooksman, D. R. CD138 mediates selection of mature plasma cells by regulating their survival. *Blood* **129**, 2749–2759 (2017).

48. O'Connor, B. P. *et al.* BCMA Is Essential for the Survival of Long-lived Bone Marrow Plasma Cells. *J. Exp. Med.* **199**, 91–97 (2004).

49. Yeh, T., Okano, T., Naruto, T. & Yamashita, M. APRIL-dependent lifelong plasmacyte maintenance and immunoglobulin production in humans. (2020).

50. Spencer, J. A. *et al.* Direct measurement of local oxygen concentration in the bone marrow of live animals. *Nature* **508**, 269–273 (2014).

51. Woods, K. & Guezguez, B. Dynamic Changes of the Bone Marrow Niche: Mesenchymal Stromal Cells and Their Progeny During Aging and Leukemia. *Front. Cell Dev. Biol.* **9**, 1–17 (2021).

52. Itkin, T. *et al.* Distinct bone marrow blood vessels differentially regulate haematopoiesis. *Nature* **532**, 323–328 (2016).

53. Bixel, M. G. *et al.* Flow Dynamics and HSPC Homing in Bone Marrow Microvessels. *Cell Rep.* **18**, 1804–1816 (2017).

54. Belnoue, E. *et al.* APRIL is critical for plasmablast survival in the bone marrow and poorly expressed by early-life bone marrow stromal cells. *Blood* **111**, 2755–2764 (2008).

55. Louie, J. K. *et al.* A novel risk factor for a novel virus: Obesity and 2009 pandemic influenza a (H1N1). *Clin. Infect. Dis.* **52**, 301–312 (2011).

56. Minnich, M. *et al.* Multifunctional role of the transcription factor Blimp-1 in coordinating plasma cell differentiation. *Nat. Immunol.* **17**, 331–343 (2016).

57. Low, M. S. Y. *et al.* IRF4 Activity Is Required in Established Plasma Cells to Regulate Gene Transcription and Mitochondrial Homeostasis. *Cell Rep.* **29**, 2634-2645.e5 (2019).

58. Ochiai, K. *et al.* Zinc finger-IRF composite elements bound by Ikaros/IRF4 complexes function as gene repression in plasma cell. *Blood Adv.* **2**, 883–894 (2018).

59. Iwakoshi, N. N. *et al.* Plasma cell differentiation and the unfolded protein response intersect at the transcription factor XBP-I. *Nat. Immunol.* **4**, 321–329 (2003).

60. Cenci, S. The Proteasome in Terminal Plasma Cell Differentiation. *Semin. Hematol.* **49**, 215–222 (2012).

61. Pengo, N. & Cenci, S. The role of autophagy in plasma cell ontogenesis. *Autophagy* **9**, 942–944 (2013).

62. Lam, W. Y. *et al.* Mitochondrial Pyruvate Import Promotes Long-Term Survival of Antibody-Secreting Plasma Cells. *Immunity* **45**, 60–73 (2016).

63. Shi, W. *et al.* Transcriptional profiling of mouse B cell terminal differentiation defines a signature for antibody-secreting plasma cells. *Nat. Immunol.* **16**, 663–673 (2015).

64. Pelletier, N. *et al.* The Endoplasmic Reticulum Is a Key Component of the Plasma Cell Death Pathway. *J. Immunol.* **176**, 1340–1347 (2006).

65. Nagata, S. Apoptosis and Clearance of Apoptotic Cells. *Annu. Rev. Immunol.* **36**, 489–517 (2018).

66. Chevrier, S. *et al.* CD93 is required for maintenance of antibody secretion and persistence of plasma cells in the bone marrow niche. *Proc. Natl. Acad. Sci. U. S. A.* **106**, 3895–3900 (2009).

67. Lugano, R. *et al.* CD93 promotes β1 integrin activation and fibronectin fibrillogenesis during tumor angiogenesis. *J. Clin. Invest.* **128**, 3280–3297 (2018).

68. Kao, Y. C. *et al.* The Epidermal Growth Factor-like Domain of CD93 Is a Potent Angiogenic Factor. *PLoS One* **7**, 1–11 (2012).

69. Delogu, A. *et al.* Gene repression by Pax5 in B cells is essential for blood cell homeostasis and is reversed in plasma cells. *Immunity* **24**, 269–281 (2006).

70. Rozanski, C. H. *et al.* CD28 Promotes Plasma Cell Survival, Sustained Antibody Responses, and BLIMP-1 Upregulation through Its Distal PYAP Proline Motif. *J. Immunol.* **194**, 4717–4728 (2015).

71. Njau, M. N. *et al.* CD28 –B7 Interaction Modulates Short- and Long-Lived Plasma Cell Function. *J. Immunol.* **189**, 2758–2767 (2012).

72. Utley, A. *et al.* CD28 Regulates Metabolic Fitness for Long-Lived Plasma Cell Survival. *Cell Rep.* **31**, 107815 (2020).

73. Glatman Zaretsky, A. *et al.* T Regulatory Cells Support Plasma Cell Populations in the Bone Marrow. *Cell Rep.* **18**, 1906–1916 (2017).

74. Wang, Y. & Bhattacharya, D. Adjuvant-specific regulation of long-term antibody responses by ZBTB20. *J. Exp. Med.* **211**, 841–856 (2014).

75. Chevrier, S. *et al.* The BTB-ZF transcription factor Zbtb20 is driven by Irf4 to promote plasma cell differentiation and longevity. *J. Exp. Med.* **211**, 827–840 (2014).

76. Van Driel, M. *et al.* CD44 variant isoforms are involved in plasma cell adhesion to bone marrow stromal cells. *Leukemia* **16**, 135–143 (2002).

77. Amanna, I. J., Carlson, N. E. & Slifka, M. K. Duration of Humoral Immunity to Common Viral and Vaccine Antigens. *N. Engl. J. Med.* **357**, 1903–1915 (2007).

78. Vieira, P. & Rajewsky, K. The half-lives of serum immunoglobulins in adult mice. *Eur. J. Immunol.* **18**, 313–316 (1988).

79. Tew, J. G., Kosco, M. H., Burton, G. F. & Szakal, A. K. Follicular Dendritic Cells as Accessory Cells. *Immunol. Rev.* **117**, 185–211 (1990).

80. Bernasconi, N. L., Traggiai, E. & Lanzavecchia, A. Maintenance of serological memory by polyclonal activation of human memory B cells. *Science (80-.).* **298**, 2199–2202 (2002).

81. Hammarlund, E. *et al.* Plasma cell survival in the absence of B cell memory. *Nat. Commun.* **8**, (2017).

82. Cambridge, G. *et al.* Serologic changes following B lymphocyte depletion therapy for rheumatoid arthritis. *Arthritis Rheum.* **48**, 2146–2154 (2003).

83. Pescovitz, M. D. *et al.* Effect of rituximab on human in vivo antibody immune responses. *J. Allergy Clin. Immunol.* **128**, 1295-1302.e5 (2011).

84. van der Kolk, L. E., Baars, J. W., Prins, M. H. & van Oers, M. H. J. Rituximab treatment results in impaired secondary humoral immune responsiveness. *Blood* **100**, 2257–2259 (2002).

85. Slifka, M. K., Antia, R., Whitmire, J. K. & Ahmed, R. Humoral immunity due to long-lived plasma cells. *Immunity* **8**, 363–372 (1998).

86. Landsverk, O. J. B. *et al.* Antibody-secreting plasma cells persist for decades in human intestine. *J. Exp. Med.* **214**, 309–317 (2017).

87. Radbruch, A. *et al.* Competence and competition: The challenge of becoming a long-lived plasma cell. *Nat. Rev. Immunol.* **6**, 741–750 (2006).

88. Amanna, I. J. & Slifka, M. K. Mechanisms that determine plasma cell lifespan and the duration of humoral immunity. *Immunol. Rev.* **236**, 125–138 (2010).

89. Odendahl, M. *et al.* Generation of migratory antigen-specific plasma blasts and mobilization of resident plasma cells in a secondary immune response. *Blood* **105**, 1614–1621 (2005).

90. Mina, M. J. *et al.* Measles virus infection diminishes preexisting antibodies that offer protection from other pathogens. *Science (80-.).* **366**, 599–606 (2019).

91. Slifka, M. K. & Amanna, I. J. Role of multivalency and antigenic threshold in generating protective antibody responses. *Front. Immunol.* **10**, 1–16 (2019).

92. Mei, H. E. *et al.* A unique population of IgG-expressing plasma cells lacking CD19 is enriched in

human bone marrow. *Blood* **125**, 1739–1748 (2015).

93. Halliley, J. L. *et al.* Long-Lived Plasma Cells Are Contained within the CD19-CD38hiCD138+ Subset in Human Bone Marrow. *Immunity* **43**, 132–145 (2015).

94. Wang, K., Wei, G. & Liu, D. CD19: a biomarker for B cell development, lymphoma diagnosis and therapy. *Exp. Hematol. Oncol.* **1**, 1–7 (2012).

95. Anderson, K. C. *et al.* Expression of human B cell-associated antigens on leukemias and lymphomas: A model of human B cell differentiation. *Blood* **63**, 1424–1433 (1984).

96. Del Nagro, C. J. *et al.* CD19 Function in Central and Peripheral B-Cell Development. *Immunol. Res.* **31**, 119–132 (2005).

97. Tedder, T. F. CD19: A promising B cell target for rheumatoid arthritis. *Nat. Rev. Rheumatol.* **5**, 572–577 (2009).

98. Cherukuri, A., Cheng, P. C., Sohn, H. W. & Pierce, S. K. The CD19/CD21 complex functions to prolong B cell antigen receptor signaling from lipid rafts. *Immunity* **14**, 169–179 (2001).

99. van Zelm, M. C. *et al.* An Antibody-Deficiency Syndrome Due to Mutations in the CD19 Gene . *N. Engl. J. Med.* **354**, 1901–1912 (2006).

100. Kanegane, H. *et al.* Novel mutations in a Japanese patient with CD19 deficiency. *Genes Immun.* **8**, 663–670 (2007).

101. Inaoki, M., Sato, S., Weintraub, B. C., Goodnow, C. C. & Tedder, T. F. CD19-Regulated Signaling Thresholds Control Peripheral Tolerance and Autoantibody Production in B Lymphocytes. *J. Exp. Med.* **186**, 1923–1931 (1997).

102. Sato, S., Hasegawa, M., Fujimoto, M., Tedder, T. F. & Takehara, K. Quantitative Genetic Variation in CD19 Expression Correlates with Autoimmunity. *J. Immunol.* **165**, 6635–6643 (2000).

103. Kozmik, Z., Wang, S., Dörfler, P., Adams, B. & Busslinger, M. The promoter of the CD19 gene is a target for the B-cell-specific transcription factor BSAP. *Mol. Cell. Biol.* **12**, 2662–2672 (1992).

104. Arumugakani, G. *et al.* Early Emergence of CD19-Negative Human Antibody-Secreting Cells at the Plasmablast to Plasma Cell Transition. *J. Immunol.* **198**, 4618–4628 (2017).

105. Brynjolfsson, S. F., Mohaddes, M., Kärrholm, J. & Wick, M. J. Long-lived plasma cells in human bone marrow can be either CD191 or CD19–. *Blood Adv.* **1**, 835–838 (2017).

106. Bhoj, V. G. *et al.* Persistence of long-lived plasma cells and humoral immunity in individuals responding to CD19-directed CAR T-cell therapy. *Blood* **128**, 360–370 (2016).

107. Woodford-Thomas, T. & Thomas, M. L. The leukocyte common antigen, CD45 and other protein tyrosine phosphatases in hematopoietic cells. *Semin. Cell Biol.* **4**, 409–418 (1993).

108. Bataille, R., Robillard, N., Pellat-Deceunynck, C. & Amiot, M. A cellular model for myeloma cell growth and maturation based on an intraclonal CD45 hierarchy. *Immunol. Rev.* **194**, 105–111 (2003).

109. Medina, F., Segundo, C., Campos-Caro, A., González-García, I. & Brieva, J. A. The heterogeneity shown by human plasma cells from tonsil, blood, and bone marrow reveals graded stages of increasing maturity, but local profiles of adhesion molecule expression. *Blood* **99**, 2154–2161

(2002).

110. Hermiston, M. L., Zikherman, J. & Zhu, J. W. CD45, CD148, and Lyp/Pep: critical phosphatases regulating Src family kinase signaling networks in immune cells. *Immunol. Rev.* **228**, 288–311 (2009).

111. Zikherman, J., Doan, K., Parameswaran, R., Raschke, W. & Weiss, A. Quantitative differences in CD45 expression unmask functions for CD45 in B-cell development, tolerance, and survival. *Proc. Natl. Acad. Sci. U. S. A.* **109**, (2012).

112. Szodoray, P. *et al.* Integration of T helper and BCR signals governs enhanced plasma cell differentiation of memory B cells by regulation of CD45 phosphatase activity. *Cell Rep.* **36**, 109525 (2021).

113. Irie-Sasaki, J. *et al.* CD45 is a JAK phosphatase and negatively regulates cytokine receptor signalling. *Nature* **409**, 349–354 (2001).

114. Kasper, C. *et al.* letters Structural basis of cell – cell adhesion by NCAM. *America (NY).* **7**, 389–393 (2000).

115. Van Acker, H. H., Capsomidis, A., Smits, E. L. & Van Tendeloo, V. F. CD56 in the immune system: More than a marker for cytotoxicity? *Front. Immunol.* **8**, 1–9 (2017).

116. Mace, E. M., Gunesch, J. T., Dixon, A. & Orange, J. S. Human NK cell development requires CD56-mediated motility and formation of the developmental synapse. *Nat. Commun.* **7**, 1–13 (2016).

117. Pellat-Deceunynck, C. *et al.* Expression of CD28 and CD40 in human myeloma cells: A comparative study with normal plasma cells. *Blood* **84**, 2597–2603 (1994).

118. Kaiser, U., Auerbach, B. & Oldenburg, M. The neural cell adhesion molecule NCAM in multiple myeloma. *Leuk. Lymphoma* **20**, 389–395 (1996).

119. Barillé, S., Collette, M., Bataille, R. & Amiot, M. Myeloma cells upregulate interleukin-6 secretion in osteoblastic cells through cell-to-cell contact but downregulate osteocalcin. *Blood* **86**, 3151–3159 (1995).

120. Peceliunas, V., Janiulioniene, A., Matuzeviciene, R. & Griskevicius, L. Six color flow cytometry detects plasma cells expressing aberrant immunophenotype in bone marrow of healthy donors. *Cytom. Part B - Clin. Cytom.* **80 B**, 318–323 (2011).

121. Kiselyov, V. V., Soroka, V., Berezin, V. & Bock, E. Structural biology of NCAM homophilic binding and activation of FGFR. *J. Neurochem.* **94**, 1169–1179 (2005).

122. Bühring, H. J. *et al.* Novel markers for the prospective isolation of human MSC. *Ann. N. Y. Acad. Sci.* **1106**, 262–271 (2007).

123. Battula, V. L. *et al.* Isolation of functionally distinct mesenchymal stem cell subsets using antibodies against CD56, CD271, and mesenchymal stem cell antigen-1. *Haematologica* **94**, 173–184 (2009).

124. Anders, S., Pyl, P. T. & Huber, W. HTSeq-A Python framework to work with high-throughput sequencing data. *Bioinformatics* **31**, 166–169 (2015).

125. Love, M. I., Huber, W. & Anders, S. Moderated estimation of fold change and dispersion for RNA-

seq data with DESeq2. *Genome Biol.* **15**, 1–21 (2014).

126. Cossarizza, A. *et al.* Guidelines for the use of flow cytometry and cell sorting in immunological studies (third edition). *Eur. J. Immunol.* **51**, 2708–3145 (2021).

127. Mei, H. E. *et al.* Blood-borne human plasma cells in steady state are derived from mucosal immune responses. *Blood* **113**, 2461–2469 (2009).

128. Chilosi, M. *et al.* CD138/syndecan-1: a useful immunohistochemical marker of normal and neoplastic plasma cells on routine trephine bone marrow biopsies. *Mod. Pathol.* **12/12**, 1101–1106 (1999).

129. Soh, K. T. *et al.* CD319 (SLAMF7) an alternative marker for detecting plasma cells in the presence of daratumumab or elotuzumab. *Cytom. Part B - Clin. Cytom.* **100**, 497–508 (2021).

130. Heinrich, P. C. *et al.* Principles of interleukin (IL)-6-type cytokine signalling and its regulation. *Biochem. J.* **374**, 1–20 (2003).

131. Riese, J. *et al.* Expression of interleukin-6 and monocyte chemoattractant protein-1 by peritoneal sub-mesothelial cells during abdominal operations. *J. Pathol.* **202**, 34–40 (2004).

132. Neiva, K. G. *et al.* Endothelial cell-derived interleukin-6 regulates tumor growth. *BMC Cancer* **14**, 1–11 (2014).

133. Rozanski, C. H. *et al.* Sustained antibody responses depend on CD28 function in bone marrow-resident plasma cells. *J. Exp. Med.* **208**, 1435–1446 (2011).

134. Jash, A. *et al.* ZBTB32 Restricts the Duration of Memory B Cell Recall Responses. *J. Immunol.* **197**, 1159–1168 (2016).

135. Yoon, H. *et al.* ZBZB32 is an early repressor of the class II transactivator and MHC class II gene expression during B cell differentiation to plasma cells. **189**, 2393–2403 (2013).

136. Ponta, H., Sherman, L. & Herrlich, P. A. CD44: From adhesion molecules to signalling regulators. *Nat. Rev. Mol. Cell Biol.* **4**, 33–45 (2003).

137. Reyes, R., Cardeñes, B., Machado-Pineda, Y. & Cabañas, C. Tetraspanin CD9: A key regulator of cell adhesion in the immune system. *Front. Immunol.* **9**, 1–9 (2018).

138. Yoon, S. O., Lee, I. Y., Zhang, X., Zapata, M. C. & Choi, Y. S. CD9 may contribute to the survival of human germinal center B cells by facilitating the interaction with follicular dendritic cells. *FEBS Open Bio* **4**, 370–376 (2014).

139. Hynes, R. O. Integrins. *Cell* **110**, 673–687 (2002).

140. Mezu-Ndubuisi, O. J. & Maheshwari, A. The role of integrins in inflammation and angiogenesis. *Pediatr. Res.* **89**, 1619–1626 (2021).

141. Fan, T. J., Han, L. H., Cong, R. S. & Liang, J. Caspase family proteases and apoptosis. *Acta Biochim. Biophys. Sin. (Shanghai).* **37**, 719–727 (2005).

142. Shamas-Din, A., Brahmbhatt, H., Leber, B. & Andrews, D. W. BH3-only proteins: Orchestrators of apoptosis. *Biochim. Biophys. Acta - Mol. Cell Res.* **1813**, 508–520 (2011).

143. Thorens, B. & Mueckler, M. The SLC2 (GLUT) Family of Membrane Transporters. *Mol. Aspects*

Med. **34**, 121–138 (2014).

144. Fotiadis, D., Kanai, Y. & Palacín, M. The SLC3 and SLC7 families of amino acid transporters. *Mol. Aspects Med.* **34**, 139–158 (2013).

145. Kabashima, K. *et al.* Plasma cell S1P1 expression determines secondary lymphoid organ retention versus bone marrow tropism. *J. Exp. Med.* **203**, 2683–2690 (2006).

146. Jourdan, M. *et al.* An in vitro model of differentiation of memory B cells into plasmablasts and plasma cells including detailed phenotypic and molecular characterization. *Blood* **114**, 5173–5181 (2009).

147. González-Fernández, A., Gilmore, D. & Milstein, C. Age-related decrease in the proportion of germinal center B cells from mouse Peyer's patches is accompanied by an accumulation of somatic mutations in their immunoglobulin genes. *Eur J Immunol* **24**, 2918–2921 (1994).

148. Wagner, S. D. & Neuberger, M. S. SOMATIC HYPERMUTATION OF IMMUNOGLOBULIN GENES. *Annu. Rev. Immunol.* **14**, 441–457 (1996).

149. Chu, P. G. & Arber, D. A. CD79 : A Review. **9**, 97–106 (2001).

150. Wilkinson, S. T. *et al.* Partial plasma cell differentiation as a mechanism of lost major histocompatibility complex class II expression in diffuse large B-cell lymphoma. *Blood* **119**, 1459–1467 (2012).

151. Scalise, M., Pochini, L., Console, L., Losso, M. A. & Indiveri, C. The Human SLC1A5 (ASCT2) amino acid transporter: From function to structure and role in cell biology. *Front. Cell Dev. Biol.* **6**, 1–17 (2018).

152. Grootjans, J., Kaser, A., Kaufman, R. J. & Blumberg, R. S. The unfolded protein response in immunity and inflammation. *Nat. Rev. Immunol.* **16**, 469–484 (2016).

153. Jin, M. Unique roles of tryptophanyl-tRNA synthetase in immune control and its therapeutic implications. *Exp. Mol. Med.* **51**, 1–10 (2019).

154. Haines, R. J., Pendleton, L. C. & Eichler, D. C. Argininosuccinate synthase: At the center of arginine metabolism. *Int. J. Biochem. Mol. Biol.* **2**, 8–23 (2011).

155. Rosenzweig, A., Blenis, J. & Gomes, A. P. Beyond the warburg effect: How do cancer cells regulate One-Carbon metabolism? *Front. Cell Dev. Biol.* **6**, 1–7 (2018).

156. Kim, H. & Park, Y. J. Links between Serine Biosynthesis Pathway and Epigenetics in Cancer Metabolism. *Clin. Nutr. Res.* **7**, 153 (2018).

157. Zhu, Z. & Leung, G. K. K. More Than a Metabolic Enzyme: MTHFD2 as a Novel Target for Anticancer Therapy? *Front. Oncol.* **10**, 1–9 (2020).

158. Shetty, S. & Varshney, U. Regulation of translation by one-carbon metabolism in bacteria and eukaryotic organelles. *J. Biol. Chem.* **296**, 100088 (2021).

159. Yadati, T., Houben, T., Bitorina, A. & Shiri-Sverdlov, R. The Ins and Outs of Cathepsins: Physiological Function and Role in Disease Management. *Cells* **9**, (2020).

160. Dong, C. *et al.* Loss of FBP1 by Snail-Mediated Repression Provides Metabolic Advantages in Basal-like Breast Cancer. *Cancer Cell* **23**, 316–331 (2013).

161. Grasmann, G., Smolle, E., Olschewski, H. & Leithner, K. Gluconeogenesis in cancer cells – Repurposing of a starvation-induced metabolic pathway? *Biochimica et Biophysica Acta - Reviews on Cancer* (2019).

162. Horváth, G. *et al.* CD19 is linked to the integrin-associated tetraspans CD9, CD81, and CD82. *J. Biol. Chem.* **273**, 30537–30543 (1998).

163. Brosseau, C., Colas, L., Magnan, A. & Brouard, S. CD9 tetraspanin: A new pathway for the regulation of inflammation? *Front. Immunol.* **9**, 1–12 (2018).

164. Théry, C. *et al.* Molecular characterization of dendritic cell-derived exosomes: Selective accumulation of the heat shock protein hsc73. *J. Cell Biol.* **147**, 599–610 (1999).

165. Schilling, S., Wasternack, C. & Demuth, H. U. Glutaminyl cyclases from animals and plants: A case of functionally convergent protein evolution. *Biol. Chem.* **389**, 983–991 (2008).

166. Schwartz, S. L. *et al.* Role of helical structure and dynamics in oligoadenylate synthetase 1 (OAS1) mismatch tolerance and activation by short dsRNAs. *Proc. Natl. Acad. Sci. U. S. A.* **119**, 1–12 (2022).

167. Spitaels, J., Van Hoecke, L., Roose, K., Kochs, G. & Saelens, X. Mx1 in Hematopoietic Cells Protects against Thogoto Virus Infection. *J. Virol.* **93**, 1–15 (2019).

168. Perng, Y. C. & Lenschow, D. J. ISG15 in antiviral immunity and beyond. *Nat. Rev. Microbiol.* **16**, 423–439 (2018).

169. Sun, F. *et al.* Topology, antiviral functional residues and mechanism of IFITM1. *Viruses* **12**, (2020).

170. Kondoh, M. *et al.* Induction of hepatic metallothionein synthesis by endoplasmic reticulum stress in mice. *Toxicol. Lett.* **148**, 133–139 (2004).

171. Parsell, D. A. & Lindquist, S. The function of heat-shock proteins in stress tolerance: Degradation and reactivation of damaged proteins. *Annu. Rev. Genet.* **27**, 437–496 (1993).

172. Zhang, J. *et al.* The role of cystatin C in multiple myeloma. *Int. J. Lab. Hematol.* **44**, 135–141 (2022).

173. Zhang, W. *et al.* Cystatin C regulates major histocompatibility complex-II-peptide presentation and extracellular signal-regulated kinase-dependent polarizing cytokine production by bone marrow-derived dendritic cells. *Immunol. Cell Biol.* **97**, 916–930 (2019).

174. Tizon, B. *et al.* Induction of autophagy by cystatin C: A mechanism that protects murine primary cortical neurons and neuronal cell lines. *PLoS One* **5**, (2010).

175. Wake, C. T. Molecular biology of the HLA class I and class II genes. *Mol. Biol. Med.* **3**, 1–11 (1986).

176. Saha, D. *et al.* Hemoglobin Expression in Nonerythroid Cells: Novel or Ubiquitous? *Int. J. Inflam.* **2014**, 1–8 (2014).

177. Bejjani, F., Evanno, E., Zibara, K., Piechaczyk, M. & Jariel-Encontre, I. The AP-1 transcriptional complex: Local switch or remote command? *Biochim. Biophys. Acta - Rev. Cancer* **1872**, 11–23 (2019).

178. Yan, S. F. *et al.* Hypoxia-associated induction of early growth response-1 gene expression. *J. Biol. Chem.* **274**, 15030–15040 (1999).

179. Gharib, S. A. *et al.* Transcriptional landscape of bone marrow-derived very small embryonic-like stem cells during hypoxia. *Respir. Res.* **12**, 63 (2011).

180. Liebermann, D. a & Hoffman, B. *Gadd45 Stress Sensor Genes*. *Advances in experimental medicine and biology* vol. 793 (Springer New York, 2013).

181. D'Souza, A. R. & Minczuk, M. Mitochondrial transcription and translation: overview. *Essays Biochem.* **62**, 309–320 (2018).

182. Castro, C. D. & Flajnik, M. F. Putting J Chain Back on the Map: How Might Its Expression Define Plasma Cell Development? *J. Immunol.* **193**, 3248–3255 (2014).

183. Caunt, C. J. & Keyse, S. M. Dual-specificity MAP kinase phosphatases (MKPs): Shaping the outcome of MAP kinase signalling. *FEBS J.* **280**, 489–504 (2013).

184. Nus, M. *et al.* NR4a1 deletion in marginal zone B cells exacerbates atherosclerosis in mice. *Arterioscler. Thromb. Vasc. Biol.* 2598–2604 (2020).

185. Lin, B. *et al.* Conversion of Bcl-2 from Protector to Killer by Interaction with Nuclear Orphan Receptor Nur77/TR3. *Cell* **116**, 527–540 (2004).

186. Ronchetti, D. *et al.* A compendium of long non-coding RNAs transcriptional fingerprint in multiple myeloma. *Sci. Rep.* **8**, 10–18 (2018).

187. Moroney, J. B., Vasudev, A., Pertsemlidis, A., Zan, H. & Casali, P. Integrative transcriptome and chromatin landscape analysis reveals distinct epigenetic regulations in human memory B cells. *Nat. Commun.* **11**, 1–18 (2020).

188. Kim, G., Ng, H. P., Chan, E. R. & Mahabeleshwar, G. H. Kruppel-like factor 6 promotes macrophage inflammatory and hypoxia response. *FASEB J.* **34**, 3209–3223 (2020).

189. Racca, A. C. *et al.* Low oxygen tension induces Krüppel-Like Factor 6 expression in trophoblast cells. *Placenta* **45**, 50–57 (2016).

190. Igaz, P., Tóth, S. & Falus, A. Biological and clinical significance of the JAK-STAT pathway; lessons from knockout mice. *Inflamm. Res.* **50**, 435–441 (2001).

191. Doria-Rose, N. A. & Joyce, M. G. Strategies to guide the antibody affinity maturation process. 137–147. *Curr.Opin.Virol*. **11**, 137-147 (2016).

192. Jensen, B. G. S. *et al.* Selective Expression of CD45 Isoforms Defines CALLA' Monoclonal B-Lineage Cells in Peripheral Blood From Myeloma Patients as Late Stage B Cells. *Blood*. **78**, 711-719 (1991).

193. Van Spriel, A. B. *et al.* The Tetraspanin Protein CD37 Regulates IgA Responses and Anti-Fungal Immunity. *PLoS Pathog*. **5**, 1–11 (2009).

194. Knobeloch, K. *et al.* Targeted Inactivation of the Tetraspanin CD37 Impairs T-Cell-Dependent B-Cell Response under Suboptimal Costimulatory Conditions. **20**, 5363–5369 (2000).

195. Koumpis, E. *et al.* Pathology - Research and Practice CD56 expression in multiple myeloma : Correlation with poor prognostic markers but no effect on outcome. *Pathol. - Res. Pract.* **225**, 153567 (2021).

196. Turner, J. S. *et al.* SARS-CoV-2 infection induces long-lived bone marrow plasma cells in humans. *Nature.* **595**, 421-425 (2021).

197. Cao, X. *et al.* Irradiation induces bone injury by damaging bone marrow microenvironment for stem cells. *Proc. Natl. Acad. Sci. U. S. A.* **108**, 1609–1614 (2011).

198. Beura, L. K. *et al.* Normalizing the environment recapitulates adult human immune traits in laboratory mice. *Nature* **532**, 512–516 (2016).

199. Zhong, L. *et al.* Single cell transcriptomics identifies a unique adipose lineage cell population that regulates bone marrow environment. *Elife* **9**, 1–28 (2020).

200. Scheller, E. L. *et al.* Region-specific variation in the properties of skeletal adipocytes reveals regulated and constitutive marrow adipose tissues. *Nat. Commun.* **6**, (2015).

201. Ewalt, M. D. & Gratzinger, D. Classical Endothelial Markers Fail to Highlight Bone Marrow Sinusoids in the Marrow of Healthy Patients and Patients with Myelodysplastic Syndromes. *Blood* **124**, 4170–4170 (2014).

202. Schoenhals, M. *et al.* Hypoxia favors the generation of human plasma cells. *Cell Cycle* **16**, 1104–1117 (2017).

203. Carroll, V. A. & Ashcroft, M. Role of hypoxia-inducible factor (HIF)-1α versus HIF-2α in the regulation of HIF target genes in response to hypoxia, insulin-like growth factor-I, or loss of von Hippel-Lindau function: Implications for targeting the HIF pathway. *Cancer Res.* **66**, 6264–6270 (2006).

204. Wu, D. & Yotnda, P. Induction and testing of hypoxia in cell culture. *J. Vis. Exp.* **54**, e2899 (2011).

205. Tokoyoda, K., Egawa, T., Sugiyama, T., Choi, B. & Nagasawa, T. Cellular Niches Controlling B Lymphocyte Behavior within Bone Marrow during Development. **20**, 707–718 (2004).

206. Ding, L. & Morrison, S. J. Haematopoietic stem cells and early lymphoid progenitors occupy distinct bone marrow niches. *Nature* **495**, 231–235 (2013).

207. Greenbaum, A. *et al.* CXCL12 in early mesenchymal progenitors is required for haematopoietic stem-cell maintenance. *Nature* **495**, 227–230 (2013).

208. Peled, A. *et al.* The chemokine SDF-1 activates the integrins LFA-1, VLA-4, and VLA-5 on immature human CD34+ cells: role in transendothelial/stromal migration and engraftment of NOD/SCID mice. *Blood* **95**, 3289–3296 (2000).

209. Schweitzer, K. M. *et al.* Constitutive expression of E-selectin and vascular cell adhesion molecule-1 on endothelial cells of hematopoietic tissues. *Am. J. Pathol.* **148**, 165–175 (1996).

210. Katayama, Y., Hidalgo, A., Peired, A. & Frenette, P. S. Integrin α4β7 and its counterreceptor MAdCAM-1 contribute to hematopoietic progenitor recruitment into bone marrow following transplantation. *Blood* **104**, 2020–2026 (2004).

211. Caraux, A. *et al.* Mobilization of plasma cells in healthy individuals treated with granulocyte colony-stimulating factor for haematopoietic stem cell collection. *Immunology* **132**, 266–272 (2011).

212. Wilmore, J. R., Jones, D. D. & Allman, D. Improved resolution of plasma cell subpopulations by flow cytometry HHS Public Access. *Eur J Immunol* **47**, 1386–1388 (2017).

213. Xu, C. *et al.* Stem cell factor is selectively secreted by arterial endothelial cells in bone marrow.

Nat. Commun. **9**, 1–13 (2018).

214. Morcos, M. N. F. *et al.* SCA-1 Expression Level Identifies Quiescent Hematopoietic Stem and Progenitor Cells. *Stem Cell Reports* **8**, 1472–1478 (2017).

215. Upadhyay, G. Emerging Role of Lymphocyte Antigen-6 Family of Genes in Cancer and Immune Cells. *Front. Immunol.* **10**, 819 (2019).

216. Cyster, J. G. *et al.* Regulation of B-lymphocyte negative and positive selection by tyrosine phosphatase CD45. *Nature* **381**, 325–328 (1996).

217. Naka, T., Fujimoto, M. & Kishimoto, T. Negative regulation of cytokine signaling: STAT-induced STAT inhibitor. *Trends Biochem. Sci.* **24**, 394–398 (1999).

218. Starr, R. *et al.* A family of cytokine-inducible inhibitors of signalling. *Nature* **387**, 917–921 (1997).

219. Mohr, E. *et al.* Dendritic Cells and Monocyte/Macrophages That Create the IL-6/APRIL-Rich Lymph Node Microenvironments Where Plasmablasts Mature. *J. Immunol.* **182**, 2113–2123 (2009).

220. Wols, H. A. M., Underhill, G. H., Kansas, G. S. & Witte, P. L. The Role of Bone Marrow-Derived Stromal Cells in the Maintenance of Plasma Cell Longevity. *J. Immunol.* **169**, 4213–4221 (2002).

221. Diehl, S. A. *et al.* STAT3-Mediated Up-Regulation of BLIMP1 Is Coordinated with BCL6 Down-Regulation to Control Human Plasma Cell Differentiation. *J. Immunol.* **180**, 4805–4815 (2008).

222. Rodríguez-Bayona, B., Ramos-Amaya, A., López-Blanco, R., Campos-Caro, A. & Brieva, J. A. STAT-3 Activation by Differential Cytokines Is Critical for Human In Vivo–Generated Plasma Cell Survival and Ig Secretion. *J. Immunol.* **191**, 4996–5004 (2013).

223. Addo, R. K. *et al.* Single-cell transcriptomes of murine bone marrow stromal cells reveal niche-associated heterogeneity. **11**, 1372–1379 (2019).

224. Bossen, C. & Schneider, P. BAFF, APRIL and their receptors: Structure, function and signaling. *Semin. Immunol.* **18**, 263–275 (2006).

225. Laurent, S. A. *et al.* γ-secretase directly sheds the survival receptor BCMA from plasma cells. *Nat. Commun.* **6**, (2015).

226. Zocchi, M. R., Poggi, A., Crosti, F., Tongiani, S. & Rugarli, C. Signalling in human tumour infiltrating lymphocytes: The CD28 molecule is functional and is physically associated with the CD45R0 molecule. *Eur. J. Cancer* **28**, 749–754 (1992).

227. Bhatta, A., Chan, M. A. & Benedict, S. H. Engagement of CD45 alters early signaling events in human T cells co-stimulated through TCR + CD28. *Cell. Immunol.* **353**, 104130 (2020).

228. Van Spriel, A. B. *et al.* The tetraspanin CD37 orchestrates the α4β1 integrin-Akt signaling axis and supports long-lived plasma cell survival. *Sci. Signal.* **5**, 1–13 (2012).

229. Männe, C. *et al.* Salmonella SiiE prevents an efficient humoral immune memory by interfering with IgG + plasma cell persistence in the bone marrow. **116**, 7425–7430 (2019).

230. Schippers, A. *et al.* β 7 integrin controls immunogenic and tolerogenic mucosal B cell responses. *Clin. Immunol.* **144**, 87–97 (2012).

231. Eyer, K. *et al.* Single-cell deep phenotyping of IgG-secreting cells for high-resolution immune monitoring. *Nat. Biotechnol.* **35**, 977–982 (2017).

232. Taillardet, M. *et al.* The thymus-independent immunity conferred by a pneumococcal polysaccharide is mediated by long-lived plasma cells. **114**, 4432–4440 (2009).

233. Xu, D. & Hemler, M. E. Metabolic activation-related CD147-CD98 complex. *Mol Cell Proteomicsell Proteomics* **4**, 1061–1071 (2006).

234. Kassambara, A. *et al.* RNA-sequencing data-driven dissection of human plasma cell differentiation reveals new potential transcription regulators. *Leukemia* **35**, 1451–1462 (2021).

235. Maness, P. F. & Schachner, M. Neural recognition molecules of the immunoglobulin superfamily: Signaling transducers of axon guidance and neuronal migration. *Nat. Neurosci.* **10**, 19–26 (2007).

236. Cheng, M., Chen, Y., Xiao, W., Sun, R. & Tian, Z. NK cell-based immunotherapy for malignant diseases. *Cell. Mol. Immunol.* **10**, 230–252 (2013).

237. Kelly-Rogers, J., Madrigal-Estebas, L., O'Connor, T. & Doherty, D. G. Activation-Induced Expression of CD56 by T Cells Is Associated With a Reprogramming of Cytolytic Activity and Cytokine Secretion Profile In Vitro. *Hum. Immunol.* **67**, 863–873 (2006).

238. Roothans, D., Smits, E., Lion, E., Tel, J. & Anguille, S. CD56 marks human dendritic cell subsets with cytotoxic potential. *Oncoimmunology* **2**, 6–9 (2013).

239. Van Acker, H. H. *et al.* Interleukin-15 enhances the proliferation, stimulatory phenotype, and antitumor effector functions of human gamma delta T cells. *J. Hematol. Oncol.* **9**, 1–13 (2016).

240. Kato, J. *et al.* Contribution of neural cell adhesion molecule (NCAM) to hemopoietic system in monkeys. *Ann. Hematol.* **87**, 797–807 (2008).

241. Skog, M. S. *et al.* Expression of neural cell adhesion molecule and polysialic acid in human bone marrow-derived mesenchymal stromal cells. *Stem Cell Res. Ther.* **7**, 1–12 (2016).

242. Walmod, P. S., Kolkova, K., Berezin, V. & Bock, E. Zippers make signals: NCAM-mediated molecular interactions and signal transduction. *Neurochem. Res.* **29**, 2015–2035 (2004).

243. Ditlevsen, D. K. *et al.* The role of phosphatidylinositol 3-kinase in neural cell adhesion molecule-mediated neuronal differentiation and survival. *J. Neurochem.* **84**, 546–556 (2003).

7. Supplement

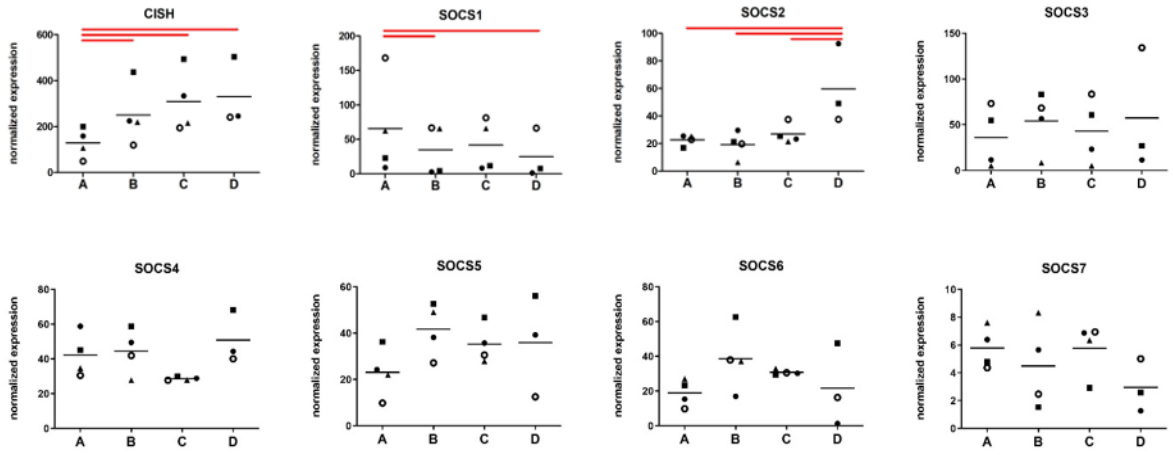

Supplemental figure 1: Gene expression of SOCS family members in BMPC. Plots show gene expression for individual donors (indicated by different symbols) as well as averages (horizontal lines). Colored lines indicate significant (adjusted p-Value > 0.05) and differential gene expression (red: fold change > 2).

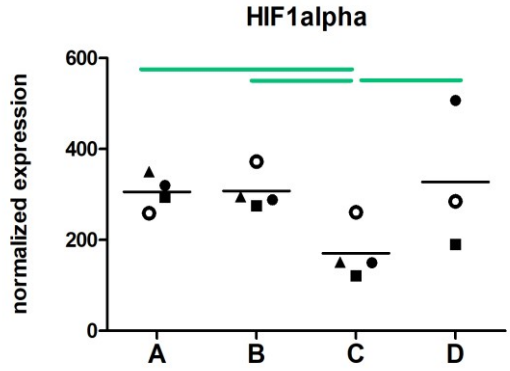

Supplemental figure 2: Gene expression of HIF1α in BMPC. Plots show gene expression for individual donors (indicated by different symbols) as well as averages (horizontal lines). Colored lines indicate significant (adjusted p-Value > 0.05) and differential gene expression (green: fold change > 1.7).

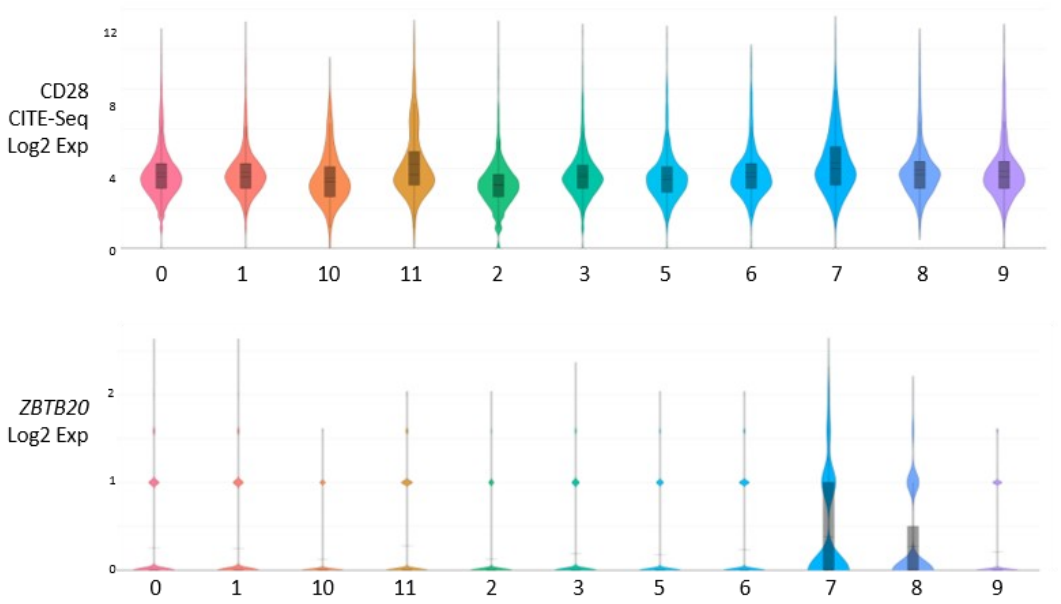

Supplemental figure 3: Protein or transcript levels of CD28 and ZBTB20 detected by single cell RNA sequencing and combined CITE-Seq in BMPC clusters. Violin plots display relative expression levels of transcripts for CD28, *ZBTB20* and *CD9* in clusters included in BMPC single cell transcriptome analysis.

8. Abbreviations

AID (gene: AICDA)	Activation-induced cytidine deaminase
AP	Alkaline phosphatase
APRIL	A proliferation-inducing ligand
ASC	Antibody secreting cell
ATF6	Activating Transcription Factor 6
ATG5	Autophagy related gene 5
Bach2 (gene: BACH2)	BTB Domain And CNC Homolog 2
BC	B cell
Bcl6 (gene: BCL6)	B cell lymphoma 6
BCMA	B cell maturation antigen
BCR	B cell receptor
Blimp-1 (gene: PRDM1)	B lymphocyte-induced maturation protein 1
BM	Bone marrow
BSA	Bovine serum albumin
CAR	CXCL12-abundant reticular cells
cDNA	Complementary deoxyribonucleic acid
CDR	Complementarity determining region
CDR-H3	Heavy chain complementarity determining region 3
CSM	Cell staining medium
CSR	Class switch recombination
CXCL12	C-X-C motif chemokine 12
CXCR4	C-X-C chemokine receptor type 4
CyTOF	Cytometry by time of flight
DAB	3, 3 -diaminobenzidine
DAPI	4’,6-Diamidin-2-phenylindol

DC	Dendritic cell
DNA	Deoxyribonucleic acid
ECM	Extracellular matrix
EDTA	Ethylenediaminetetraacetic acid
EF	Extrafollicular
ER	Endoplasmic reticulum
Fab	Antigen-binding fragment
FACS	Fluorescence activated cell sorting
Fc	Crystallizable fragment
FCS	Fetal calf serum
FFPE	Formalin-fixed paraffin-embedded
FGFR	fibroblast growth factor receptor
Fv	Fragment variable region
GC	Germinal center
H2O2	Hydrogen peroxide
HRP	Horse raddish peroxidase
HSC	Hematopoietic stem cell
HSPC	Hematopoietic stem and progenitor cell
IFN-γ	Interferon γ
Ig	Immunoglobulin
IL-21	Interleukin 21
IL-6	Interleukin 6
IRE1	Inositol-requiring enzyme 1
IRF-4 (gene: IRF4)	Interferon regulatory factor 4
LCA	Leukocyte common antigen
LFA-1	Lymphocyte function-associated antigen 1
LLPC	Long-lived plasma cell

MGUS	Monoclonal gammopathy of undetermined significance
MHC	Major histocompatibility complex
MM	Multiple myeloma
MMR	Measles, mumps and rubella
MOMP	Mitochondrial outer membrane pore
MSC	Mesenchymal stromal cell
NCAM1	Neural cell adhesion molecule 1
NK	Natural killer
Pax5 (gene: PAX5)	Paired box 5
PBS	Phosphate-buffered saline
PC	Plasma cell
PFA	Paraformaldehyde
PI3K	phosphatidylinositol 3-kinase
RNA	Ribonucleic acid
Sca-1	Stem cell antigen 1
SFK	Src family kinase
SHM	Somatic hypermutation
SI	Small intestine
SIPC	Small intestine plasma cell
SLPC	Short-lived plasma cell
TACI	Transmembrane activator and CAML interactor
TC	T cell
TGF-β	Transforming growth factor β
TLR	Toll like receptor
UPR	Unfolded protein response
V(D)J	Variable (diversity) joining
VCAM-1	vascular cell adhesion molecule 1

VH	Heavy chain variable region
VL	Light chain variable region
VLA-4	Very late antigen 4
Xbp-1 (gene: XBP1)	X-box binding protein 1

9. Acknowledgments

I sincerely thank all who supported me in obtaining my doctoral degree. I thank Henrik Mei for giving me the opportunity to work in this exciting research field at the DRFZ as well as for his excellent scientific supervision. I thank Hyun-Dong Chang and Andreas Radbruch for the fruitful scientific discussions and support of my project. My gratitude goes to the entire TRR130 for the excellent environment for the scientific discourse with members of the scientific community as well as the financial support and opportunities for further training through the organization of workshops and meetings.

I would like to thank Heike Hirseland, Axel Schulz, Marie Burns and all former group members for the collaborative, supportive and friendly environment in the lab. I thank Simon Reinke and Antje Blankenstein of the BCRT, and Hayo Rieger of the Bundeswehrkrankenhaus Berlin for their valued collaboration in the collection of bone marrow samples. My gratitude goes to all donors of bone marrow samples which made this entire work possible at all. I thank the lab managers for providing buffers, media and help whenever needed. I thank my father, Gerald Niedobitek, for the collaboration and expertise in immunohistochemical analyses, and Katja Wolff and Ann-Kathrin Höls at the Institute of Pathology of the Unfallkrankenhaus Berlin for their support in the lab.

I especially thank my father for his mentoring and constant motivation. I thank my family, friends and Julien for being there for me. I am especially grateful to Rebecca Cornelis and Padmavathy Ramanarayanan for their invaluable companionship.